NJPST

NIGERIAN JOURNAL OF POLYMER SCIENCE AND TECHNOLOGY

A PUBLICATION OF THE POLYMER INSTITUTE OF NIGERIA

Vol. 14, 2019. ISSN 1119-4111

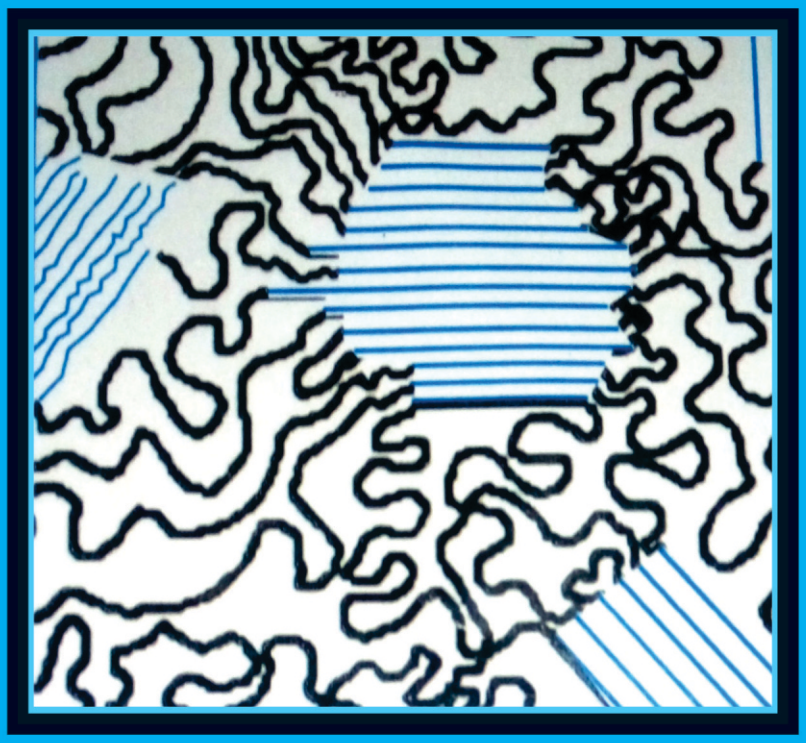

POLYMER INSTITUTE
OF NIGERIA

ANA INDUSTRIES LTD.

Nigerian Journal of Polymer Science and Technology

Volume 14, 2019

ISSN: 1119-4111

A PUBLICATION OF THE POLYMER INSTITUTE OF NIGERIA

Editor-in-Chief
Prof. S. M. Gumel

Nigerian Journal of Polymer Science and Technology

ISSN: 1119-4111 Volume 14, 2019

EDITORIAL BOARD

Editor-in-Chief
Prof. S. M. Gumel
(smgumel.chm@buk.edu.ng)

Technical Secretary, Editorial Board
Dr. Magaji Ladan
(mladan.chm@buk.edu.ng)

Associate Editors

Prof. Peter O. Nkeonye	Department of Textile Science and Technology, A.B.U., Zaria.
Prof. Stephen S. Ochigbo	Department of Chemistry, FUT, Minna, Niger State.
Prof. Issac O. Igwe	Department of Polymer and Textile Engineering, FUT Owerri, Imo State.
Dr. Shehu Umar	Department of Metallurgical and Materials Engineering, A.B.U., Zaria.
Dr. Amali Ejila	Nigerian Institute of Leather and Science Technology (NILEST), Zaria.
Dr. Clement Gonah	Glass Technology Unit, Department of Industrial Design, A.B.U., Zaria
Dr. Peter S. Dass	Department of Chemistry, Modibbo Adama University of Technology, Yola.
Dr. Peter S. Dass	Department of Chemistry, Modibbo Adama University of Technology, Yola.

NATIONAL OFFICERS AND COUNCIL MEMBERS OF THE POLYMER INSTITUTE OF NIGERIA (PIN)

Engr. (Dr.) Innocent Akuvue, FPIN	Chairman, Board of Directors
Chief Alexis N. Ajuebon, FPIN	Immediate Past Board Chairman
Prof. P. A. P Mamza, FPIN, FICCON	President
Dr. J. E Imanah, FPIN	Immediate Past President
Prof. B. T Nwufo, FPIN	Secretary to the Board
Dr. (Mrs) C. D Igwebike-Ossi	Vice President (Operations)
Dr. F. O Biotidara, FPIN	Vice President (Finance)
Engr. (Dr.) F. P Momoh	General Secretary
Engr. (Dr.) N. C Iheaturu	Assistant Secretary General
Prof. P. M Ejikeme	Treasurer
Dr. M. B Dalen	Publicity Secretary
Engr. (Mrs) G. O Ihekweme	Membership Secretary
Chief A. S. Ogunkoya	Lagos District
Prof. Onyewuchi Akaranta	Port Harcourt District
Mr. Inegbedion Festus	Auchi District
Dr. Owen Egharevba	Benin District
Prof Emmanuel Osabohien	Warri District
Prof. Isaac Igwe	Owerri District
Mr. Oboh Johnson	Zaria District
Dr. (Mrs.) Clementina Igwebike-Ossi	Anambra/Enugu/Ebonyi District
Mr. Ishaya G. Kure	Jos District
Mr. Noble Alu	Abuja District
Dr. (Mrs) Doris Boryo	Adamawa/Bauchi/Gombe Chapter
Prof. Victor Adeola Fofoola, (Acting)	Ondo/Ekiti Chapter

Mr. Godfrey Okorie	Oyo/Ogun Chapter
Prof. D.S Oguniyyi	Ilorin Chapter
Prof. A. A. Salisu	Kano/Jigawa Chapter
Prof. S. Achi (Acting)	Kaduna Chapter
Dr. Olumuyiwa Turoti	Osun Chapter
Dr. Misbahu M. Ladan (Acting)	Sokoto/Kebbi/Zamfara Chapter
Dr. Micheal Eneji	Kogi/Niger Chapter

PAST & PRESENT PRESIDENT(S) OF THE POLYMER INSTITUTE OF NIGERIA

1. Chief Engr. K. Ogunade, FPIN	1989 – 1995
2. Ms. May Ikokwu, FPIN	1995 – 1998
3. Dr. T. O Odozi, FPIN	1998 – 2001
4. Dr. P. C. O Nzelu, FPIN	2001 – 2005
5. Dr. E. J Asore, FPIN	Oct., 2005 – Dec., 2005
6. Prof. B. T Nwufo, FPIN	Dec., 2005 – Oct., 2011
7. Dr. J. E Imanah, FPIN	2011 – 2015
8. Prof. P. A. P Mamza, FPIN, FICCON	2015 – till date

CORRESPONDENCE

Editor-in-Chief
Prof. S. M Gumel, FCSN, FPIN, FCAI
(smgumel.chm@buk.edu.ng)

All rights reserved

No part of this publication may be reproduced or stored in retrieval system, transmitted in any form or by any means, electronic, mechanical, photocopying, recording, or otherwise without the prior written permission of the Editor/publishers.

Published by:
POLYMER INSTITUTE OF NIGERIA

Nigerian Journal of polymer Science and Technology

Information to Authors

Scope of the Journal

The Journal is devoted to publishing original research and short communications in all aspects of Polymer Science and Technology (Engineering). Articles in the related discipline of Materials Science Technology will also be considered for publication.

Preparation of Manuscript

Manuscript should be written in the third person in an objective, formal and impersonal style.The SI system should be used for all scientific and laboratory data. The full stop should not be included in abbreviations, example m (not m.) ppm not (p.p.m.). All mathematical expressions should be included in the manuscript. Care should be taken to distinguish between capital and lowercase letters, between zero (0) and letter (O), between the numeral (1) and letter (I), etc. Mathematical expressions should fit into a single column when set in type. Fractional powers are preferred to root signs and should always be used in more elaborate formulas. The solids (/) should be used instead of the horizontal lines for fractions whenever possible. Numbers that identify mathematical expressions should be enclosed in parentheses. Refer to equations in the text as "Eq. (1)", etc., or "Equation (1)", etc., at the beginning of a sentence.

Content

All pages must be numbered consecutively. A manuscript would normally include a title, abstract, keywords, introduction, materials and methods, results and discussion, conclusions and references.

i. **Title page**: A short title which should be concise but informative must be provided. This should be followed by the names and full addresses of all authors. E-mail addresses of the corresponding authors must be included.
ii. **Abstract**: The abstract should not be more 220 words. It should give concise factual information about objectives of the work, the methods used, the results obtained and the conclusions reached.
iii. **Keywords**: The authors should list below the abstract keywords for information retrieval purposes. The keywords should identify with main point in the paper.
iv. **Abbreviations and Notations**: Nomenclature must be listed at the

beginning of the paper and should conform to the system of standard SI units. Acronyms and abbreviations should be spelt out in full at their first appearance in the text.

v. **Text**: Papers should be typed single column, with double line spacing on one side of the paper only with ample margins on all sides. The text should be divided into sections each with a separate heading, numbered consecutively. The section heading be typed on a separate line and should be bold.

vi. **Conclusionsand Recommendations**: The conclusions should summarise the findings, clearly stating the contributions and their relevance. Recommendations for implementation or for areas of further work on the subject matter should be made.

vii. **Acknowledgements**: These should be brief and relevant. The names of funding organizations should be written in full. Dedications are not permitted.

viii. **References**: References to publish work should be indicated at the appropriate place in the text, according to the Harvard system (i.e. using author(s)' name(s) and date), with a reference list in alphabetical order, at the end of the manuscript. All references in this list should be indicated at some point in the text and vice versa. Papers by more than two authors but with same first author should be listed by year sequence and alphabetically within each year.

Examples of layout of reference are given below:

Book

Onyeyili, I.O. (2003) Analysis of statistically Determine Structures. El' DemakPublishers, Enugu.

Thesis

Ihueze, C.C. (2005) Optimum Buckling Response Model of GRP Composites. Ph.D. Thesis, University of Nigeria, Nsukka.

Journal

Umerie, S.C., Ogbuagu, A.S., Ogbuagu, J.O. (2004) Stabilisation of palm oils by using Ficusexasprata leaves in local processing methods. *Bioresources Technology*, 94: 307-310.

Conference

Menkiti, M.C., Ugodulunwa, F.X.O., Onukwuli, O.D. (2007) studies on the coagulation and flocculation of coal washery effluent. *Proceedings of the 37th annual conference of the Nigerian Society of Chemical Engineers*, Enugu, 22-24 November, pp169-184.

ix. **Illustrations**: All figures whether line drawings, graphs or photographs should be given a figure number be Arabic numeral in ascending order as reference is first made to them in the text (e.g. Fig. 1). Tables are to be similarly numbered. Captions of figures should be below the respective figures while captions of table should be above the respective tables. The measured quantity with the units, usually in brackets, and the numerical scale should be given alongside the ordinate and abscissa of every graph. All illustrations including chemical structures should be placed in the appropriate places within the text.

x. **Submission of Manuscript**: Manuscript should be submitted to the Editor-in-Chief via pineditor2017@gmail.com.

xi. Manuscripts are considered for acceptance on the understanding that the work described is original and have not been published or submitted for consideration elsewhere and that the author has obtained necessary authorization for publication of the material submitted. Submission of a multi-authored manuscript implies the consent of all the participating authors. A processing fee of N3, 000.00 (Three thousand naira only) is charged per manuscript. Make payment to PIN National Account, Polymer Institute of Nigeria account number **0006664735** at Union Bank Plc. A publication fee for accepted manuscript of **NGN10, 000.00** (Ten Thousand Naira) is charged and should be remitted to Polymer Institute of Nigerian Account number **0006664735** at Union Bank Plc.

xii. **Copyright**: By submitting a manuscript, the authors agree that the copyright for the article is transferred to the Polymer Institute of Nigeria, if and when the article is accepted for publication.

xiii. **Disposal of Material**: Once published, all copies of the manuscript and correspondence will be held for three months before disposal. Authors must contact the Technical secretary if they wish to have any material returned

Contents

Nigerian Journal of Polymer Science and Technology, 2019, Vol. 14, pp1-8

Received: 12/07/2018 Accepted: 14 August, 2019

EFFECT OF CARBONIZATION TEMPERATURE ON THE REINFORCEMENT PROPERTIES OF GROUND RICE HUSK USED AS FILLER IN NATURAL RUBBER VULCANIZATE

M. O. Ihuezor*, U. K. Ehigiator, A. O. Imasuen, F. Inegbedion

Department of Polymer Technology, Auchi Polytechnic, Auchi Edo State Nigeria

*Corresponding author: ihuezormervyn@gmail.com

Abstract

The production of fillers from local agricultural wastes (rice hulls) is one of the most viable ways of transforming agricultural wastes to valuable materials. Moreover, the effect of carbonization temperature on the reinforcement properties of ground rice husk in natural rubber vulcanizate was studied. Rice hulk carbonized at specific temperatures "300^{o}C, 400^{o}C, 500^{o}C, 600^{o}C, 700^{o}C and 800^{o}C and ground to fine particles were incorporated into natural rubber using standard method. Cured test pieces were obtained and subjected to hardness test, abrasion resistance test and tensile strength test. The carbon black obtained from rice husk at carbonization temperature of 600^{0}C gave the highest reinforcement properties: hardness 67 IRHD, abrasion resistance 58.5%, tensile strength 11.0MPa, elongation at break 892.5% and elastic modulus 1.9MPa. These values were closely followed by those of 700^{0}C.

Keywords: Natural rubber, Rubber filler, Rice husk, Carbonization, Reinforcement.

1.0 Introduction

In recent time there is growing interest in producing rubber based products (such as shoe sole, door mats, etc) using agricultural wastes such as rice husk as fillers (Ajay, 2012). Rice husks are amongst the most widely available agricultural wastes in many rice producing countries around the world. The milling generates a waste material - the husk surrounding the dried rice paddy. Globally, approximately 600 million tons of rice paddies are produced annually. This makes rice husks one of the largest readily available but also one of the most under-utilized resources, on an average 20% of the rice paddy is husks, giving an annual total production of 120 millions tons (http:/crentionism org). Rice husks have very low nutritional value and as they take very long to decompose are not appropriate for composite or manure.

Rice husks removed during rice refining create disposal problem due to less commercial interest. Also handling and transportation of rice husk is problematic due to its low bulk density. Therefore the 600 million tons of rice produced globally constitute environmental pollution if not disposed off properly. The global environment awareness has led to research ways of an effective utilization of rice by-product (husk) (Giddel and Jivan, 2007). One of such ways is the carbonization of rice husk at various temperatures 300^{o}C, 400^{o}C, 500^{o}C, 600^{o}C, 700^{o}C and 800^{o}C,

and its utilization as filler in rubber vulcanizate. It revealed how best carbon black form of rice husks can be effectively utilized as fillers for industrial manufacturing operations such as shoe sole production. However, the hydrated silica in the rice husks undergoes structural transformations depending on the carbonization temperature.

Carbonization is the conversion of an organic substance into carbon or a carbon-containing residue through pyrolysis or destructive distillation (McNaught and Wilkinson, 1997). It is considered as a complex process in which many reactions take place concurrently such as dehydrogenation, condensation, hydrogen transfer and isomerization and residual content of foreign element. Rice husk undergoes this process in a carbonizing furnace to obtain its carbon black state or form (Francis, 2011 and Eguaikhide,2013). Carbon black is derived from petrochemical sources but the unstable price of crude oil has led to the search for filler that are derived from other sources (Ski,1970). Several attempts have been made to use rice husk ash (RHA) as filler for natural and synthetic rubbers. Most of them indicated that RHA is moderately reinforcing fillers, in that the reinforcing effect is not as good as silica and carbon black but is better than talcum, clay or calcium carbonate ($CaCO_3$) (Sae-Oui, et al, 2002; Arayapranee, et al,2005). Haxo and Mehta (1975) revealed the possibility of using ground RHA obtained by a special burning condition as moderately reinforcing filler for natural rubber (NR).The influences of RHA incorporation on mechanical properties and fatigue behavior of epoxidized natural rubber (ENR) were also investigated. It was found that rice husk ash (RHA) has potential as Semi-reinforcing filler for ENR vulcanizates (Ishak and Bakari, 1995; Ishak, et al 1997). In this study, the potential of carbonized rice husk were assessed for use in natural rubber vulcanizates.

2.0 Materials and Methods

2.1 Materials

Rice husks were obtained from a local rice mill in Auchi town, Edo state. The rice husks were air-dried and carbonized at different fixed temperatures viz: 300^{o}C, 400^{o}C, 500^{o}C, 600^{o}C, 700^{o}C and 800^{o}C. The carbonized rice husks were ground into fine particulate powder, passed through sieve of mesh size 100 micrometer and stored in clean, dry and transparent polyethylene sack.

2.1.1 Sources of Other Materials

The natural rubber (NSR-10) used as the base polymer was purchased from Rubber Research institute of Nigeria (RRIN), Iyanomo, Edo State. The remaining compounding additives such as zinc oxide, stearic acid, 1,2-dihydro -2,2,4-Trimethyl quinoline (TMQ), N-Isopropyl N-phenyl – para-phenylene diamine (IPPD), mercantobenzothiazyl disulphide (MBTS), Tetramethyl thiuram disulphide (TMTD), Sulphur and processing oil were sourced commercially and used as supplied.

Table 1: The Formulation

Additives	Parts Per Hundred Rubber
Natural Rubber	100
Filler (CRH*)	50.0
Stearic Acid	2.0
Zinc Oxide	5.0
TM Q	1.0
IPPD	0.5
TMTD	1.5
MBTS	1.50
Processing oil	5.00
Sulphur	2.00

Carbonized Rice Husk (CRH*) -300 ^{0}C, 400 ^{0}C, 500 ^{0}C, 600 ^{0}C, 700 ^{0}C and 800 ^{0}0C

2.2 Compounding and Vulcanization

The additives were incorporated into the polymer using formulation based on parts by weight (PBW). The compounding was done on a water cooled Laboratory two-roll mill size (180 x 360mm) in accordance with ASTM-D3182. The mill was kept at maximum temperature of about 70^{o}C, so as to avoid scorching of the mix (http:/rubbertech.word press.com). Moreover, fillers used were based on the individual carbonization temperature 300^{o}C, 400^{o}C, 500^{o}C, 600^{o}C, 700^{o}C and 800^{o}C of the rice husks, hence six (6) formulations. The sheet rubber compound was allowed for maturation at room temperature for 24hours.

Vulcanization of the compounded rubber mixes were carried out using an electrically heated and hydraulically operated compression moulding machine in accordance to ASTM-D1632-09. Cure temperature of 150^{o}C at 15 minutes were selected for vulcanizing the test pieces..

2.2.1 Assessment of Vulcanizates Properties

Some mechanical properties such as hardness and tensile properties (tensile strength, elongation break, elastic modulus were determined using American society for testing and materials (ASTM) and German Institute for Standardization methods. ASTM-D1415 (1983) was used for hardness and DIN 53504 -05 (1994) for tensile properties. The abrasion resistance was determined using the British Standards Institute testing method BS 903 Part A4.

3.0 Results and Discussion

Table 2: Mechanical properties of rubber vulcanizates

MECHANICAL PROPERTIES	TEMPERATURES					
	300^0C	400^0C	500^0C	600^0C	700^0C	800^0C
Hardness IRHD	60	61	63	67	65	64
Abrasion Resistance index (%)	7.1	14.2	23.1	58.5	55.5	45.3
Tensile strength (MPa)	3.0	4.3	5.6	11.0	10.9	5.1
Elongation at break (%)	157.0	344.8	375.1	892.5	714.7	382.3
Modulus of elasticity (MPa)	2.3	2.0	1. 9	1.9	1.9	1.8

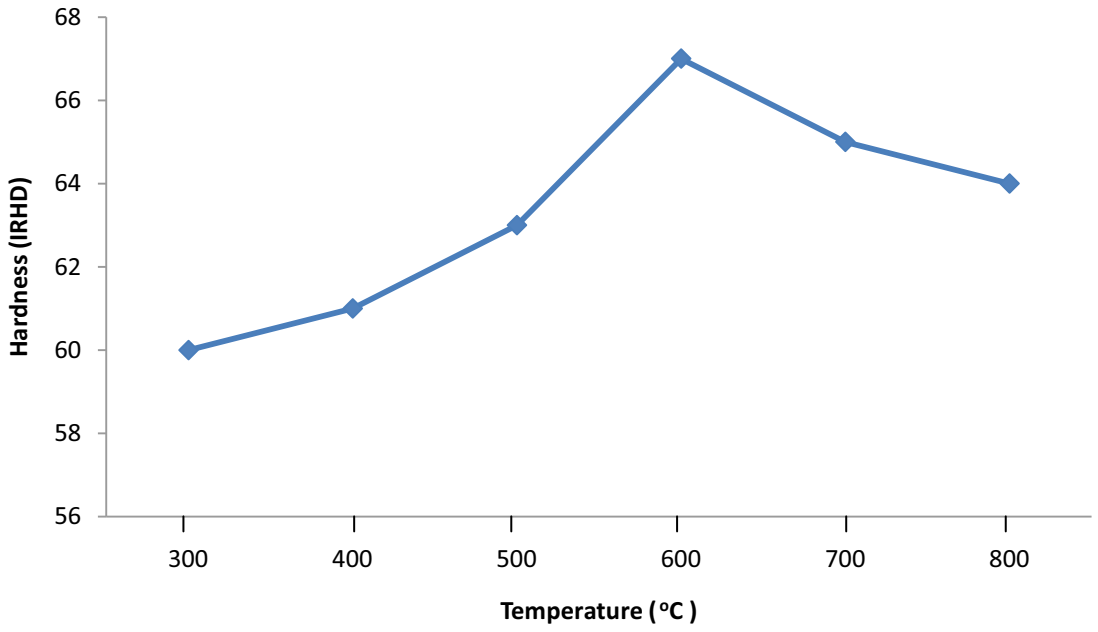

Figure 1: Plot of hardness-temperature curve of carbonized rice husk filled natural rubber vulcanizates

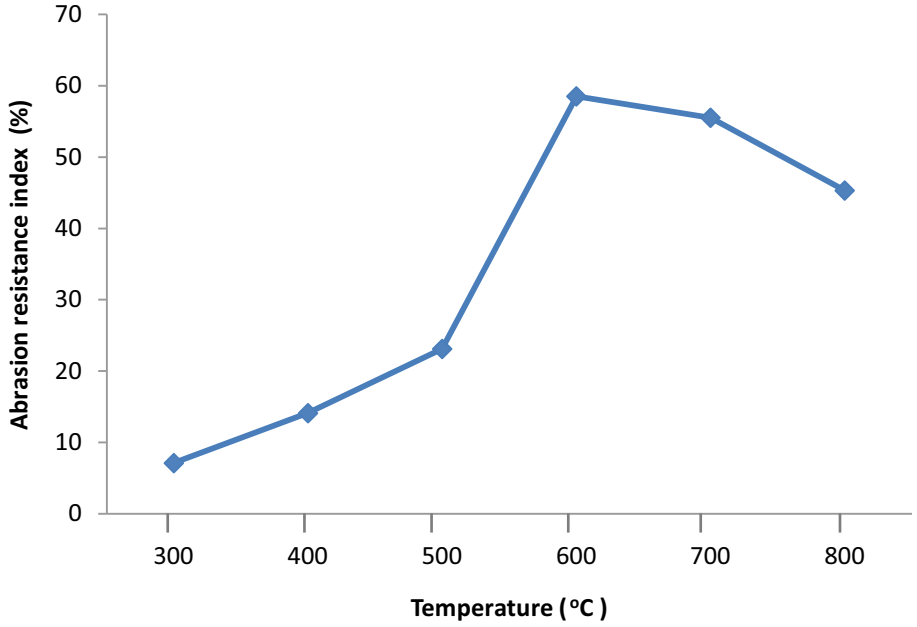

Figure 2: Plot of abrasion resistance – temperature curve of carbonized rice husk filled natural rubber vulcanizates

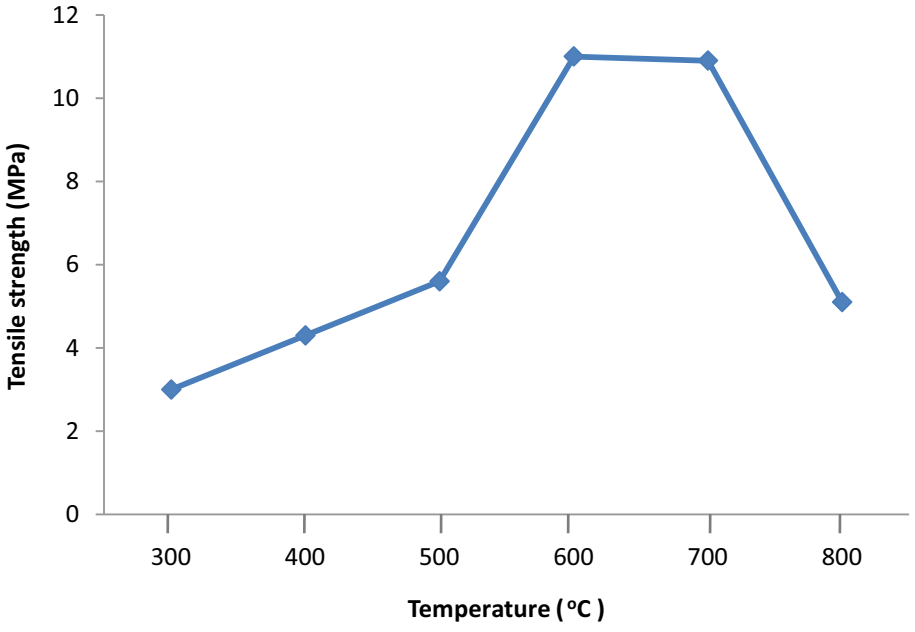

Figure 3: Plot of tensile strength – temperature curve of carbonized rice husk filled natural rubber vulcanizates

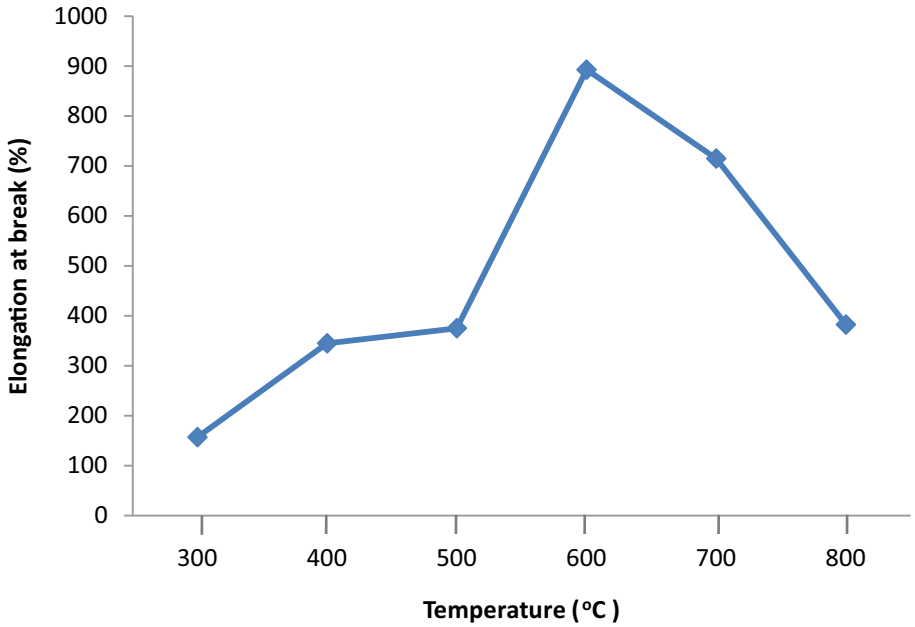

Figure 4: Plot of elongation at break – temperature curve of carbonized rice husk filled natural rubber vulcanizates

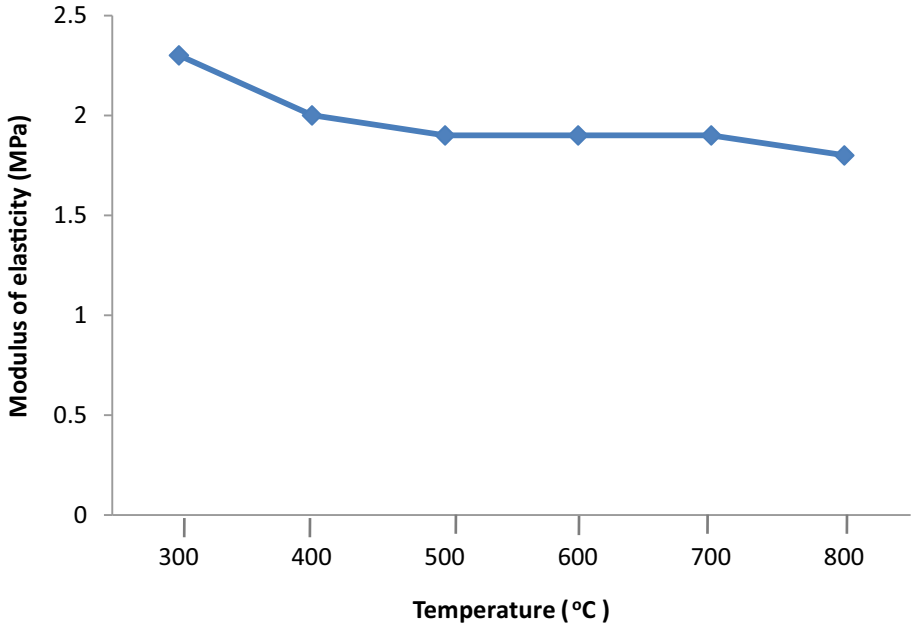

Figure 5: Plot of modulus of elasticity – temperature curve of carbonized rice husk filled natural rubber vulcanizates.

The hardness of the rubber vulcanizate was at its peak on carbonization temperature of 600°C as shown in figure 1 above. This result shows the highest level of carbon content conversion and degeneration of the opaline silica (Si_2O_4. $2H_2O$) (Mitani, et al, 2005) present in the rice husk to silicon (iv) oxide (S_iO_2). Carbon black is a well known mineral filler which possesses high level of reinforcement potentials (Blow and Hepburn,1982)

In figures 2, 3 and 4 above, the results for abrasion resistance, tensile strength and elongation at break (% EAB) of the natural rubber vulcanizates filled with carbonized rice husk filler were also at their peak at the carbonization temperature of 600^{o}C respectively. These were closely followed by 700^{o}C carbonization temperature. It is a well known fact that silica (S_iO_2) is a non-black reinforcing filler. After the degeneration of opaline silica which occur in hydrated form (S_{i2} $O_4.2H_2O$) to yield silicon (iv) oxide or silica as otherwise called, S_iO_2, posed or imparted some reinforcement properties to the natural rubber vulcanizate. Hence, the results obtained at carbonization temperature of 700^{o}C were of higher values compared to those of $\leq$ 500^{o}C. The result on modulus of elasticity at 100% strain shown in figure 5 revealed a progressive decrease in modulii as carbonization temperatures were increased up to 500^{o}C. The modulii remain constant at carbonization temperature range 500^{o}C to 700^{o}C and the least modulus value was obtained at 800^{o}C. Carbonized rice husk consist of carbon black, silica and lots of metal oxide such as calcium oxide (CaO), magnesium oxide (MgO,) ferrous oxides (Fe_2 O_3) etc. Sarkawi and Aziz (2007) revealed that silica-filled (VN3) natural rubber vulcanizates have lower modulii at 100% strain compared to those filled with ground rice husk powder (180 mirco meter) and carbon-black filler (N330). Carbonization process leads to increased silica content and reduction in organo-cellulose material present in carbonized rice husk filler. Hence lesser modulii at higher carbonization temperatures were recorded for carbonized rice husk-filled natural rubber vulcanizates.

4.0 CONCLUSION

The results obtained above show that the best carbonization temperature for rice husk should be at 600^{o}C . There was a clear indication that among all the carbonized fillers used, ground rice husk filler carbonized at 600^{0}C gave the optimum values. This observation might be due to increase in surface area which leads to more interaction between the filler and the rubber matrix. Thus, it should have a high potential for being utilized as such, especially when coupled with the fact that it is cheap as well as renewable. Its use could resolve the agricultural problem and environmental issues effectively.

REFERENCES

Ajay, K. (2012). Properties and industrial application of rice husk : a review. International Journal of Emerging Technology and Advanced Engineering (IJETAE) ISSN 225-2459. Vol.2 pp 240 - 248.

Arayapranee, W., Na-Ranong, N. and Rempel, G.L.(2005). Application of rice husk ash as filler in the natural rubber industry, Journal of Applied Polymer Science. 98:34-41

ASTM D1415 (1983). Method for testing hardness of rubber vulcanisate. American Society for Testing and Materials International.

Blow, C.M. and Hepburn,C.(1982). Rubber Technology and Manufacture. Second edition, Butterworth Scientific, London.pp 35-37, 270-271

Din 53504-05 (1994). Testing of rubber and elastomer. Determination of tensile stress-strain properties. The German Institute for Standardization.

Eguaikhide , A. (2013). Rheological and mechanical properties of natural rubber compounds filled with carbonized palm kernel husk and carbon black (N-330). Science Journal of chemistry. vol.1. Pp 50-55

Francis, U.O (2011). Effect of

carbonization temperature on wear rate behaviour of rice husk ash reinforced epoxy composites. Journal of Science and Technologies. ISSN-1583-1078, Pp172-182.

Giddel, M.R. and Jivan, A.P. (2007). Waste to wealth potential of rice husk in India: a literature review. International conference on clear technologies and environment management, PEC, Pondichery. India. January 4-5.

Haxo, H.E and Mehta, P.K.(1975). Ground rice-hull ash as a filler for rubber. Rubber Chemistry and technology, 48(2):271-288.

http:/crentionism org. Doheny scientific expedition, Havasupai canyon, Arisona.

Ishak, Z.A.M and Bakar A.A.(1995). An investigation on the potential of rice husk ash as fillers for epoxidized natural rubber (ENR), European Polymer Journal 31(3):259-269

Ishak,Z.A.M., Bakar, A. A.,Ishiaku, U.S., Hashim, A.S and Azahari, B.(1997). An investigation of the potential of rice husk ash as a filler for epoxidized natural rubber-ii.Fatigue behaviour. European Polymer Journal 33(1): 73-79

McNaught, A.D. and Wilkinson, A. (1997). IUPAC Compendium of Chemical Terminology. 2nd ed. Blackwell Scientific Publication. Oxford. pp 172-175.

Mitani, N; Ma, J.F. and Iwashita, T. (2005). Identification of the silicon form in xylem sap of rice (oriza sativa). Plant Cell Physiology. 46:279-283.

Sae-Oui, P., Rakdee, C. and Thanmathorn (2002). Use of rice husk ash as filler in natural rubber vulcanizates: In comparison with other commercial Fillers, Journal of Applied Polymer Science, 83: 2485 – 2493.

Sarkawi S.S and Aziz, Y (2007). Ground rice husk as filler in rubber compound. JTMKHA 539A (Babi 13). Pmd. Pp 136-147.

Nigerian Journal of Polymer Science and Technology, 2019, Vol. 14, pp9-21

Received: 03/07/2019 Accepted: 26 September, 2019

KINETICS AND THERMODYNAMIC STUDIES ON THE PRODUCTION OF BIODIESEL FROM *Balanites Aegyptiaca* OIL USING ITS SHELL AS CO-CATALYST

Disho H.[1*], Peter M. D.[1] and Susan P. A.[2]

[1] *Department of Chemistry, School of Physical Sciences, Modibbo Adama University of Technology, Yola, Adamawa State, Nigeria*
[2] *Department of Science Laboratory Technology, Adamawa State Polytechnic, Yola, Nigeria*
[*]Corresponding author : dishonihaggai@yahoo.com, +2348058008832

Abstract

Kinetics and thermodynamic studies on the production of biodiesel from Balanites aegyptiaca oil using its shell as co-catalyst was carried out by trans-esterification of the oil with methanol. First the oil was extracted from the seed kernel of Balanites aegyptiaca using a mechanical extractor. The waste fruit shell of the Balanites aegyptiaca was subjected to carbonization process to generate activated carbon which was used as co-catalyst for the trans-esterification to produce the biodiesel. The effects of temperature, time of stirring, ratio of volumes of the reactants, and concentration of the catalyst on the yield of biodiesel were monitored and recorded. The optimum values of the results obtained were used to determine the values of the kinetic and thermodynamic parameters governing the biodiesel production. The biodiesel yield obtained was 72.5%. The kinetic data obtained for the forward reaction could not fit the differential rate law for any of the orders of reaction investigated, but data for the reverse reaction, obtained by mirror-imaging of the forward reaction, followed second order kinetics with rate constant $\boldsymbol{k = 0.017239 cm^3/min}$ *at* $\boldsymbol{303K}$*. The change in entropy,* $\boldsymbol{\Delta S = 62.4JK^{-1}}$*, heat of reaction,* $\boldsymbol{\Delta H = 29{,}207Jmol^{-1}}$ *and energy of activation,* $\boldsymbol{E_a = 29{,}207Jmol^{-1}}$*. The positive value of the* ΔH *showed the reaction to be endothermic, taking in heat from the surrounding, and due to the large value of the* E_a *the reaction could not have occurred without the catalyst. It is recommended that further research be carried out to find the reaction order for the forward reaction of the trans-esterification and not finalize conclusion on the order of reaction obtained by mirror image of the process.*

Keywords: *Balanites Aegyptiaca, biodiesel, catalyst, seed oil, vegetable oil*

1.0 Introduction

The use of vegetable oils for engine fuel seemed insignificant in the past, but in the course of time such oils have been becoming as important as fossil fuel products. In fact they are becoming more important than fossil fuel products for the reasons that they are renewable energy resources and pose no environmental hazards compared to fossil fuels, the shortage of which has been predicted in addition to the environmental concerns they pose. The above issues are attracting significant attention to scientific and technological research concerning conversion of biomass into biofuels to replace fossil fuel. An important step to achieve this is the trans-esterification of vegetable oils. But if the use of vegetable oil as fuel for engines is to compete with its consumption as food then the problem is not really solved. Therefore it becomes necessary to seek for feedstocks which are considered as waste and non-edible by man and animals and convert them to forms that will be of advantage technologically. The shell of *Balanites aegyptiaca* fruit is thrown away as waste, and the oil extracted from its nut is not so much edible, especially in Northern Nigeria. It is therefore reasoned that carbonization of the fruit shell of the desert date tree can produce a catalyst to optimize the trans-esterification reaction between oil extracted from the *Balanites aegyptiaca* fruit kernel and methanol for biodiesel production. Many research works on acid and base-catalyzed trans-esterification of vegetable oils exist, but virtually little or no work is done on its catalysis by activated carbon from waste fruit shells. While the general features of the reaction mechanism of acid and base-catalyzed trans-esterification are well known, not many studies have been directed towards a better understanding of the principles and parameters governing the kinetics and thermodynamics of the trans-esterification of vegetable oils, which is instrumental in improving the commercial performance of the process. An accurate analysis of kinetic and thermodynamic data on the trans-esterification process can be very helpful for process optimization. The trans-esterification of vegetable oil is a complex process; the reaction rate and equilibrium yields are affected by numerous chemical and physical factors. Vegetable oil is composed from over 100 substances, and different oils have different compositions that can vary even for the same oil. The thermodynamic and kinetic details and models describing the processes can be drastically dependent on these factors and some other reaction parameters, such as the nature of the solvent, catalyst, and substrate (Arumugam *et al*., 2009) as well as temperature.

2.0 Materials and Methods

2.1 Sample collection: Desert date (*Balanites aegyptiaca*) fruits were purchased from the local markets in Adamawa State. The fruits were sorted to remove those with defects and unwanted materials and contaminants. The sorted fruits were tied in sacks and pounded to remove the exocarp (epicarp). The fruits now stripped of the exocarp were soaked in water for 24 hours, so that the mesocarp got softened, after which it was washed off by scrubbing and rinsing with clean water. The cleaned wet nuts were dried in the sun for 12 hours.

***2.2 Pre-treatment of raw materials*:** The pericarp or shell of the cleaned *Balanites aegytiaca* nuts were cracked with pebble, split open and the kernels removed. The kernels were put in clean polythene bags, sealed and kept ready for extraction of the *Balanites aegytiaca* oil. The shells were sorted and any unwanted parts and contaminants discarded. The sorted shells were washed and rinsed with distilled water repeatedly. The washed shells were sun-dried for two days and then crushed to small particle sizes in metal mortar and pestle. This pre-treated shell was kept in a stoppered sample container ready for carbonization and

activation processes. The kernels or the contents of the nut were packed together and kept in clean polythene bags for extraction of the oil.

2.3 Carbonization (physical activation) of Balanites aegyptiaca shell: Carbonization, otherwise known as physical activation or pyrolysis of carbonaceous substances was carried out according to the method used by Abdul *et al.* (2008). The pre-treated *Balanites aegyptiaca* shell was placed in a crucible and carbonized at the standard temperature for the carbonization of the plant fruit shell (300 - 1000^{o}C) for an activation duration of 2 hours. During the carbonization it was ensured that little or no oxygen was allowed to penetrate the sample, which otherwise would allow it to burst into flames and burn away into ash. The absence of oxygen forced the *Balanites aegyptiaca* shell material to decompose into various substances, the main of which is a black porous solid consisting mainly of elemental carbon. At the end of 2 hours the sample was left to cool down to room temperature in a desiccator. It was then removed, ground, sieved with a 300mm sieve and stored in an air-tight bottle which was labelled as AC (activated carbon). This activated carbon was used as catalyst for trans-esterification of *Balanites aegyptiaca* oil to generate biodiesel.

***2.4 Extraction of oil from Balanites aegyptiaca seed*:** The kernels of the *Balanites aegyptiaca* seeds were spread on heated coarse sand in a pan, and briskly and continuously were turned round and round until they were lightly fried. The fried kernels were shaken and gathered together, and then separated from the sand in a tray. They were allowed to cool down. The cooled kernels were gently rubbed with the palm in the tray to remove any burned parts. Unwanted parts were either hand-picked or blown away. The cleaned kernels were weighed and subjected to cold-pressed extraction using a mechanical extractor or presser to obtain clean oil.

2.5 Determination of free fatty acid in Balanites aegyptiaca oil: For the determination of the free fatty acid in the *Balanites aegyptiaca* oil that was extracted, the titration method described by (Mahesar *et al.,* 2014) was used. 0.7g of the oil was dissolved in 20cm^3 of diethylether/ethanol (1/1, v/v) and titrated against 0.1 M solution of KOH that was prepared in ethanol.

2.6 Biodiesel production from Balanites aegyptiaca seed oil: Single stage step by step trans-esterification was used in the production of biodiesel catalyzed first by the heterogeneous catalyst of CaO, then by the physically activated carbon from the *Balanites aegyptiaca* shell, and finally by both of them combined as co-catalyst.

***2.7 Determination of kinetic parameters of the trans-esterification*:** The reaction time or time of stirring, *t* to form the volume of biodiesel, V_{BD}, at a given temperature, T was determined using a stop-clock. From the stoichiometric equation of the reaction:

$$TG(l) + 3MeOH(l) \rightleftharpoons glycerol(l) + BD(l),$$

the rate of the reaction (taken as rate of formation of biodiesel), r was evaluated as

$$r = d\,V_{BD}/dt = k(V_{TG})^{x}\,(V_{MeOH})^{y}$$

where V_{BD} is volume of biodiesel formed; V_{TG} is the volume of the triglyceride or vegetable oil (*B. aegyptiaca* oil) and V_{MeOH} is the volume of methanol that were used up to form the volume of biodiesel, V_{BD} in time t; k is the rate coefficient of the reaction; x and y are the orders of the reaction with respect to the vegetable oil (triglyceride) and methanol (MeOH) respectively. Since the reaction between a biolipid (fat or oil or vegetable oil) and alcohol is always a reversible reaction, the alcohol was added in excess to ensure

complete conversion. A number of runs of the reaction at constant temperature, T and varying volume of vegetable oil, V_{TG} to yield a corresponding volume of biodiesel, $V_{BD,}$ at excess volume of methanol, V_{MeOH} using the ultimate time, t permitted the calculation of the values of the rate constant k, partial order of reaction x with respect to V_{TG}, and y with respect to V_{MeOH} algebraically. The values of x, y and k for the trans-esterification were experimentally determined by employing two experimental situations. The first situation is the one in which the volume of the vegetable oil was varied while the volume of the alcohol was kept constant. The second situation is the reverse of the case above in which the volume of the alcohol was varied while the volume of the vegetable oil was kept constant. In each of these situations the optimum values of temperature, catalyst and time of stirring were used.

2.8 Determination of thermodynamic parameters of trans-esterification for biodiesel production: Since trans-esterification is a reversible reaction, at equilibrium the free energy, ΔG = 0. But the free energy of activation E_a was calculated using Arrhenius equation $k = Aexp(-E_a/RT)$. Rate constants k, were calculated as the slopes of the kinetic graphs of production of biodiesel $V_{BD}^{-1} = kt$ at temperatures T = 25°C (298K), 30°C (303K) and 40°C (313K), in Figures 2, 3 and 4.

To determine the ΔH and ΔS of the trans-esterification, the equation

$\Delta G = \Delta G^o + RT\ ln\ (k)$ was used, where, ΔG is Gibb's free energy at non-standard states, and ΔG^o is Gibb's free energy at standard states. But since ΔG = 0 for systems at equilibrium $\Delta G^o = -\ RT\ ln\ (k)$.

Using $\Delta G^o = \Delta H^o - T\Delta S^o$

at non-standard states it becomes

$$\Delta H - T\Delta S = -\ RT\ ln\ (k)$$

$$ln\ (k) = \frac{-\Delta H + T\Delta S}{RT} = \frac{-\Delta H}{RT} + \frac{\Delta S}{R}.$$

Relating this equation to the graph of *ln(k)* vs *1/T* in Figure 6, $\frac{-\Delta H}{R}$ is the slope, *m* and $\frac{\Delta S}{R}$ is the intercept *b* on the *ln(k)* axis. From the slope, *m* and the intercept *b*, Δ*H* and Δ*S* were calculated respectively.

3.0 Results and Discussion

3.1 Free fatty acid in Balanites aegyptiaca oil: The result of the titration showed that about 9% of the oil used was free fatty acid. This meant that along with the biodiesel and glycerol that was produced as products there were by-products of water and soap. So the percentage of biodiesel obtained could not have been as it should when the oil has zero free fatty acid. This added to the difficulty, (as also reported by Freedman *et. al.,* 2007) encountered in trying to separate any unused oil left in the lower layer that settled from the post reaction mixture at the bottom of the separating funnel. It was even more difficult when the amount of oil left was small. This difficulty and shortage of equipment for delicate separation of the constituents of the lower layer informed the researcher to adopt the method of measuring the rate of the reaction by the formation of biodiesel (formed as a clear upper layer in the separating funnel) instead of the rate of consumption of the vegetable oil in the trans-esterification.

3.2 Yield of Biodiesel in its production from Balanites aegyptiaca seed oil: The yields of biodiesel in different runs using varying catalyst concentrations and time of stirring, temperature, quantitative proportion of vegetable oil to alcohol, varying volumes of vegetable oil and varying volumes of methanol are presented on Tables in Appendices I, II, III, IV, and V.

***3.3 Effect of catalyst concentration on Biodiesel yield*:** The catalyst employed for the trans-esterification was either CaO, the activated carbon from the *Balanites aegyptiaca* shell or the combination of the two as co-catalyst. From the results on Table in Appendix I it is observed that the maximum yield of biodiesel obtained was when the concentration of the catalyst was 0.3g for any of catalysts CaO, C-act and CaO/C-act. There was not much difference in the yield of biodiesel when CaO, C-act or CaO/C-act was used.

***3.4 Effect of time of stirring on biodiesel yield*:** The table in Appendix I showed that time of stirring ranged between 15-30 minutes. But within 15 minutes of stirring, the trans-esterification was completed. This timing of course corresponded to the quantities of the reactants used. Higher quantities would definitely require longer time of stirring.

***3.5 Effect of temperature on biodiesel yield*:** This is presented on the table in Appendix II. The temperature range that was considered in this investigation was from 25 – 45^{o}C. At 30 ^{o}C high yield of biodiesel was obtained using 0.3g of either activated carbon (C-act) as catalyst or the co-catalyst (C-act/CaO). Higher yield of biodiesel was obtained at 40 - 45 ^{o}C, but the biodiesel appeared cloudy or milky. The increase in temperature must have caused some changes in the biodiesel. 25 ^{o}C gave a lower yield of biodiesel.

***3.6 Effect of quantitative proportions of Balanites aegyptiaca oil to methanol on Biodiesel production*:** The equation of reaction in trans-esterification of vegetable oils shows that the proportion of triglyceride to alcohol is 1:3. 30ml of methanol which weighed 23.3g was taken as reference point. One-third the mass of the ethanol should be the required mass of the oil, i.e. 7.77g to give complete reaction. This mass of the oil is equivalent to 8.3ml. The first part of the table in Appendix III shows volumes of biodiesel obtained using varying volumes of *Balanites aegyptiaca* oil with constant volume of methanol at 30^{o}C, using 0.3g of activated carbon as catalyst and 15 minutes run time.
8.3ml of the oil happened to give the highest yield of biodiesel when it was reacted with 30 ml of methanol. Additional volume of the oil seemed to give little difference.

3.7 Determination of kinetic parameters of trans-esterification:
The table in Appendix IV shows the volumes of biodiesel obtained when the amount of vegetable oil was varied while that of alcohol was kept constant and/or in excess, at T = 30^{o}C and relatively constant time of stirring. The corresponding volumes of biodiesel (V_{BD}), vegetable oil (V_{TG}) and methanol (V_{MeOH}) in the trans-esterification can be and are kinetically related by the rate equation:

$$r = d\ (V_{BD})/dt = k(V_{TG})^{x}\ (V_{MeOH})^{y}$$

This rate equation is the differential rate law for the kinetics of a reaction where two different substances react to form products. Normally the equation should have been

$$r = d\ [BD]/dt = k[TG]^{x}[MeOH]^{y}$$

when concentration of the species are used. But in this experiment, volumes have been used because the actual composition of *Balanites aegyptiaca* oil is not known and the definite triglyceride in the oil that reacted with methanol to form biodiesel is not known, talk less of its molecular formula or molecular mass. By using the data of volumes of the species (instead of their concentrations) in the reaction at a fixed temperature, the values of x, y and k were calculated. The volumes in each run of the experiment on the Table in Appendix IV were substituted into the rate equation to determine the partial orders of the reaction x and y with respect to vegetable oil and methanol, as well as the rate constant, k. By substitution of the experimental values on the Table in

Appendix IV into the last equation above for different runs and calculating algebraically, x was found to be one.
The value of x obtained as 1 means that the partial order of reaction with respect to the triglyceride as reactant is first-order. This means that the reaction rate is directly proportional to the concentration (or amount) of the triglyceride in the reaction.

With x = 1, y was found to be equal to zero. The value of y obtained as 0 means that the partial order of the reaction with respect to the methanol as reactant is zeroth-order. As zeroth-order it means the rate of the reaction was independent of the concentration (or amount) of the methanol as a reactant. This can be accepted to be true because the amount of the methanol was provided in excess, which has a consequence of being kept constant.

Using x = 1 and y = 0, the rate coefficient was calculated as k_1 = 0.2533ml/min.
These values of x = 1 and y = 0 indicate that under this condition, the reaction proceeded with first-order and zeroth-order with respect to the triglyceride and methanol respectively.

Hence, it can be seen that in the trans-esterification of *Balanites aegyptiaca* oil, the order with respect to methanol as a reactant is zeroth-order. One or both of the following two propositions can account for this. First the volume of methanol was provided in excess compared to the volume of the vegetable oil. If the amount of the methanol used is not significant compared to the unreacted amount left in the vessel, the reaction would tend toward zero-order. The second is that the volume of methanol was not only in excess, it has the implication of being kept constant, as if little or nothing was changing in it compared to the vegetable oil. The excess volume of methanol ensured complete conversion to products as it is the case with reversible reactions, of which the reaction between vegetable oil and alcohol is one.
On the other way round, when the volume of the vegetable oil (V_{TG}) was kept constant and the volume of methanol (V_{MeOH}) varied at T = 30°C, the result is as shown on the Table in Appendix V.

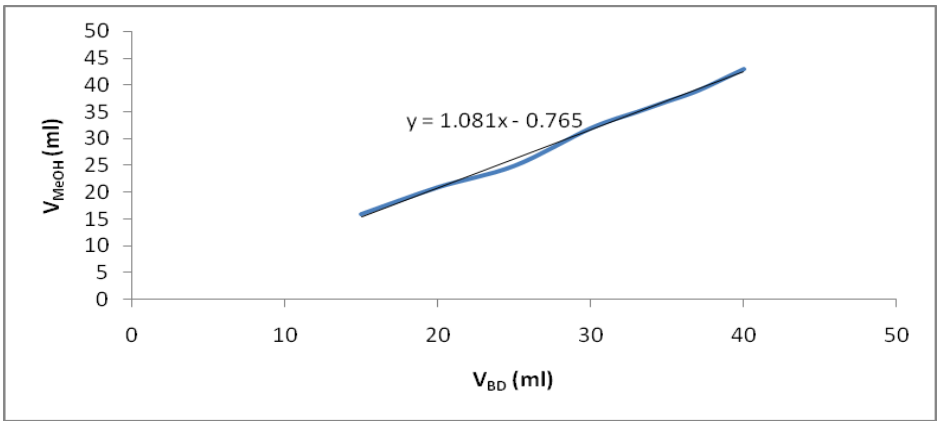

Figure 1: Graph of volume of biodiesel obtained against volume of methanol used.

On the Table in Appendix V, volume of triglyceride was kept constant and volume of methanol was varied throughout.

As before, using the rate equation,

$$r = d\,V_{BD}/dt = k(V_{TG})^x\,(V_{MeOH})^y$$

and substituting values obtained at the various experimental runs, y was found to be 1.

This shows that the reaction order with respect to methanol here is first-order. In this situation, keeping the volume of vegetable oil, $\mathbf{V_{TG}}$ constant (or in excess) and varying the volume of methanol V_{MeOH}, the order of the reaction y with respect to V_{MeOH} is first order. Zheng *et al*. (2006) showed that, in a large excess of methanol, the acid-catalyzed trans-esterification reaction of waste cooking oils is essentially a pseudo-first-order reaction. The excess of V_{TG} here implied that the order x with respect to the V_{TG} must be zero-order as earlier explained.

Substituting these values of x and y in any of the runs, gave $k_2 = 0.0707$ml/min.

Here, k_1 and k_2, though controlled by the same temperature, are not expected to be the same because different conditions were imposed in the two situations. The rate at which the trans-esterification could go in any of the situations was governed by the constraint placed on it. It can be shown there is some degree of agreement between the stoichiometric proportion of the reactants and the rate constants obtained in varying their amounts in the two cases above.

The ratio of triglyceride to methanol is triglyceride : methanol =1:3. So the relative rates must have been that the rate of consumption of the triglyceride must be three times that of methanol,.Hence,

$k_1 : k_2 = 0.2533$ml/min : 0.0707ml/min

Dividing the two values by the smaller one gives 0.2533ml/min :0.0707ml/min

$k_1 : k_2 =$ 0.0707ml/min : 0.0707ml/min

= 3.6:1 (giving room to experimental error of 20%)

***3.8 Determination of the overall order and the rate constant of the reaction*:** The overall order and the rate constant for the reaction were obtained from the combined effect of allowing the trans-esterification to occur freely. Time was the only independent variable that was monitored to get the corresponding volume of biodiesel produced. If no constraint were placed on any of the quantities of the reactants in the trans-esterification, such that the reaction was allowed to proceed in its natural course to completion and any limiting quantity was not externally imposed, the reaction would obey the rate law of the form $r = k[A][B]$

where $[A] = V_{TG}$ and $[B] = V_{MeOH}$ the volumes of the two reactants, k is the rate constant, and the overall order of the reaction would be second order.

Since the volume of triglyceride and volume of methanol initially were present in stoichiometric proportions (1:3), they must have remained so throughout the free reaction, i.e. $V_{TG}/V_{MeOH} = ⅓$ at any time t; [From: TG(*l*) + 3MeOH(*l*) glycerol(*l*) + BD(*l*)]. Focusing on the TG alone and considering the reaction to occur at second order, the rate of the reaction becomes

$r = -⅓dV_{TG}/dt = k(V_{TG})^2$ (i.e. the rate of use up of TG with time.)

But $-⅓dV_{TG}/dt = dV_{BD}/dt = k(V_{BD})^2$ (i.e. the rate of formation of BD is equal to ⅓ the rate of use up of TG with time.)

Experimentally it was easier to measure the rate of formation of biodiesel, $\mathbf{V_{BD}}$ than the rate of disappearance of vegetable oil, $\mathbf{V_{TG}}$. Therefore the rate law for the formation of biodiesel as a second order reaction would take the form:

$r = dV_{BD}/dt = k(V_{BD})^2$, and when we integrate, we have

$$\int (V_{BD})^{-2} dV_{BD} = k\int dt$$

$$V_{BD}^{-1} = -kt$$

This is the integrated rate law for a second order reaction. Experimentally it was established that 8.3ml of *Balanites aegyptiaca* oil required 30mls of ethanol to react completely in 15 minutes for the temperatures 25 - 40^{o}C. So to determine the kinetic parameters for the trans-esterification, the initial volume of

vegetable oil $\mathbf{V_{TG}}$ = 8.3ml, initial volume of methanol $\mathbf{V_{MeOH}}$ = 30mls and mass of catalyst **m-cat** = 0.3 were used to generate biodiesel. The volume of biodiesel $\mathbf{V_{BD}}$ formed at varying times **t** were recorded at three temperatures **T** = 25°C, **T** = 30°C and **T** = 40°C. The tables in Appendices VI, VIII, and X show the results.

But none of the set of values obtained at the three temperatures could fit into second order kinetic plot. Perhaps it was because the rate of the reaction was measured by monitoring the rate of formation of biodiesel instead of rate of consumption of vegetable oil. To get round the problem it was reasoned that since trans-esterification is a reversible reaction, the path followed by the forward reaction must be the path followed by the backward reaction. Therefore the corresponding values for the backward reaction were obtained by mirror-imaging. The results obtained are presented on Tables in Appendices VII, IX, and XI. Surprisingly the data obtained fit into the second order kinetic plot. The pairs of curves for both the forward and backward cases for the three temperatures are shown on Figures 2, 3 and 4.

t (min)	V_{BD} (ml)	V_{BD}* (ml)
0	0	
2	0.3	
5	15.8	
8	21.2	
10	23	
12	24.2	
15	25.3	

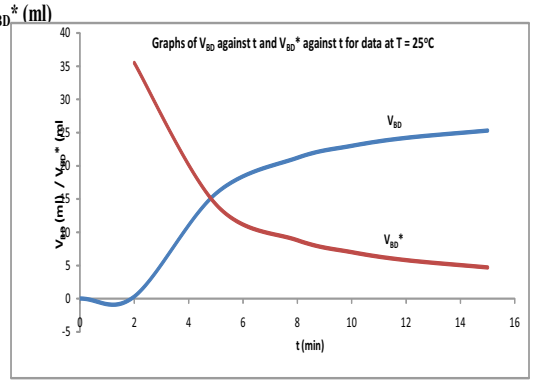

Figure 2: Graphs of volume of biodiesel for forward reaction ($\mathbf{V_{BD}}$) against time and volume of biodiesel for the backward reaction ($\mathbf{V_{BD}}$*) against time for data at **T** = 25°C.

t (min)	V_{BD} (ml)	V_{BD}* (ml)
0	0	
2	14	
5	20	
8	24	
10	25	
12	25.8	
15	26.3	

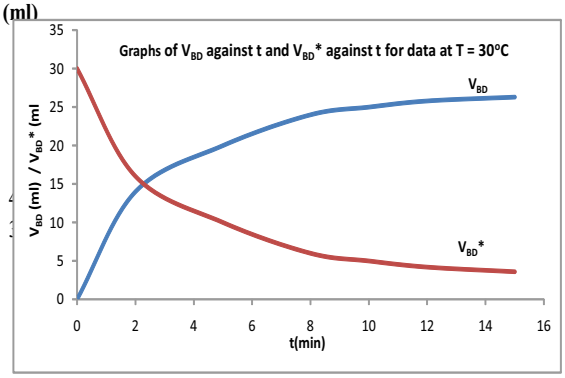

Figure 3: Graphs of volume of biodiesel for forward reaction (V_{BD}) against time and volume of biodiesel for the backward reaction (V_{BD}*) against time for data at **T** = 30°C

t (min)	V_{BD} (ml)	V_{BD}* (ml)
0	0	30.3
2	17.5	12.5
5	23.5	6.5
8	25.7	4.3
10	26.4	3.6
12	27	3

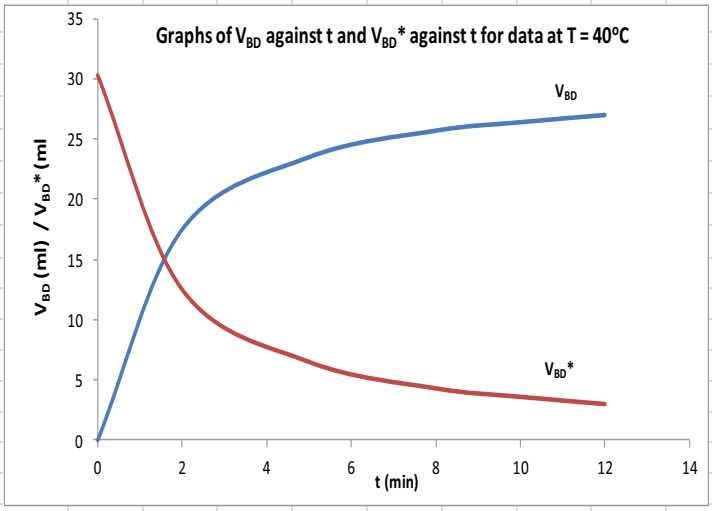

Figure 4: Graphs of volume of biodiesel for forward reaction (V_{BD}) against time and volume of biodiesel for the backward reaction (V_{BD}*) against time for data at **T** = 40°C

The data for the forward reactions for T = 25°C, 30°C and 40°C in Tables in Appendices VI, VIII, and X above could not fit into second order kinetic plots (V_{BD}^{-1} against **t**) but the ones for the backward reactions (V_{BD}*$^{-1}$ against **t**) in Tables in Appendices VII, X and XI did. These are shown in figure 5.

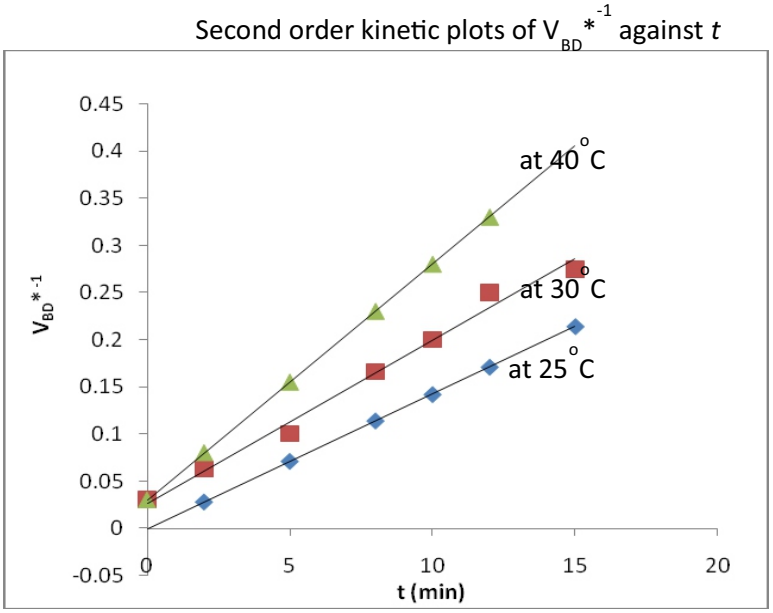

Figure 5: Second order kinetic plots of the reciprocal of volume of biodiesel for reverse reaction (V_{BD}*$^{-1}$) against time (**t**) for the production of biodiesel at temperatures of 25°C, 30°C and 40°C

The straight line plots obtained for the $\mathbf{V_{BD}}^{*-1}$ against **t** graphs show that the trans-esterification of *Balanites aegyptiaca* oil obeyed the second-order rate law. Darnoko *et al*. (2000) had carried out the kinetics of trans-esterification of palm oil and has reported that the conversion of triglycerides (TG) appeared to be second order up to 30 min of reaction time.

From the straight line graphs of $\mathbf{V_{BD}}^{*-1}$ vs **t** for temperatures of 25°C, 30°C and 40°C in figure 5, the rate constants were determined by taking the slopes of the straight lines (by least square method) as shown below. The values are presented on the table in Appendix XII. The rate constants k_1 and k_2 that were obtained for the separate experimental situations in section 3.7 at 30°C seem to have the following relationship with the rate constant, k for the overall reaction at 30°C.

k_1 = 0.2533ml/min; k_2 = 0.0707ml/min; k = 0.017239 ml/min.

$k = (k_2/ k_1)^3$

$0.017239 = (0.0707/0.2533)^3$

$0.017239 = 0.021744$

By rounding up to two decimal places we have $0.02 = 0.02$

Hence, k is the ratio of $(k_2$ *to* $k_1)$ raised to the power of three.

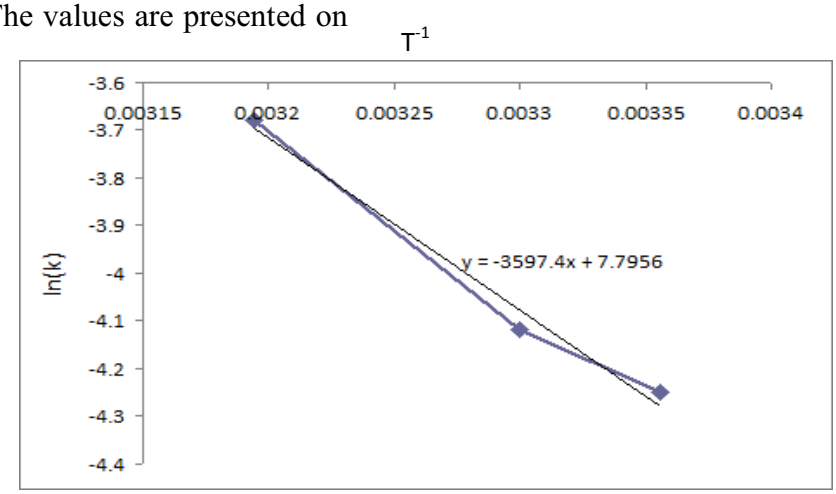

Plot of *ln(k)* vs *1/T*

Figure 6: Plot of logarithm of rate constant, *ln(k)* against inverse of temperature, *1/T*

3.12 Determination of thermodynamic parameters for the trans-esterification reaction for biodiesel production:

In determining the parameters of enthalpy (heat) of reaction, ΔH, entropy ΔS, and Gibb's free energy of activation, ΔG of trans-esterification of *Balanites aegyptiaca* oil, Arrhenius equation was used. $k = Aexp(-E_a/RT)$ … … *(1)*

where k is the rate constant, A is the Arrhenius pre-factor whose value depends on the reactants, and E_a is the activation energy of the reaction. By taking the logarithm of both sides of the equation, it gives

$ln(k) = -E_a/RT + ln(A)$ … … …*(2)*

This equation is linear when *ln(k)* is plotted against 1/T. k was determined for the varying temperatures (See table in Appendix XII). The plot of *ln(k) vs. 1/T* gave a straight line (see figure 6). The slope, $m = -E_a/R$ and the intercept $b = ln(A)$.

The slope m, and the intercept b on the *ln(k)* axis have been calculated using Least Square Method where

$$\sum_{i=1}^{n} (x_i - \overline{X})(\overline{y_i - Y})$$

$m = \frac{}{\sum_{i=1}^{n}(x_i - \overline{X})^2} = -3513\text{K}$, and

$b = \overline{Y} - m\overline{X} = 7.5$

x_i and y_i are the individual data for x-axis and y-axis respectively; X *and* Y are the means of the sets of data for x-axis and y-axis respectively.

The slope, m of the graph is $-E_a/R$ [From equation (2)] and from Figure 6

$m = -3513\text{K} = -E_a/R$

$E_a = 3513\text{K} \times R = 3513\text{K} \times 8.314\text{Jmol}^{-1}\text{K}^{-1}$

$= 29207\ \text{Jmol}^{-1}$

This is the energy of activation E_a, which also is the Gibbs free energy, ΔG. The positive and high value of it shows that the energy barrier between the reactants and the products was great, such that it was practically impossible to transform vegetable oil and ethanol to biodiesel without a catalyst for the reaction. The catalyst employed lowered the activation energy, so that the reaction began and proceeded to equilibrium where $\Delta G = 0$.

Also [From equation (2) and Figure 6], the intercept $b = ln(A) = 7.5$

$A = e^{7.5} = 1808$

A is Arrhenius factor, a constant whose value depends on the reactants of a reaction. Here 1808 is the value of A when *Balanites aegyptiaca* oil reacted with methanol.

To determine the ΔH and ΔS of the trans-esterification of *Balanites aegyptiaca* oil in biodiesel production, the equation

$\Delta G = \Delta G^o + RT\ ln\ (k)$ ... ...(3)

was used, where, ΔG is Gibb's free energy at non-standard states, and ΔG^o is Gibb's free energy at standard states. R is the universal gas constant. It functions here as a constant that relates energy to temperature in a reaction. Since trans-esterification is a reversible reaction, at equilibrium ΔG = 0

so $0 = \Delta G^o + RT\ ln\ (k)$

$\Delta G^o = -RT\ ln\ (k)$

But $\Delta G^o = \Delta H^o - T\Delta S^o$

Therefore, $\Delta H^o - T\Delta S^o = -RT\ ln\ (k)$.

At non-standard states it becomes

$$\Delta H - T\Delta S = -RT\ ln\ (k)$$

$$ln\ (k) = \frac{-\Delta H + T\Delta S}{RT} = \frac{-\Delta H}{RT} + \frac{\Delta S}{R}$$

Relating this equation to the graph of $ln(k)$ vs $1/T$, $\frac{-\Delta H}{R}$ is the slope, m and $\frac{\Delta S}{R}$ is the intercept b on the $ln(k)$ axis. Therefore, $\frac{-\Delta H}{R} = m = -3513\text{K}$ and $\Delta H = 3513\text{K} \times R = 3513\text{K}^{-1} \times 8.314\text{Jmol}^{-1}\text{K}^{-1} = 29{,}207\text{Jmol}^{-1}$ This value of ΔH shows that the trans-esterification is an endothermic reaction. It drew heat from the surrounding. The intercept, $b = \frac{\Delta S}{R}$. It is a constant that relates the change in entropy to the gas constant, giving.

$\Delta S = b \times R = 7.5 \times 8.314 = 62.4\text{JK}^{-1}$

This value of ΔS shows that the entropy increased by 62.4J per every rise in Kelvin during the trans-esterification.

4.0 Conclusion

Biodiesel was produced by trans-esterification of oil extracted from *Balanites aegyptiaca* seed, catalyzed by activated carbon which was generated from the fruit shell using carbonization by physical activation. In the course of the biodiesel production, the experimental values of temperature, time of stirring, volumes of reactants and products,

concentration of catalyst, ratios of quantities of materials were monitored and recorded. The optimum values of the results obtained were used to determine the values of the kinetic and thermodynamic parameters governing the biodiesel production from the seed oil. 30ml of methanol mixed with 0.3g of catalyst and 8.3ml of the oil and stirred for 15minutes at 30^{o}C yielded 28 ml of biodiesel. The generation of the biodiesel followed the partial first order kinetics for methanol and oil respectively, giving an overall second order for the process, with a rate constant of k = 0.017239ml/min at 30^{o}C. The activation energy of the process is E_a = 29,207Jmol^{-1}. The process is endothermic with ΔH = 29,207Jmol^{-1} and leads to increase in entropy with ΔS = 62.4JK^{-1}. It is recommended that FTIR and MS of *Balanites aegyptiaca* oil be carried out to know the specific triglyceride component that reacts with methanol to form the biodiesel. It is also recommended that further research be carried out to find out the reaction order for the forward reaction of the trans-esterification and not finalize conclusion on the order of reaction obtained by mirror image of the process.

Acknowledgement: Authors are grateful to Modibbo Adama University of Technology, Yola, Adamawa State - Nigeria for their financial support to the research work.

References

Abdul, R., Yacob, Z., Abdul, M., Ratna, S., Dewi, D., Vincinisvarri, I. (2008). "Comparison of various sources of high surface area activated carbon prepared by different activation." *The Malaysian Journal of Analytical Science.* 1(1), 12-16.

Arumugam, S., Kien Y. C., PaoloF.,Francis K., Sergey Z., and S. M. "Catalytic applications in the production of biodiesel from vegetable oils." *ChemSusChem* 2009, 2, 278 – 300.

Azcan, N., A. Danisman, "Alkali catalyzed transesterification of cottonseed oil by microwave irradiation," *Fuel*, Vol. 86, No. 17-18, 2007, pp. 2639-2644. *Fuel* 2008, 87, 1781.

Booth, H. E. "Charcoal production and Technology." FAO/ESCAP Regional Energy Development Programme. FAO, Rome 1983. http//www.fao.org/docrep

Chapagain, B. P., Yehoshua, Y. and Wiesman, Z. (2008). Desert date (*Balanites aegyptiaca*) as an arid land sustainable bioresource for biodiesel. *Journal of Bio-resource Technology.* (100)3, 1221-1226.

Corsini, A., Marchegiani, A., Rispoli. F., Sciulli, F. and Venturini, P. "Vegetable oils as fuels in diesel engine. Engine performance and emission." ScienceDirect. Energy Procedia 81 (2015) 942-949.

Darnoko, D, M. Cheryan, "Kinetics of palm oil transesterification in a batch reactor" *Journal of American Oil Chemical Society*. 2000, 77, 1263.

Davis, U.C. A Physical Chemistry Textbook/Supplementary modules. (http//www.chem.libretexts.org/Bookshelves), 1, 2019.

Freedman, B., E. H. Pryde, T. L. Mounts;"Variables affecting the yield of fatty esters from transesterified vegetable *oils." Journal of American Oil Chemists Society*. 2007, 61, 1638.

Freedman, B.; Kwolek, W.F.; Pryde, E.H. "Transesterification of soybean *oil"; Journal of the American Oil Chemical Society.* 2008, *62*, 663.

Freedman, B., R. O. Butterfield, E. H. Pryde, "Transesterification of soybean *oil."Journal of the American Oil Chemical Society*. 2009, 63, 1375.

Gao, Y. Y., C hen, W. W., Lei, H. W., Lin, X. Y. and Ruan, R. (2009). "Biodiesel processing and production via transesterification of tallow kernel oil." *Journal of Biomass and Bioenergy.* 32, 311-320

Komers, K., F. Skopal, R. Stloukal, J. Machek. "Kinetics and mechanism of the KOH-catalyzed methanolysis of rapeseed oil for biodiesel production." *European Journal of Lipid Science and Technology.* 2002, 104, 728.

Mahesar, S.A., S. T. H. Sherazi, Abdul Rauf Khaskheli, Aftab A. Kandhro. "Analytical approaches for free fatty acids assessment in oils and fats." *Analytical methods*, 2014, 6, 4956 – 4963.

Noureddini, H., D. Zhu. "Kinetics of transesterification of soybean oil." *J. Am. Oil Chem. Soc.* 2004, 74, 1457.

Sivasamy, A., Yoo C., Paolo F., Francis K., Sergey Z., and Stanislav M. (2009). "Catalytic applications in the production of biodiesel from vegetable oils." *ChemSusChem*, 2, 278 – 300.

Verla, A. W ., Horsfall, M (Jnr), Verla, E. N., Spiff, A. I., Ekpete, O. A., (2012). "Preparation and characterization of activated carbon from fluted pumpkin (*Telfairia accidentalis)* Hook. F seed shell." *Asian Journal of Natural and Applied Sciences*. 1(3), 39-50.

Zheng, S., Kates, M., Dube, M.A. *and* McLean, D.D., "Acid-catalyzed production of biodiesel from waste frying oil," *Biomass & Bioenergy*, *30*, *267*-272, Jan.*2006*.

Nigerian Journal of Polymer Science and Technology, 2019, Vol. 14, pp22-31

Received: 7/06/2019 Accepted: 07/07/2019

POLY MALTOSE ACRYLATE -GRAFT-ACRYLIC ACID HYDROGEL: A COPOLYMER WITH POTENTIAL APPLICATION IN ORAL DRUG DELIVERY.

* Haruna M., Suleiman M. and Musa Y.

**Department of Pure and Industrial Chemistry, Bayero University, P.M.B. 3011, Kano Nigeria*

*Corresponding Author: harunam.chm@buk.edu.ng

Abstract

Hydrogels are crosslinked polymers that have recently been used in agriculture, environmental remediation and medical applications as drug carriers. In this research maltose was modified to maltose-acrylate by reaction with acryloyl chloride. Poly maltose acrylate-graft-acrylic acid copolymer hydrogel was also synthesized via free-radical polymerization initiated with potassium persulphate (KPS) and N,N-methylene bisacrylamide (MBA) as a crosslinking agent. The synthesized hydrogel was characterized by FTIR, SEM and DSC. The swelling capacity of the synthesized hydrogel was evaluated in various pH media ranging from pH 1-12 at 25^{o}C. The hydrogel showed a good swelling capacity ranging from 107-1711% depending on the pH of the media and higher swelling ability was observed in basic media. Diphenylhydramine hydrochloride (DPH) as model drug was loaded into the polymeric hydrogel via post-loading method, the concentration of DPH loaded and released was measured using UV-visible spectrophotometer at 229.91nm where 99.5% DPH loading was achieved. The drug release (in-vitro) of the DPH loaded hydrogel in simulated gastric fluid (SGF) and simulated intestinal fluid (SIF) at 37^{o}C for 48hrs was also evaluated. The results obtained show that the hydrogel released 86% and 98% of DPH drug in SGF and SIF respectively. The hydrogel also exhibited excellent fluid absorption and retention capacity. The results obtained in this work suggest that the hydrogel has promising applications in DPH drug delivery system.

Keywords: DPH, Hydrogel, Maltose, Poly maltose acrylate-g-acrylic acid, Swelling

1.0 Introduction

Hydrogels are three-dimensional crosslinked polymeric network that are capable of imbibing and retaining large amount of water or biological fluid (Ashwani *et al*., 2014). They are hydrophilic, polymeric networks capable of absorbing large amount of water or biological fluids but do not dissolve (Shaikh *et al.,* 2015). Similarly, hydrogels are smart enough to respond to fluctuations of environmental stimuli (pH, temperature, ionic strength, electric field, presence of enzyme etc) (Enas *et al.,* 2013). Hydrogels swell or shrink accordingly (Das, 2013). In their swollen state, they resemble natural living tissue because of their softness and high-water content (Rakesh, 2008). It is generally agreed that, for a material to be classified as hydrogel, it should absorb at least 10% w/w water and must be insoluble in it (Rithe *et al*.,2014). The water holding capacity of the hydrogels arise mainly due to the presence of hydrophilic groups, amino, carboxyl and hydroxyl groups, in the polymer chains (Snezana, 2011). Hydrogels, when fully swollen, show some unique properties such as being soft and rubbery and having low interfacial tension with

water and biological fluids. These unique properties of hydrogels have made them similar to extra cellular matrix in living tissues (Ullah, 2015). For hydrogels, there are less chances of negative immune response due to low interfacial tension with body fluids which reduces cell adhesion. Many hydrogels have enhanced tissue permeability and drug residence time owing to their mucoadhesive and bioadhesive properties which make them very good vehicles for drug delivery (Rizwan et al., 2017). The beauty of these materials is, because of their excellent biocompatibility, they found applications in many areas such as biomaterials (Lu *et al*., 2009)., drug delivery (Kumar et al., 2017). Owing to their softness, hydrophilicity, super-absorbancy, visco-elasticity, biodegradability and their similarity with extra cellular matrix they are used in tissue engineering and regenerative medicine (Rana *et al*., 2015)., contact lenses (Zhang *et al*., 2011)., and water retention to disposable diapers (Chirani *et al*., 2014). In recent years, many researchers reported the advantages of using hydrogels in drug delivery over conventional method. The later has always been found to be associated with problems and limitations (Rithe *et al*., 2014). This research is aimed at synthesizing biocompatible and biodegradable polymeric hydrogel by grafting acrylic acid on maltose and uses it for drug delivery application.

2.0 Materials and Methods

2.1 Materials

Maltose (95%, BDH), Acryloyl Chloride (98%), Acrylic Acid (99% Xilong Chemicals), Methyl Ethyl Ketone (99%, Burgoyne Burbigdes & CO. India.), Butan-2-ol (Guangdang Guanghoa Chemical factory Co Ltd China), Potassium Persulphate (98%, Kermel), N'N-methylenebisacrylamide (MBA) (97%, BDH Chemicals), Hydrochloric Acid (98%, Sigma-Aldrich), Ethanol (98%, Qualikem) and Sodium Hydroxide (98%, LOBA), All other reagents were of analytical grade and used as obtained without further purification.

2.2 Methods

2.2.1 Test for Reducing Sugars

The test was carried out using Fehling's solution: Fehling's solution was prepared by combining solutions A and B;

Solution A: Copper (II) sulphate (17.32g) was dissolved in de-ionized water and the volume made up to 250cm^3 in a volumetric flask.

Solution B: Sodium potassium tartrate (86.5g) was dissolved in warm water, sodium hydroxide (30g) was also separately dissolved in water, and the two solutions were mixed and made up to 250 cm^3 in a volumetric flask.

Equal quantity of solutions A and B were transferred to a dry flask and mixed thoroughly and 1.25g of maltose was dissolved in water and made up to 250cm^3 in a volumetric flask. Fehling's solution (25cm^3) was put in a test-tube and boiled, followed by addition of maltose solution gradually until the blue colour turned to red.

2.2.2 Preparation of Maltose Acrylate

The conversion of maltose to maltose-acrylate was carried out using a modified method suggested by Shantha and Harding (2001). A solution of maltose (25g) in water (75ml) was maintained at pH 10.5 with sodium hydroxide (1M), and acryloyl chloride (3 ml) was added drop wise. The mixture was stirred at 20°C for 15min, and then neutralized with sodium hydroxide (1M). The resulting solution was extracted with methyl ethyl ketone (3×20ml), then with Butan-2-ol (3×25ml), and finally evaporated to give maltose acrylate.

2.2.3 Synthesis of Poly maltose acrylate-graft-acrylic acid (Poly MA-g-AA) Hydrogel

The synthesis was carried out according to a modified procedure reported by Ahmed *et al*., (2016). The monomers were taken in (1:1) ratio, maltose-acrylate (2g, 1M) was placed in a three-neck volumetric flask equipped with a set of condenser and magnetic stirrer at 50^{o}C for 10min followed by addition of acrylic acid (5ml, 1M) and the mixture was allowed to homogenize. MBA (0.5g, 0.1M) cross-linker was added and the mixture allowed to stir for 15min, then potassium persulphate (0.5g, 0.1M) initiator was added, the temperature was raised to 80°C ± 2°C and the polymerization was allowed to proceed for 2hrs under nitrogen. The resulting gels were washed thoroughly with de-ionised water followed by washing with ethanol to remove any residual monomer and dried in an oven at 50-60°C.

2.3 Fourier Transforms Infrared Spectroscopy (FTIR)

The spectra of the monomer and the synthesized hydrogel were recorded on a CARRY 630 FTIR spectrophotometer Agilent Technologies. All spectra were recorded at 25ºC and frequency range of 4000–650 cm^{-1}.

2.4 Determination of Percentage Swelling of the Hydrogel

The percentage swelling studies of Poly maltose-acrylate-co-acrylic acid hydrogel was determined by immersing known weights of dry drug-free hydrogel in various buffer solutions (pH 1-12) at 25^{o}C for 24hrs. After excess water on the surface was removed with filter paper, the weight of the swollen sample (hydrogel) was taken using the equation:

$$\% \text{ swelling} = \frac{\text{Wt} - \text{Wo}}{\text{Wo}} 100\%$$

where

Wo = initial weight of hydrogel
Wt = final weight of hydrogel

2.5 Preparation of DPH Calibration Curve

The stock solution of DPH was prepared by dissolving 25mg of DPH in 100ml of distilled water. The calibration solutions of DPH in the range of 5.0-40.0 µg/ml were obtained by appropriate dilution of the stock solution.

2.6 Drug Loading

The loading of the drug into the synthesized hydrogel was carried out via post loading method: 1g (1000mg) of hydrogel was dispersed in 200ml of solution containing 1mg/ml of DPH to suck up the total amount of the drug solution. After 24hr, the completely swollen hydrogel loaded with drug was dried.

2.6.1 Determination of Amount of DPH Loaded

The amount of drug loaded into the hydrogel was determined after swelling the hydrogel in a solution containing known concentration of drug, the remaining solution was collected and analyzed using UV-Visible spectrophotometer (Perkin Elmer) at 229.91nm. The difference between the amount of drug initially employed and the drug content in the residual solution was considered as the amount of drug loaded.

2.7 *In-Vitro* DPH Release

The *in-vitro* drug release was carried out by placing 1g of each drug loaded hydrogel into 100ml of aqueous buffer solution (SGF: pH 1.2 and SIF: pH 7.4) in a 150ml rubber-bottle at 37°*C* ± 0.2°C. The bottles were shaken on an INNOVA 4000 INCUBATOR SHAKER with reciprocating motion of 100rpm. At periodic intervals, 5ml of samples were removed from the release

medium and replaced with fresh enzyme-free SGF and SIF. The samples removed were analyzed using UV-Spectrophotometer (Perkin Elmer λ35). at a wavelength of 229.91nm. The percentage drug release was calculated using the equation by Sadeghi (2011):

Percentage drug released = Rt/L × 100

where: Rt = final amount of drug released at time t and L= initial amount of drug loaded

2.8 Scanning Electron Microscopy (SEM)

The surface morphology of poly Maltose acrylate-g-acrylic acid hydrogel before and after DPH loading was analysed using scanning electron microscope Phenom proX model.

2.9 Differential Scanning Calorimetry (DSC)

The thermal stability of poly Maltose acrylate-g-acrylic acid hydrogel was determined using differential scanning calorimetry (DSC). The sample was placed on the aluminium crucible pressed and sealed. This was followed by repeated heating and cooling and cycles. A wide temperature scan in heat, cool, heat cycles were generated by up to 120 thermocouples arranged in several layers. The analysis was carried out using DSC 1 Star System-Mettler Toledo Instrument.

3.0 RESULTS and Discussion

3.1 Fourier Transform Infrared Spectroscopy (FTIR)

FTIR spectrum of maltose acrylate (Figure 1) with absorption bands at 3268 cm^{-1}(OH stretching) due to hydroxyl group, peak at 2929 cm^{-1}due to C-H alkane stretching (sp^3), peak at 1722 cm^{-1} due to C=O (carbonyl of carboxylic acid), vinyl unsaturation at 1640 cm^{-1} due to C=C (alkene), stretching vibration at 1019 cm^{-1} due to C-O vibration.

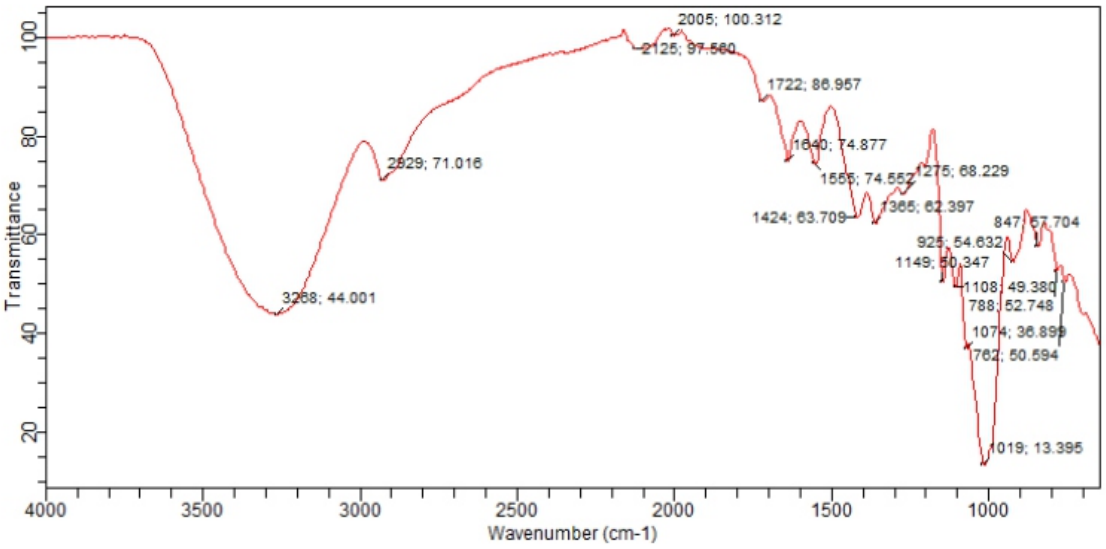

Figure. 1: FTIR Spectrum of Maltose Acrylate

FTIR spectrum of poly maltose acrylate-g-acrylic acid hydrogel (Figure 2) shows the presence of peak at 3398 cm^{-1} due to OH stretching, peak at 2933 cm^{-1} due to C-H alkane stretching (sp^3), shift of band from 1700 cm^{-1} to 1704cm^{-1} due to carbonyl group C=O was observed, a peak at 1156 cm^{-1} due to secondary hydroxyl group C-O

and neutralization of C=C confirmed the formation of the gel and grafting the acrylic acid onto maltose acrylate.

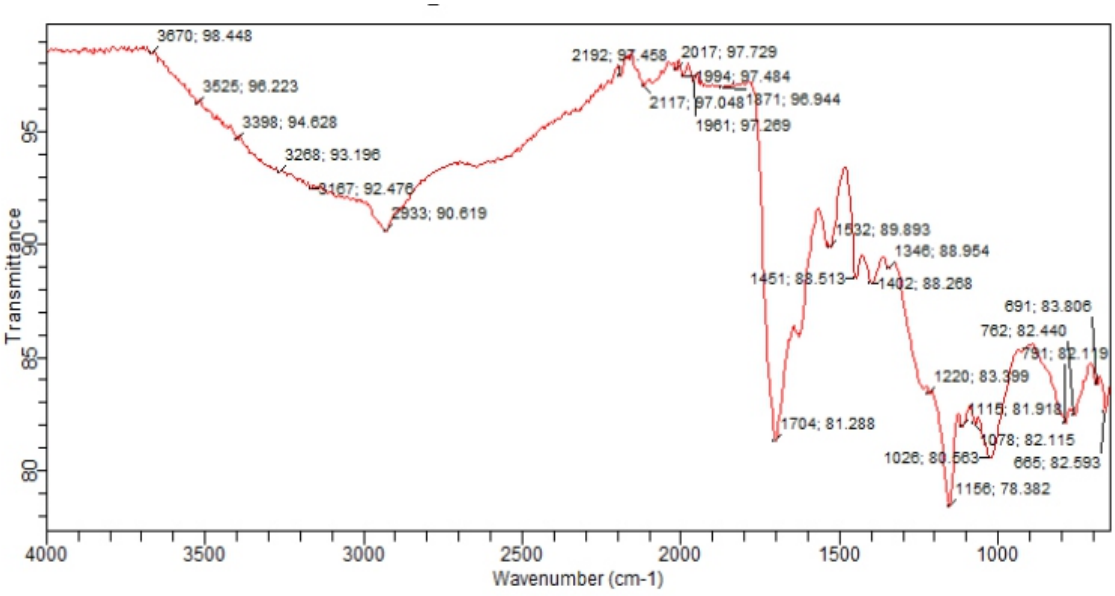

Figure 2: FTIR Spectrum of MA-g-AA Hydrogel

3.2 Percentage Swelling

The percentage swelling of the synthesized hydrogel at various pH ranging from 1-12 is shown in figure 3. The swelling studies indicated that, the hydrogel are sensitive to changes in pH of their environment. A maximum percentage swelling was oberved in basic media, the lower percentage swelling behavior of the hydrogel in acidic media can be ascribed to the protonation of most of the carboxylate groups which decreases the repulsion of anionic groups thereby leading to a decreased swelling rate. However, increase in pH of the media, converts the carboxyl groups to COONa groups as a result of neutralization by NaOH and subsequent ionization depending on the pH of the medium, this was in accordance with (Sadeghi, 2011). Similarly, when a hydrogel is brought into contact with water or a buffer solution, the solution diffuses into the network and a volume phase transition occurs, resulting in the expansion of the hydrogel. Diffusion involves the migration of fluid into the hydrogel or dynamically formed spaces between the hydrogel chains. Swelling of the hydrogel involves large segmental motion resulting, ultimately, in the increased separation of the hydrogel chains. The swelling behavior was followed by the degree of swelling, until equilibrium, was reached.

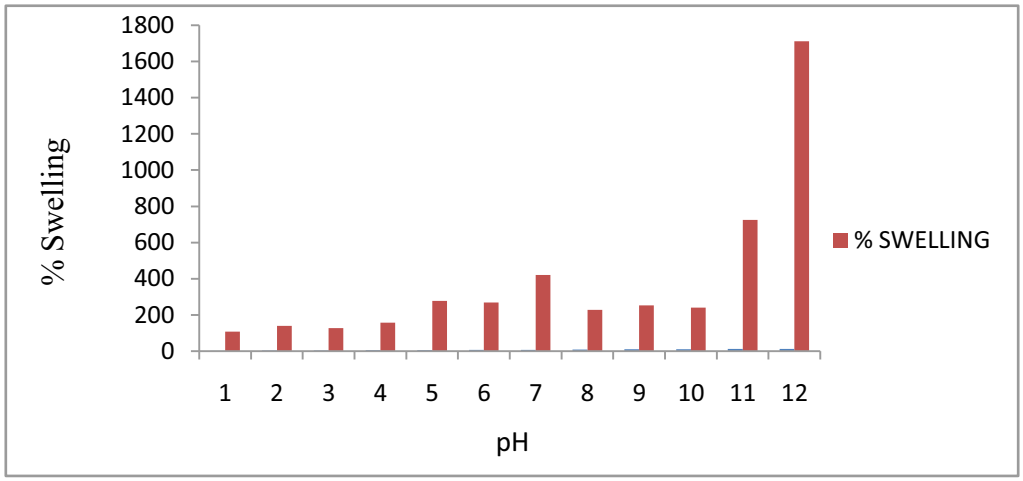

Figure 3: Percentage swelling of poly MA-g-AA Hydrogel

The swelling equilibrium occurs when the values of the osmotic force driving the solvent into the network and of the elastic force of the stretched sub-chains become equal. The equilibrium water content of a pH sensitive hydrogel is a function of the cross-link ratio and the network structure, i.e. its hydrophilicity, which in turn depends on the degree of ionization of the functional groups (Eid, 2001).

3.3 Drug Loading

After 24 hrs of post-loading the Diphenylhydramine hydrochloride (DPH) drug in to the hydrogel, UV-visible spectrophotometric measurements have confirmed that 99.5% of the drug was successfully loaded into the hydrogel.

3.4 DPH Percentage Release (*In-Vitro)* Study

Figure 4 shows the *in-vitro* release profile of diphenylhydramine hydrochloride drug from poly maltose acrylate-g-acrylic acid hydrogel in enzyme-free simulated gastric fluid (SIF) and simulated intestinal fluid (SIF). It can be seen from the figure that during the first five hours, the release was found to be 7.5% in SGF and 8% in SIF and at the end of 48 hrs the release was 86% in SGF and 98% in SIF. The low release in SGF compared to the SIF can be attributed to the pH sensitivity of the hydrogel.

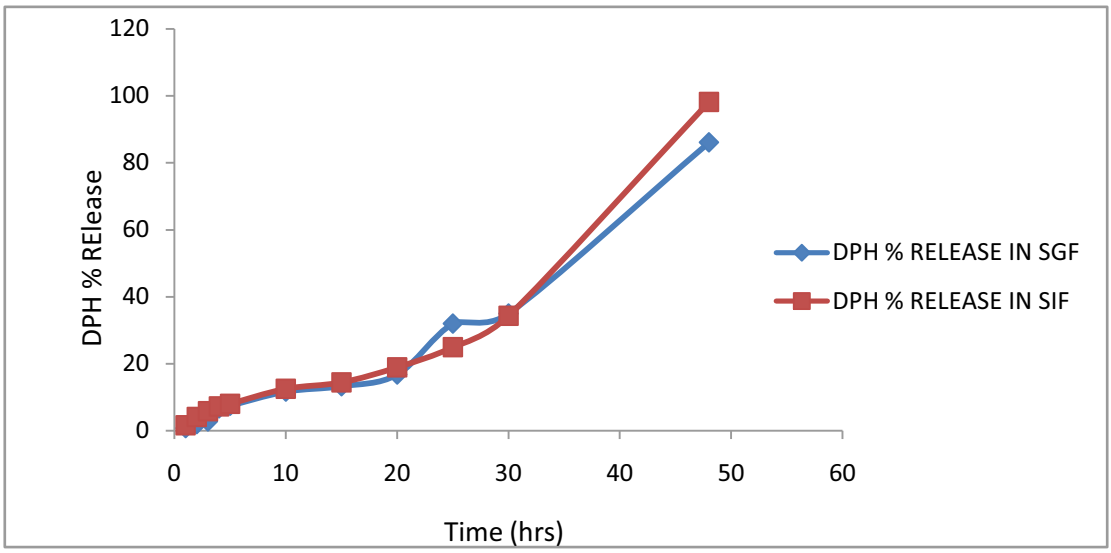

Figure 4: Percentage DPH release by poly maltose acrylate-g-acrylic acid hydrogel in SGF and SIF

3.5 Scanning Electron Microscopy (SEM)

The surface morphology of poly maltose acrylate-g-acrylic hydrogel before and after diphenylhydramine hydrochloride drug loading is shown in Figures 5 and 6 respectively. The micrograph of poly maltose acrylate-g-acrylic acid hydrogel before DPH loading appeared to be smooth while after loading, a rough surface was observed.

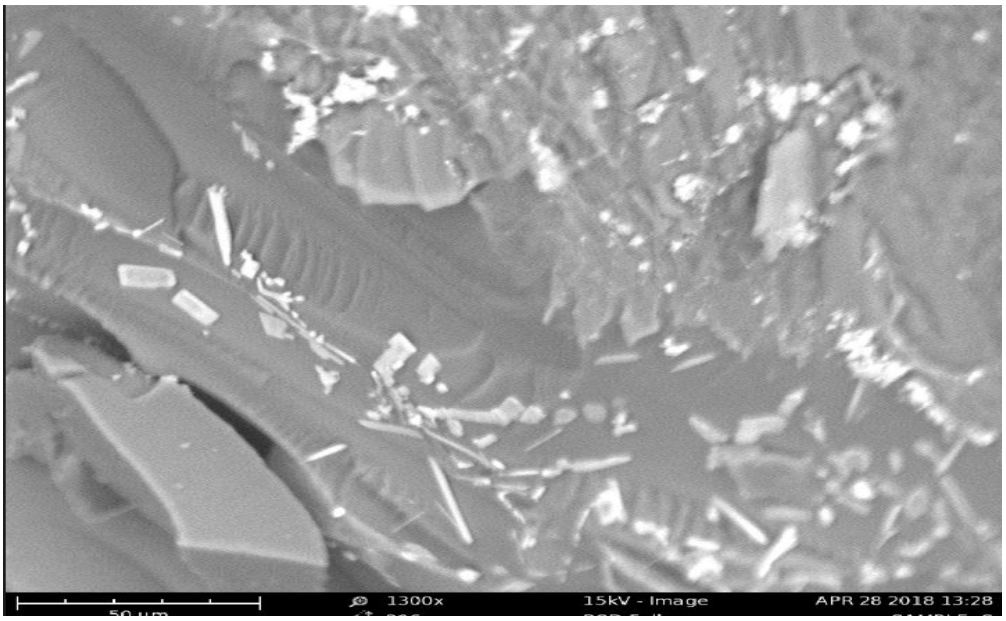

Figure 5: SEM of poly MA-g-AA before DPH Loading

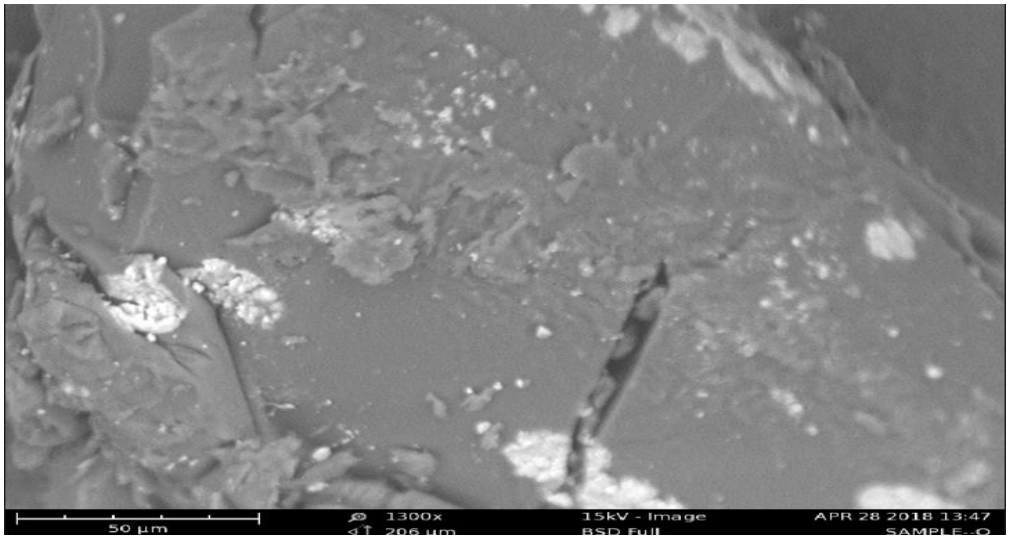

Figure 6: SEM of poly MA-g-AA after DPH Loading

3.6 Differential Scanning Calorimetry (DSC)

The DSC thermogram of poly maltose acrylate-g-acrylic acid hydrogel is presented in figure 7. A sharp exothermic transition around 96^{o}C and a second broad exothermic transition at around 264^{o}C. This confirmed that the hydrogel has satisfactory thermal stability that is required for an effective controlled drug delivery system.

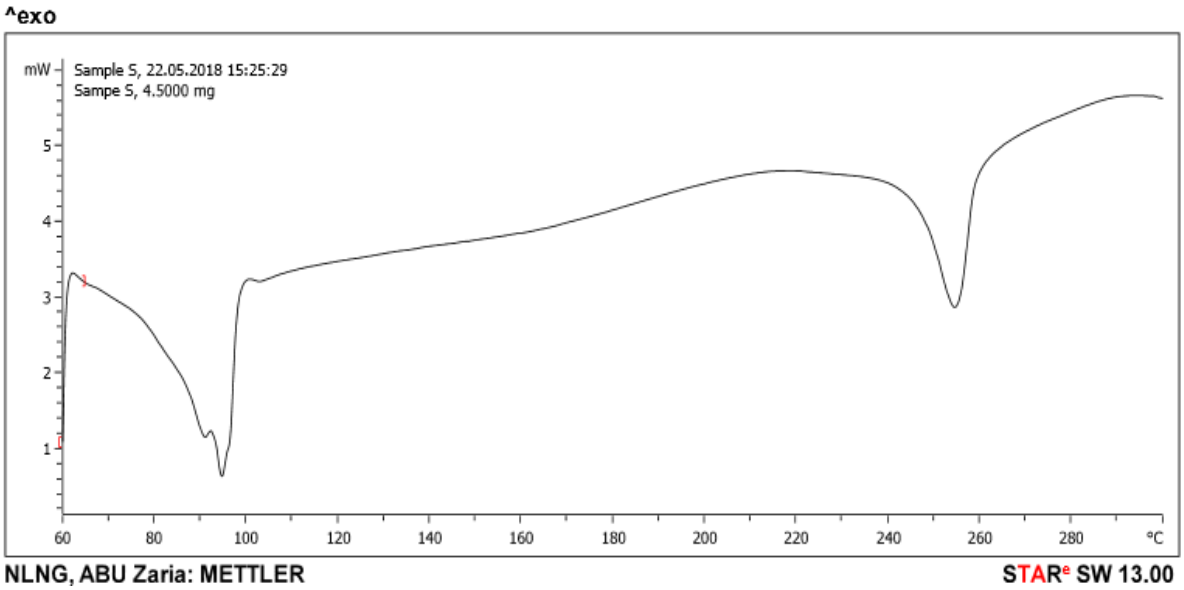

Figure 7: DSC graph of poly MA-g-AA hydrogel

Conclusion

Poly maltose acrylate-g-acrylic acid hydrogel was successfully synthesized via free-radical polymerization initiated with potassium persulphate (KPS) and N,N-methylene bisacrylamide (MBA) as a crosslinking agent as confirmed by FTIR spectroscopy. The hydrogel was found to have excellent fluid absorption and retention ability. The hydrogel has promising

application as drug carrier for application in controlled drug delivery systems due to the efficiency it exhibited in DPH loading and release both in SGF and SIF. Also, DSC and SEM analyses have indicated that the hydrogel has high thermal stability and good surface morphology.

References

Ahmed G.I., Farag A. H., Hamada A. W., Hamza M. (2016) "Synthesis, Characterization, Swelling Studies and Dye Removal of Chemically Crosslinked Acrylic Acid/Acrylamide/N,N Dimethyl Acrylamide Hydrogels)" *American Journal of Applied Chemistry* 4(6): 221-234

Ashwani G., Manju, N., Shikha, B., and Gitika, A.D. (2014) "Superporous Hydrogel Composites of Acrylamide Using Starch-silicone Dioxide Coprecipitate as Composite Agent" *British Journal of Pharmaceutical Research* **4** (3): 338-351.

Chirani N., Hocine L.Y., Lukas G., Federico L.M., Soumia C. and Silvia F. (2016) "History and Application Hydrogels" *Journal of Biomedical Sciences* Vol. 4: No. 2, 2254-2279

Das N. (2013) "Preparation, Methods and Properties of Hydrogel: A Review" *International Journal of Pharmacy and Pharmaceutical Sciences* 5: 112-117

Eid M. (2001) "In vitro release studies of vitamin B12 from poly N-vinyl pyrrolidone /starch hydrogels grafted with acrylic acid synthesized by gamma Radiation" *National Centre For Radiation Research and Technology*.

Enas M.A., Aggora F. S., Ahmed M. A, Ahmed T. E. (2013) "An innovative method for preparation of nanometal hydroxide superabsorbent hydrogel Carbohydrate Polymers*" Journal of Advanced Research,* 91: 693–698

Ezra A.K., Nermin O., Oguz, O. (2007) "Prepartion of homogeneous polyacrylamide by free radical crosslinking copolymerization" *European Polymer Journal* Vol. **43**: 2913–2921

Kumar D., Jyoti, P., Vinit R. and Pramendra K. (2017) "A Review on the Modification of Polysaccharide Through Graft Copolymerization for Various Potential Applications" *The Open Medicinal Chemistry Journal*. Vol. **4:** (2) 109-126

Lu D.R., Xiao C.M. and Xu S.J. (2009) "Starch-based completely biodegradable polymer materials" *Express Polymer Letters* Vol. **3**: No. 6, 366–375

Rakesh K.M., Mahesh D. and Ajit, K.B. (2008) "Synthesis and Characterization of Pectin/PVP Hydrogel Membranes for Drug Delivery System" *American Association of Pharmaceutical Scientist.* Vol. **9**: No. 2, 395-403

Rana P., Ganarajan G. and Preeti K. (2015). "Review on Preparation and Properties Hydrogel Formulation" *World Journal of Pharmacy and Pharmaceutical Sciences*. Volume 4, Issue 12, 1069-108.

Rithe S.S., Pravin G.K. and Shashank T.M. (2014) "Preparation and Analysis Of Novel Hydrogels Prepared From The Blend Of Guar Gum And Chitosan: Cross-Linked With Glutaraldehyde" International

Journal of Materials Science and Engineering: (MSEJ), Vol. **1**: No. 2, 1-15

Rizwan M., Rosiyah Y., Aziz H., Muhammad Y., Ahmad D.A., Vidhya S., Faridah S. and Cheyma N.A., (2017) "pH Sensitive Hydrogels in Drug Delivery: Brief History, Properties, Swelling, and Release Mechanism, Material Selection and Applications" 3 *journal of polymers* **9**: 137 498-512

Sadeghi M. (2011) "Synthesis of starch-g-poly (acrylic acid-co-2-hydroxy ethyl methacrylate) as a potential pH-sensitive hydrogel-based drug delivery system" *Turk J Chem* 35: 723 – 733.

Shaikh M., Nitin. S., Gramopadhye, A.A. Wardole and Shrikant, V. L. (2015) Starch-Acrylic Acid Hydrogel: Synthesis, Characterization and Drug Release Study. *World Journal of Pharmacy and Pharmaceutical Sciences* 4: 942-954.

Shantha K.L. and Harding D.R.K. (2001) "Synthesis and Evaluation of Sucrose-Containing Polymeric Hydrogels for Oral Drug Delivery" *Journal of Applied Polymer* Science 84: 2597–2604.

Snezana I.S., Ljubisa N., Vesna N., Slobodan P., Mihajlo S., Ivana M.R., (2011) "Stimuli-Sensitive Hydrogels for Pharmaceutical and Medical Applications" FACTA University Series: Physics, Chemistry and Technology Vol. **9**: No 1, pp. 37 - 56

Ulijn R.V., Bibi N., Jayawarna V., Thornton P.D., Todd S.J., Mart R.J., Smith A.M., and Gough J.E. (2007) "Bioresponsive hydrogels" *Materials Today* 10: 40–48

Ullah F., Othman M.B.H., Javed F., Ahmad Z., Akil H.M. (2015) "Classification, processing and application of hydrogels" A review. *Journal of Materials Science and Engineering.* 57: (3), 414–433.

Zhang R., Huang Z., Xue M., Yang J., & Tan T. (2011) "Detailed characterization of an injectable hyaluronic acid-polyaspartylhydrazide hydrogel for protein delivery." *Carbohydrate Polymers*, Vol. 85, No. 4, pp 717-725

Nigerian Journal of Polymer Science and Technology, 2019, Vol. 14, pp32-38

Received: 19/11/2018 Accepted: 09/08/2019

Extraction of Lignin from the Soda Extract of Defatted and Ethanol Extracted Cashew Nut Shell

Salehdeen M. U.[1*], Isa Y.[2] and Esther F. O [1].

[1] *Department of Pure And Industrial Chemistry, Kogi State University, Anyigba, Kogi State, Nigeria*
[2] *Department of Chemistry, Federal University, Lokoja, Kogi State, Nigeria*

*Correspondingauthor:Email: umar_chemist@yahoo.com

Abstract
In this study, lignin and hemicellulose soda extracts from the defatted and ethanol extracted cashew nut shell (DAECNS), were precipitated using 6M HCl. The pH was adjusted to 1 and 7 to compare the relative effect of pH on the recoverable weight yield which amounted to 7.00 g and 6.00 g respectively. Further hydrolysis of the above gave acid insoluble of 80% in both cases and tests on these were positive for lignin and negative for sugars. This implies that careful pH control can be used to isolate lignin from its mixture with hemicellulose.

Key words: Biomas, Cashew nut shell, Hemicellulose, Lignin,

1.0 Introduction

One component of lignocellulosic biomass, lignin, has long been viewed as a low-value or waste product in the wood pulping industry. The most common pulping process is the Kraft process, where lignin is dissolved in hot sodium hydroxide and sodium sulfide Azadi *et al;* (2013).

The top three pulping processes are the Kraft process, the sulfite process, and the soda lignin process. These three processes produce 60–100 Ktonnes of Kraft lignin, 1 M tonne of lignosulfonates, and 5–10 Ktonnes of Sulfur-free soda lignin per year, respectively Bugg and Rahmanpour (2015). Typically, lignin is used as a fuel to fire pulping boilers Stewart, (2008).

There is a vast collection of literature on lignin processing, including improving the recovery of lignin from biomass, de-polymerization of lignin into monomers by chemical and/or biological means, and upgrading of the de-polymerized lignin monomers to industrially relevant chemicals, which have been described in several other recent reviews Ragauskas *et al*., 2014).

Lignin monomers provide an opportunity for green aromatic-based compounds Lavoie *et al.,* 2011*).*

Lignin is the key biorenewable source of aromatic compounds with phenolics, for example, vanillic acid, syringic acid, ferulic acid, syringol, guaiacol, and eugenol attracting the interest of polymer chemists Calvo-Flores and Dobado (2010). They are also valuable building blocks for synthesis of bisphenols, aliphatic-aromatic polyesters,

polyethylene terephthalate mimics, and epoxy resins Fache *et al.,* (2015). In addition, there is strong interest in the continued development of polyurethane precursors originating from renewable resources Kuhire *et al.,* 2015).

Carbon fibers produced from lignin based materials require a lower amount of thermo-stabilization and possess high tensile strength Kadla *et al.,* (2002). Lignin has been used to produce various polymers like ARBOFORM, polyesters and polyurethanes and various polymer blends with PVC, polyolefins, and rubbers are being currently developed. Nagel *et al.,* (2002*)*. Lignin has also been used as slow release nitrogenous fertilizers for soil and catalyst for the Kraft pulping process Northey, (2002). Due to its hydrophobic nature, lignin can be used in the manufacture of gypsum wallboards.
Studies on the lignin extracted from black liquor, depending on wood type, extraction method, and pulping process, have been reported earlier García *et al.,* (2009). The lignin extracted from black liquor consists of many aromatic rings in the chemical structure. The chemical structure is complicated and can often be identified by the presence of poly-propane units such as p-hydroxyphenyl (or p-coumaryl alcohol), guaiacyl (or coniferyl alcohol), and syringyl (or sinapyl alcohol) Toledano *et al*., (2014).
Accordingly, its high aromaticity gives rise to relatively high thermal stability and carbon yield, being considered as a potential candidate as biomass-based carbon materials. The lignin polymer contains aryl alkyl ether as one of the weakest types of link between its constituent C6 -C3 units. These are split by the sulfur chemicals or alkali used at high temperatures during pulping, thus breaking down the polymer into smaller fractions. The phenolic hydroxyl groups in lignin, plus the sulphonic acid groups ($-SO_3H$) introduced into the degraded lignin molecules during pulping, help to make the material soluble in the alkaline pulping liquors.

Liquefaction processes produce monophenolic compounds that can be converted to liquid fuels by hydrodeoxygenation Ouyang *et al;* (2015*)*. Monomeric, aromatic-based compounds have also been obtained by steam treatment followed by base-de-polymerization to generate two fractions: a monomeric fraction and a dimeric and trimeric fraction Macfarlane *et al.,* (2014). The yield of the monomeric fraction was as great as 15 wt% of the initial lignin and included phenolic species such as vanillin, guaiacol, phenol, and catecol Macfarlane *et al*., (2014).

Mankind has utilized biomass throughout history to produce heat for warmth and cooking; biochemical, such as the ethanol and lactic acid produced by fermentation and bio-fiber, such as those used in clothing and other textiles Brown and Brown (2013). Present-day utilization of lignocellulosic biomass instead of petroleum in the production of chemicals and fibers could contribute to the improvement of environmental quality, national security, and rural economic development Brown and Brown (2013).

Cashew nut shell cellulose encrusting matter appears to form considerable proportion of the shell. The extraction of this component, using method of lignin extraction in pulp and mill or some other newer processes will avail the polymer and chemical industry additional renewable material for chemical conversions as well as add value to cashew nut plantation owners and cashew nut processors.

The importance of this study rest on the information it reveals about the lignin

composition in cashew nut shell. Lignin itself is composed of important monomer units that can provide an opportunity for green aromatic-based raw materials for the polymer and allied industries.

This research is aimed at isolating cellulose encrusting matter (lignin) from n-hexane defatted and ethanol extracted cashew nut shell for quantitative and chemical characterization. It is also intended to estimate its relative proportion in the shell and subsequently identify the structural unit making up the lignin through chemical characterization.

Therefore, the soda extract obtained from defatted-ethanol extracted shell was treated with 6M hydrochloric acid. Each sample at various pH was concentrated and filtered, the extract was further subjected to hydrolysis; both the filtrate and the residual were subjected to various test i.e. Bial test, Molisch test, iodine test, test for intact and extracted lignin using phloroglucinol-HCl.

2.0 Materials and method

2.1 Materials

Soda extract containing lignin from cashew nut shell, 10% iron (111) chloride, 6M hydrochloric acid, 2.5N hydrochloric acid, conc. sulphuric acid, phloroglucinol solution, orcinol solution, phenolphthalein and methyl orange, all were obtained from the Chemistry Laboratory, Kogi State University, Anyigba.

2.2 Method

The cashew nut shell sample was obtained from Anyigba in Dekina Local Government Area of Kogi State. After shelling and preliminary extractions with n-hexane (de-fat) and ethanol (i.e. removal of extractives) respectively, it was finally extracted exhaustively with NaOH in a delignification process.

2.2.1 Sample Collection and Preparation

The soda extract used in the present work was obtained from the cashew nut shell that had been treated with fat soluble solvent n-hexane (de-fat) and its extractives removed. The soda extract is the component of the treated shell that dissolved in NaOH.

Soda soluble extraction was carried out using 17.5 % sodium hydroxide solution. Eight grams of sample was wrapped carefully with glass wool and weighed. The sample was treated with this solution in a liquor ratio of 1:20 (gram: volume basis). It was boiled in a beaker for an hour and then decanted repeatedly for 30 times when extraction was visibly completed. All solution so decanted were added up and distilled to effect volume reduction. The solution left over in the distiller was cooled and made up to 1000 ml in a volumetric flask.

2.3 Lignin/ Hemicellulose Extraction

The soda extract had initial pH value of about 13. This was acidified to pH 7 and pH 1 in a separate process with hydrochloric acid. The precipitates formed in either case were filtered, washed, dried at 105 $^{\circ}$C, cooled in a desiccator and weighed. Using the formula below, the relative percentage of the precipitate relative to the original weight of material was evaluated;

$$\text{Weight of the precipitate (g)} \quad \text{Weight of DAECNS (g)} \times 100$$

The precipitates formed at various pH were tested for the presence of lignin and sugars, using phloroglucinol/HCl for lignin according to John *et al*., (1966) on one hand, and Molisch's and Bial's test for carbohydrates and pentose on the other hand.

2.4 Lignin isolation by hydrolysis of Hemicellulos

Four mills (4 ml) of 6 N HCl was introduced to 0.34 g each of samples of precipitated biomas above, they were heated to boil for three hours (3 hr), thereafter the solutions were filtered through a pre-weighed filter paper, then washed with distilled water until the filtrates were neutral. The filter papers were dried at 105 °C for one (1 hr), cooled and weighed.

Weight of residue (g) Weight of precipitate taken (0.34g) × 100

The residues were tested for the presence of lignin and simple sugars, using phloroglucinol/HCl for lignin according to John (1966) on one hand, and Molisch's and Bial's test for carbohydrates and pentose on the other hand. Similar tests were done on the filtrates.

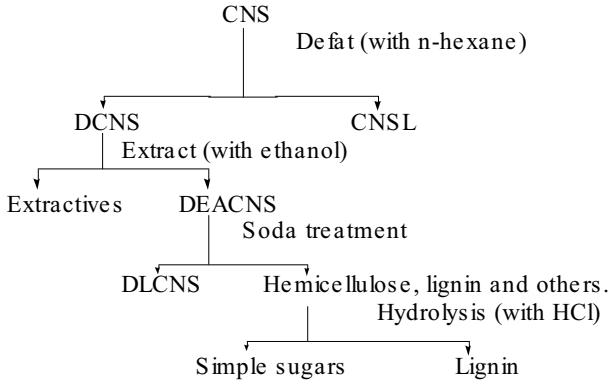

Figure 1: Schematic procedure for route analysis of component parts of cashew nut shell.

3.0 Results and Discussion

The result of the analysis (Table 1) shows the percentage composition of Lignin/Hemicellulose at various pH values relative to defatted and alcohol extracted cashew nut shell (DAECNS), this estimated that about 87.5% of lignin/hemicellulose was present in the DAECNS at pH 1 , on the other hand, about 75.5% of lignin /hemicellulose was constituted in the DAECNS at pH 7, the greater value obtained at pH 1 is in agreement with the view of Mussatto *et al.,* (2007) who also reported greater yield at this pH .

Table 1: Percent composition of Lignin/Hemicellulose at various pH relative to DAECNS

pH	Percent (%)
1.0	87.5
7.0	75.5

Keys: DAECNS = Defatted alcohol extractive cashew nut shell

Table 2 shows the qualitative test for the lignin/ hemicellulose in the DAECNS. The extract was positive to both the Wiesner's test and the Bial's /Molisch's test, in line with the report of John (1966). A brilliant red color develops, owing to the presence of coniferaldehyde group in the lignin. Bial's tests, indicates that the black liquor obtained from cashew nut shell contains the pentose.

Table 2: Qualitative test for Lignin/ Hemicellulose in DAECNS

Ph	Lignin	Hemicellulose
1.0	+	+
7.0	+	+

Keys
+ = Present
- = Absent

Table 3 shows the percentage yield of both the lignin/hemicellulose after the acid hydrolysis, showing that at the pH values of 1 and 7 contain the same amount of lignin at 80%, which simply means that a greater amount of hemicellulose was present at pH value 1 compared to that at pH value 7.

Table 3: Estimate of lignin in lignin/hemicellulose extract

pH of Hydrolysed extract	Percent %
1.0	80
7.0	80

Table 4 shows that the crude extract was positive to the Wiesner's test at both the pH value 1 and 7 after the acid hydrolysis. On the other hand, the crude extract was negative to the carbohydrate test after the acid hydrolysis at both pH values, implying that the hydrolysis step eliminated carbohydrates that were co-precipitated with lignin.

Table 4: Qualitative test for carbohydrates and lignin in the residue after acid hydrolysis

Hydrolysed extract of pH	Carbohydrates		Lignin
	Fehling's	Bial's	
1.0	-	-	+
7.0	-	-	+

Further, the result of the analysis (Table 5) shows that the filtrate obtained after the acid hydrolysis was positive to the carbohydrate test (Fehling's and Bial's test). This can be interpreted to mean that the co-precipitated carbohydrate was solubilized in the hydrolysis step so that the filtration step was used to effectively separate it from the lignin. This position was re-enforced by the fact that test on the filtrate using Wiesner's reagent showed negative outcome.

Table 5: Qualitative test for carbohydrates and lignin in the filtrate after acid hydrolysis

Hydrolysed extract of pH	Carbohydrates		Test for Lignin with Wiesner's reagent
	Fehling's Reagents	Bial's reagent	
1.0	+	+	-
7.0	+	+	-

4.0 Conclusion

This study has shown that cashew nut shell has reasonable quantity of recoverable lignin which can be isolated using pH control method. As lignin is known to dissolve in high alkaline pH in excess of pH 12, the soda insoluble components of the defatted, ethanol extracted cashew nut shell (DEACNS) can be separated. This will give a filtrate containing the solution of lignin and dissolved carbohydrates like hemicelluloses. As the solution is acidified, the carbohydrate fractions are precipitated and removed by filtration. Lignin is precipitated at much lower pH of 7 and below. As the solution is further acidified and heated any encrusting carbohydrate is degraded and removed by filtration to give lignin.

The delignification procedure was able to remove the lignin from hemicellulose by way of breaking down the hemicelluloses to soluble simple sugars. Appropriate test for the various carbohydrates revealed their presence in the resulting solution and no lignin was found. The residue on the other hand revealed the presence of lignin when tested.

REFERENCES

Azadi, P., Inderwildi, O.R., Farnood, R., King, D.A. (2013). Liquid fuels, hydrogen and chemicals from lignin: A critical review. *Renew of Sustainable Energy Rev.*,21, 506–523.

Brown, R.C., Brown, T.R. (2013). Biorenewable Resources: Engineering New Products from Agriculture ; John Wiley & Sons: New York, NY, USA,.

Bugg, T.D.H., Rahmanpour, R. (2015). Enzymatic conversion of lignin into renewable chemicals .Current Opinion in Chemical Biology.,29, 10–17.

Calvo-Flores, F.G., Dobado, J.A. 2010. Lignin as renewable raw material. ChemSusChem. 3, 1227–1235.

Fache, M., Boutevin, B., Caillol, S. (2015). Vanillin, a key-intermediate of biobased polymers. *European Polymer Journal*,68,488–502.

García A, Toledano A, Serrano L, Egüés I, González M, Marín F, Labidi J. (2009). Characterization of lignins obtained by selective precipitation. *Separation and Purifation Technol,* 68,193.http://doi.org/10.1016/j.seppur.2009.05.001.

John M. H. (1966), Lignin production and detection in wood. *U.S. Forest* November.

Kadla JF, Kubo S, Gilbert RD, Venditti RA(2002). **Lignin- based Carbon Fibers.** In Chemical Modification, Properties, and Usage of Lignin. Edited by: Hu TQ. New York, USA:

Kluwer Academic/Plenum Publishers;121-138.

Kuhire, S.S., Avadhani, C.V., Wadgaonkar, P.P. (2015). New poly (ether urethane)s based on lignin derived aromatic chemicals via a-b monomer approach: Synthesis and characterization. *European Polymer Journal*,71, 547–557

Lavoie, J.M., Bare, W., Bilodeau, M. (2011). Depolymerization of steam-treated lignin for the production of green chemicals. *Bioresource and Technology*, 102 , 4917–4920. [CrossRef] [PubMed.

Mussatto, S.I, Fernandes, M., Roberto, I.C. (2007). Lignin recovery from brewer's spent grain black liquor. Carbohydr Polym, 70, 218. https://doi.org/10.1016/j.carbpol.2007.03.021.

Nagel, H., Pfitzer, J., Nagele, E., Inone, E.R., Eisenreich, N., Eckl, W., Eyerer, P(2002). Arboform-A thermoplastic, processable material from lignin and natural fibers. In Chemical Modification, Properties, and Usage of Lignin. Edited by: Hu TQ. New York, USA: Kluwer Academic/Plenum Publishers; 2002:101-120.

Northey RA (2002). The Use of Lignosulphonates as Water Reducing Agents in the Manufacture of Gypsum Wallboard In Chemical Modification, Properties, and Usage of Lignin. Edited by: Hu TQ. New York, USA: Kluwer Academic/Plenum Publishers:139-150.

Macfarlane, A.L., Mai, M., Kadla, J.F. (2014). Bio-based chemicals from biorefining: Lignin conversion and utilisation.In Advances in Biorefineries: Biomass and Waste Supply Chain; Woodhead Publishing: Cambridge,UK, pp. 659–692.

Mussatto, S.I., Fernandes, M., Roberto, I.C (2007). Lignin recovery from brewer's spent grain black liquor. *Carbohydrate Polymers*, 70, 218. https://doi.org/10.1016/j.carbpol.2007.03.021.

Ouyang, X.P., Zhu, G.D., Huang, X.Z., Qiu, X.Q. (2015). Microwave assisted liquefaction of wheat straw alkali lignin for the production of monophenolic compounds. *Journal of Energy Chemistry.*24, 72–76.

Ragauskas, A.J., Beckham, G.T., Biddy, M.J., Chandra, R., Chen, F., Davis, M.F. (2014). Davison, B.H.; Dixon, R.A.; Gilna, P.; Keller, M.; et al. Lignin valorization: Improving lignin processing in the biorefinery. *Science* 2014, 344, 1246843.

Stewart, D.(2008). Lignin as a base material for materials applications. Chemistry, application and economics, Industrial Crops Production, 2008,27, 202–207.

Toledano, A., Serrano, L., Labidi, J. (2014**)**. Improving base catalyzed lignin depolymerization by avoiding lignin repolymerization. *Fuel,* 116, 617–624.

Nigerian Journal of Polymer Science and Technology, 2019, Vol. 14, pp39-52

Received: 30/09/2018 Accepted: 26 September, 2019

EFFECT OF FIBER MODIFICATION ON MECHANICAL PROPERTIES OF *SUGARCANE (Saccharumofficinarum)/GLASS FIBER* REINFORCED EPOXY RESIN HYBRID COMPOSITE.

[*1]Birniwa A. H., [1]Abdullahi S. S., [2] Abdulkadir A., and [3] Sani S.

[1] *Department of Polymer Technology, Hussaini Adamu Federal Polytechnic Kazaure, P.M.B 5004 , Jigawa State.*

[2] *Rabiu Musa Kwankwaso, College of Advance and Remidial Studies,Tudun Wada, Kano.*

[3] *Department of Pure and Applied Chemistry, Usmanu Danfodiyo University Sokoto. PMB 2346, Sokoto.*

Abstract

Sugarcane (Bagasse) was extracted to remove the juice by mechanical process. A portion of sugarcane fiber was subjected to 6% alkaline, then0.125% potassium permanganate, andlater 6% benzoyl peroxide treatment respectively. Also this research work deal with the hybrid effect of composite made of sugarcane/glass fibers which are fabricated by hand lay-up method using epoxy and hardener of ratio 2:1. The mechanical properties of this hybrid composite are determined by testing like Tensile and flexural strength which wereevaluated experimentally according to American Society for Testing of Material (ASTM) standards. The result of the test shows that hybrid composite of treated benzoyl peroxide sugarcane/glass fiber (TBP/GFHC) on the mechanical properties possesses better properties than that of untreated, alkaline, and potassium permanganate treated sugarcane fiber composite. The effect of alkali, potassium permanganate and benzoyl peroxide treatments of sugarcane fiber on the mechanical structure and Functional Group was examined using Fourier Transform infrared spectroscopic (FT-IR). FT-IR analyses confirmed the lowering of hemicelluloses and lignin contents by benzoyl treatment of the sugarcane fiber. Furthermore, the improved hybrid composite showed resistance to acid, alkali and also possessed lower water absorption. The sugarcane fiber composite/glass fiber hybrid composites have the properties which advice their relevance for application in the building and construction.

Key words*: Composite, Epoxy-resin, Sugarcane-fiber.*

1.0 Introduction

The use of natural fibers as reinforcements for composite has attracted more interest of industries(Şahin and Mehmet, 2018). Fibers reinforced polymer composites have many applications as class of structural materials because of their ease of fabrication, relatively low cost and superior mechanical properties compared to polymer resins(Sumit*et al*., 2018). For example in the automotive industry, the effort to reduce weight in order to improve fuel economy and to comply with tighter governmental regulations on safety and emission has led to the introduction of increasing amounts of plastics and composites materials in place of the traditionally used steels (Mathur, 2006). Natural fibers have different origins such as wood, pulp, cotton, bark, bagasse, bamboo, cereal straw, and vegetable (e.g., munja, flax, jute, sun hemp, sisal, banana, pineapple and ramie). These fibers are mainly made of

cellulose, hemicelluloses, lignin and pectin's, with a small quantity of extractives. Compared to glass fiber and carbon fibers, natural fibers provide many advantages, such as, abundance and low cost, biodegradability, flexibility during processing and less resulting machine wear, minimal health hazards, low density, desirable fiber aspect ratio, and relatively high tensile and flexural modulus(Maneesh*et al.,* 2012)**.** The effect of fiber length on mechanical properties of composite was presented by Sherif*etal.,(*2012).Along with holding the fiber together, the matrix has the chief function of transferring applied load to the fibers. Failure of specimen takes place may be due to insufficient length of fiber for stress distribution. An optimum length of 5mm was considered for present experimentation. Mohd*et al*.,(2015).

Nowadays, composites have become one of the most important engineering materials in various applications. The demands for composites are steadily increasing as composites are more preferred compared to other materials such as metals and ceramics (Dadrasi, *et al*., 2019). The main reason for this is because composites are relatively cheaper and have high availability. On top of that, the properties of composites can be altered according to the desired applications (Gang *et al*; 2018). However, the trend of the world today leans toward biodegradable materials which are more environmental friendly,these hybrid composites materials are also sustainable as it comes from renewable resources (Xue*et al*., 2007). Even though composites have many uses in the industry, it is actually a better idea to apply hybrid composite.

Hybrid composites are a type of composite where either one or both of the constituent materials; matrix and reinforcement are of biological origin (Singal and Tiwari.,2014). As mentioned earlier, at least one of the constituent materials of the hybrid composite must be of biological origin. In this study, bagasse fibers are used as the reinforcement for the hybrid composite. Bagasse is the residue of sugar cane after the process of juice extraction,sugar canes are largely produced throughout the world as it is very important in the sugar milling industry (Punyapriya and Acharya, 2010). This means that, bagasse which is the residue/waste materials are also produced in large quantity along with the sugar canes. Most sugar milling industry uses the bagasse as the fuel resource of the industry itself (Nazari*et al*., 2008). However, the quantityof bagasse produced by the world is about 54 million dry tons every year (Satyanarayana*et al*., 2008). Even though bagasse is used as fuel resource of the sugar milling industry, there would still be a large amount of unused bagasse which will become waste material. Thus, it is quite important to make good use of this waste product which is produced in such large quantity.The need for hybrid composite materials are rising. Thus, it has become necessary to find a new product especially composites which have potential to solve this worldwide problem.

In this study, the potential of bagasse (sugar cane residue) to be used as hybrid composite was analyzed and discussed. The mechanical properties of the sugarcaneparticle reinforced hybrid composite are the main focus to determine the potential of the sugar cane residue. As bagasse has high availability throughout the world (Sumit*et al*., 2018;Satyanarayana*et al*., 2008), there would be no problem regarding the sustainability of this material. Thus, this study will be mainly focusing on the mechanical properties of the bagasse particle reinforced hybrid composite. The effect of

bagasseparticle weight fraction towards the mechanical properties of the resulting hybrid composite is also one of the main concerned. The main aim of this research is to fabricate blend convectional composite using hand lay-up method.

2.0 Experimental

2.1 Materials

The epoxy resin Bis (phenol-A-diglycidyl-ether), crosslinker HY-951 and the glass fiber were obtained from NYCIL Nigeria Limited, Lagos. Epoxy resin was used as a matrix material with the grade LM-556 and density of 1.3 ± 0.2 g/cm^3. The *Saccharumofficinarum* fiber was obtained from a local farm in Gada village, Kazaure local government, Jigawa state.

2.2 Extraction of Fiber from Sugarcane stalks

The *S.officinarum* fiber was extracted using water retting process. Thus, the bark of The *S.officinarum*fiber was cut from its tree was soaked in a trough of water at room temperature for 7 days. After which the water fed on the pectin, lignin and other impurities contained in the fiber. It produced an unpleasant odor with gummy materials. The fiber appeared fresh and milky in a sheath of networked structure. The resulting fiber were removed by hand scratching and carded with a soft nylon brush. This was then washed with tap water several times and allowed to dry for three days under shade (Gumel and Tijjani 2017; Velmurugan, *et al*., 2012;).The dried fiber was brushed using a hand nylon brush resulting in a fine strand of the material ready for treatment and composite fabrication.

2.3 Sugarcane Fiber SamplesPre-Treatment

This particularly focused on the modification of filler surface to improve the interfacial adhesion between filler particles (hydrophilic) and polymer macromolecules (generally hydrophobic) and their dispersion the composite.

2.3.1 Alkali Treatment

The fiber was first washed with non-ionic 2% detergent solution several times. It was later immersed in 5% sodium hydroxide solution (NaOH) for three hours at 96 ^{o}C, in a thermostat machine. This is to activate the hydroxyl (OH^-) groups on the cellulose within the fiber and to introduce the sodium ion (Na^+) on the fiber backbone. At higher concentration above 5%, excess delignification of natural fibers can occur, resulting in a weaker or damaged material. The fiber was then washed thoroughly with distilled water and dried in an air oven at 70°C for 24 hours. The fiber was designated as alkali-treated *S.officinarum*(Sumit*et al* 2018).

2.3.2 Permanganate Treatment

The Fibre was washed with 2% detergent and soaked in 2% NaOH for one hour and then soaked in 0.2% potassium permanganate (KMnO4) for ten minutes. At higher permanganate concentrations, degradation of cellulosic fibre occurred which resulted in the formation of polar groups between the fibre and the matrix. The permanganate soaked fibre was put into thermostatic water bath at 50ºC for two hours to catalyze the reaction, washed with distilled water and dried at 70°C for twenty four hours. The fibre was designated as potassium permanganate treated *S. officinarum,*(Sumit*et al* 2018; Gumel and Tijjani 2017).

2.3.3 Peroxidation: The fiber was washed with 2% non-ionic detergent solutions and soaked in 2% NaOH solution for 1 hour, it was subsequently immersed inside benzoyl peroxide (around 6% concentration) solution

in acetone for 30 minutes. Some portion were immersed in hydrogen peroxide instate of benzyl peroxide for comparing between them. Complete decomposition of peroxide was achieved by heating the solution at higher temperature 180^0C. The *S. officinarum*fiber was designated as benzoyl treated (Lingtong*et al*., 2018).

2.4 Polymer Matrix

The epoxy resin is a class of thermosetting polymer that cross link when polymerize in the presence of a hardener. Specifically the epoxy herein used is of LM 556 grade and density of 1.3 ± 0.2 g/Cm^3. While the crosslinker used was HY-951. The matrix material was prepared with a mixture of the epoxy resin and hardener HY-951 in the volume ratio of 2:1 (Niharika and Acharya, 2013).

2.5 Composite preparation

2.5.1 Composite Fabrication (Hand Lay-Up Method)

For a hybrid composite, the sugarcane and glass fibers each of 0.3gwere weighed and place intomold cavity as reinforcement, length of the fiber were 15cm long,after the The mold is made from metal iron, with at least six cavities; each cavity has 150mm ×150mm, and 13mm and 13mm respectively. The mold has dumb-bell shape. Then the mold were firstly cleaned with either toilet paper or clean pieces of cloth to clean the dust/dirty. Then the surface of each cavity was coated with a blue seal as a releasing agent. 0.6g of blended sugarcane fiber was dispersed into the each mold cavity as reinforcements. The epoxy resin (60ml) and the hardener (40ml) were mixed together into the ratio 2:1, and stirred it gently until homogeneous (same). (Daniella *et al*., 2009 ;Abubakar, 2004).Then the mixture of epoxy and hardener was poured into the mold cavity until each of the mould cavity was filled. It wasthen allowed cure for 1:30-2:00 hours at a room temperature. After the composite was cured, then the sharp knife ends were used to remove the composite from the mold(Arrakhiz*et al*., 2013Xie et al., 2010).

curing process, test samples were cut to the required sizes prescribed in the ASTM standards.

Table 1: Formulation Table of Composite Fabrication

S/N	MATERIALS	COMPOSITION
1	Epoxy resins	$60cm^3$
2	Hardener	$40cm^3$
3	Sugarcane/ glass fiber	0.6gm
4	Curing temperature	Room temperature
5	Releasing agent	Blue seal

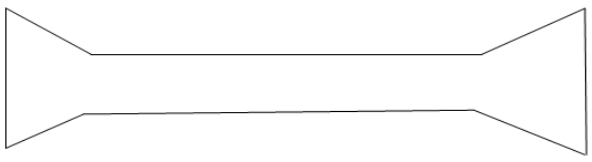

Figure. 1. Diagrammatical presentation of composite

2.6 Water Absorption Test

Water absorption is used to determine the amount of water absorbed under specified condition. The test specimen was manufactured as per ASTM standard D570. The water absorption is expressed as increasing weight percent.The high moisture absorption capacity of natural fibers adversely affects adhesion with a hydrophobic matrix and, as a result, it may cause material degradation and loss of strength**.**

The composite was pre- weight (W_1) and immersed in their respective cylinder contained distilled water for 24hours. After the sample was dried by pressing both side of the composite with tissue paper and re-weight (W_2). The % weight loss/weight gained of the composite was evaluate using equation% weight = $\frac{w2-w1}{w1} \times 100\%$ (Venkateshwaran*et al*., 2011)

Where W_1 = initial weight, w_2 = final weigh of the sample

2.7 Chemical Resistance Test

The chemical test of the composite was conducted using acid and base (H_2SO_4, HCl and KOH. The acid and base used was 10% in 90ml of water. In accordance with ASTDM standard D -570. The composite sample was tested using each chemical, the average value was evaluated, composite was pre-weight (w_1) and dipped into the respective cylinders at room temperature for 24 hours. After sample has been washed with distilled water and dried by pressing with side of the sample with tissue paper and re-weighted immediately as (w_2).The weight gain/ loss of the samples was calculated as percentage.Percentage weight gain/loss = $\frac{w2-w1}{w1} \times 100\%$

Where; w_1 and w_2 are initial and final of the sample respectively

2.8 Mechanical Testing

2.8.1 Tensile Test

Samples of the composite were tested for their tensile strength using an Instron Universal Testing Machine, IX, Model 4302, Instron, A crosshead speed of 5mm per minute was used. An ASTM D-638 standard was adopted for this purpose (Gang *et al*., 2018).

2.8.2 Flexural Test

The Instron IX 4302 machine was also used for the flexural tests, using the 3-point bending fixture according to ASTM D-790. Across-head speed of 5 mm per minute was used. The dimension of test samples was typically 60 x 6 x 2 mm. The average results were obtained from 3 specimens that were tested. The value of flexural strength (σ) was calculated according to equation 1 $\sigma = \frac{3FL}{2dh^3}$. (1)

In equation 1, F is the maximum load recorded (N), L is the sample span (mm), d is the sample diameter (mm), and h is the width (mm). (Gang *et al*., 2018; Bai*et al*., 1999).

2.9 Fourier Transform Infrared Analysis (FTIR) The Agilent technology (cary 630 FTIR) Fourier transformed infrared spectroscopy machine was used, the machine required no any sample preparation the spectra of all the treated and untreated (sugarcane fiber) and the polymeric was required from 4000-650cm^{-1}

3.0 Results and Discussion

3.1 Moisture Absorption Test Moisture absorption capacity is another crucial factorto be taken in an account when

considering the effect of water on the composite materials developed; the results are presented in figure 2.

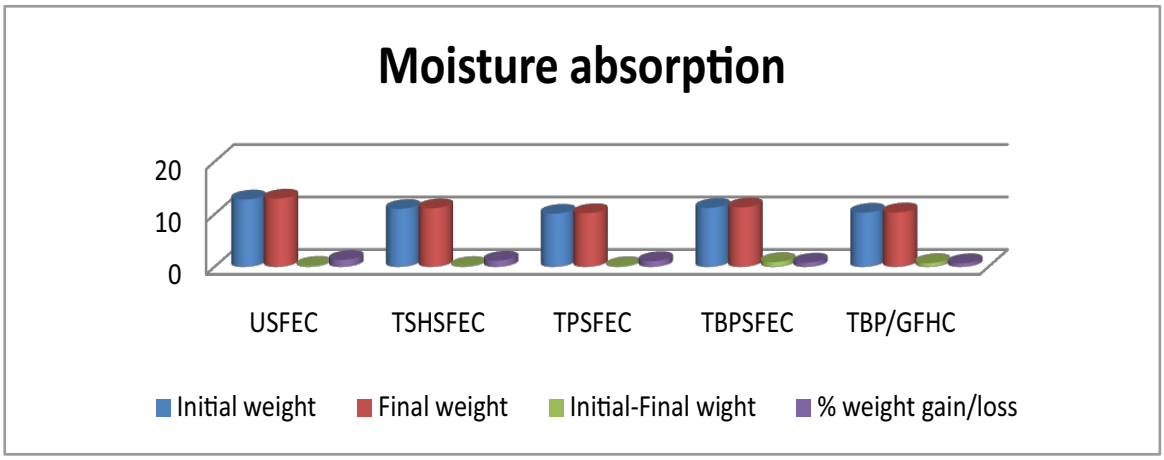

Figure 2: Moisture absorption test

KEY

1. **USFEC:** *Untreated Sugarcane Fiber Epoxy Composite*
2. **TSHSFEC:***Treated Sodium Hydroxide Sugarcane Fiber Epoxy Composite*
3. **TPSFEC:***Treated Permanganate Sugarcane Fiber Epoxy Composite*
4. **TBPSFEC:** *Treated Benzoyl Peroxide Sugarcane Fiber Epoxy Composite*
5. **TBP/GFHC:** *Treated Benzoyl Peroxide with Glass Fiber Hybrid Epoxy Composite*

From the result obtained in the figure 2, it observed that all the composite sample absorbed water; however TBP/GF HC absorbed the least amount of 0.68% after 24 hours in water. The USFEC absorbed as high as 1.32% which is expected due to it is hydrophilic nature and the presence of OH, polar groups and other substance. The TSHSFEC and TPSFEC absorbed more water than TBP/GF HC which indicates that TBP/GFHC might be ideal for chemical modification of sugarcane fiber composite. Although the epoxy resin composite absorbed water, which was unexpected as the weight should remain constant throughout the water absorption treatment. This may have been due to cracks and void during production. Similar research was conducted by (Josephine andBenjamin.,2016*)*.

3.2 Chemical Resistance Test

Chemical resistance tests are used to find the ability of a composite to withstand exposure to acids, alkalis, and other chemicals(Jawaid*et al*., (2011)The chemical resistance tests of these hybrid composites were performed in order to find out whether these composites products are resistant to chemicals. The weight loss/gain for the untreated, and treated samples of sugarcane fiber/glass fibers reinforced hybrid composites with different chemicals were shown in figure 3. It was shown clearly evident that weight gain and loss was observed for some chemical reagent.From the result obtained, the weight increase of the composites was least for aqueous solutions, and this was to be expected as a result of the hydrophobicity of the fiber. It was also observed from the figure 4.

Thattreated composites also have weight loss in H_2SO_4 like TBPSFEC and TBP/GFHC. The reason is due to the attack of the sulpuric hydrocarbons on the cross linked epoxy hybrid system. The positive values indicate that the composite materials were swollen with gel formation rather than dissolving in chemical reagents. It was further observed that composites were also resistant to water. This epitomes clearly that the sugarcane/glass fiber epoxy hybrid composites are substantially resistant to almost all chemicals except potassium hydroxide. Therefore, observations suggest that these hybrid composites can be used in aerospace, automobile, and marine applications for making water and chemical storage tanks. (Wang *et al*., 2007).

3.3 Mechanical Test

3.3.1 Tensile Strength Test:

The mechanical properties of sugarcane fiber composite filled epoxy resins hybrid composite were determine by universal testing machine (Testometric material testing machine with model 0500-10074) at test speed 10.00mm/min cross head –speed under displacement control mode, the result are presented in the figure 6.From the result obtained as shown in figure 6 above, indicated that the TBP/GFHC had the highest tensile strength of 242.45kgf. This shows that the TBP/GFHC improved the tensile strength of the USFEC which recorded 148.55kgf.This indicates of the ability of benzoyl peroxide to modify the fiber. TSHSFEC and TPSFEC recorded value of 178.20 and 194.40kgf respectively. The result for TSHSFEC and TPSFEC might be easily considered and anomalies as these agents have been reported to improve fiber composite strength. However, poor tensile strength could be due to the variety of sugarcane used, method of collection, and processing. (Josephine *et al.,* 2016).

3.3.2 Flexural Strength Test: The flexural test of composite was determined using Testometric material testing machine with model no 0500-10074 at test speed 2.130mm/min at strain rate under displacement control mode. The result obtained as shown in the figure 7, shows that the TBP/GFHC at 33.900kgf has more tendencies to accommodate high flexural strength than other treated and untreated fiber epoxy composite due to the modification of benzoyl peroxide. Before yield point, which was during application it was more to resist major deformation at break at 2.988 which was lower than that TSHSFEC deformation at 7.178,this means that TBP/GFHC has a high deflection.USFEC and TSHSFEC has been proved by other research to be the promising using other fiber, hence it is major negative response have may be due to the sugarcane variety, processing and handling.(Josephine *et al.*, 2016).

3.3 Fourier Transform Infrared Analysis (FTIR)

FTIR Analysis was conducted for both treated and untreated fiber to investigate the reaction take place within the cellulose of the fiber. The Agilent technology (cary 630 FTIR) was used, the machine require no any sample preparation. The spectra for both treated and untreated sugarcane fiber, polymeric material was required from 4000-650cm^{-1} the result are presented in table 2.From the result in table (2), strong broad band observed around 3335 cm^{-1} in the spectra was due to the hydrogen bonded O-H stretching vibrations of sugarcanefiber. Hydroxyl groups were also involved in hydrogen bonding with the carboxyl groups, cellulose, pectin, lignin, hemicelluloses that were available on the fiber surface of natural fiber. The medium intensity band at 2802cm^{-1} was attributed to the C-H stretching frequency in methyl and

methylene groups. The absorption band at 1032cm^{-1} was due to the vibrations of adsorbed water molecule in the non-crystalline region of cellulose which appeared as a shoulder in the spectra. The peak at 1423cm-1 was caused by CH_2 symmetric bending. The band at 1544cm^{-1} was assigned to C=C showing the presence of aromatic (symmetric) arising from polysaccharides. The peak at 1035 cm^{-1} was assigned to Symmetric C-OH stretching of lignin (Cao *et al*, 2012; Jonoobi, *et al*., 2010; Amine *et al*.,2001).

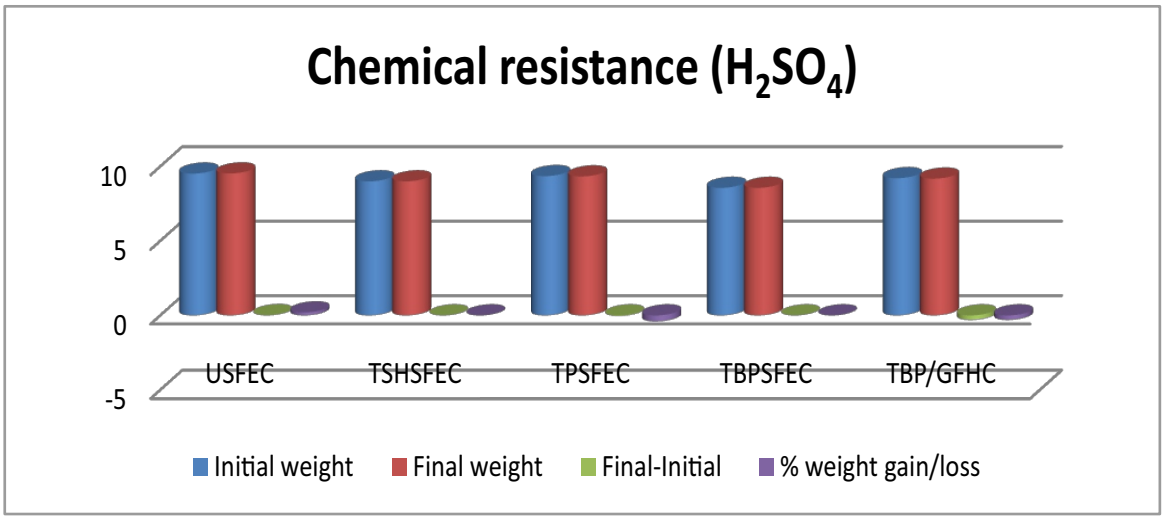

Figure 3. Chemical Resistance Acid (H_2SO_4) Test

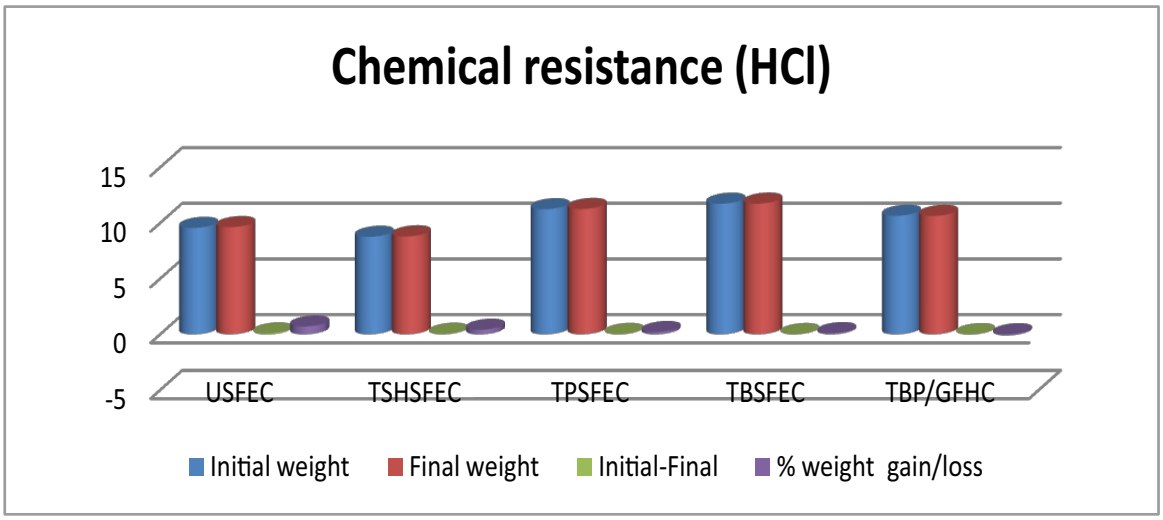

Figure 4. Chemical Resistance Acid (HCl) Test

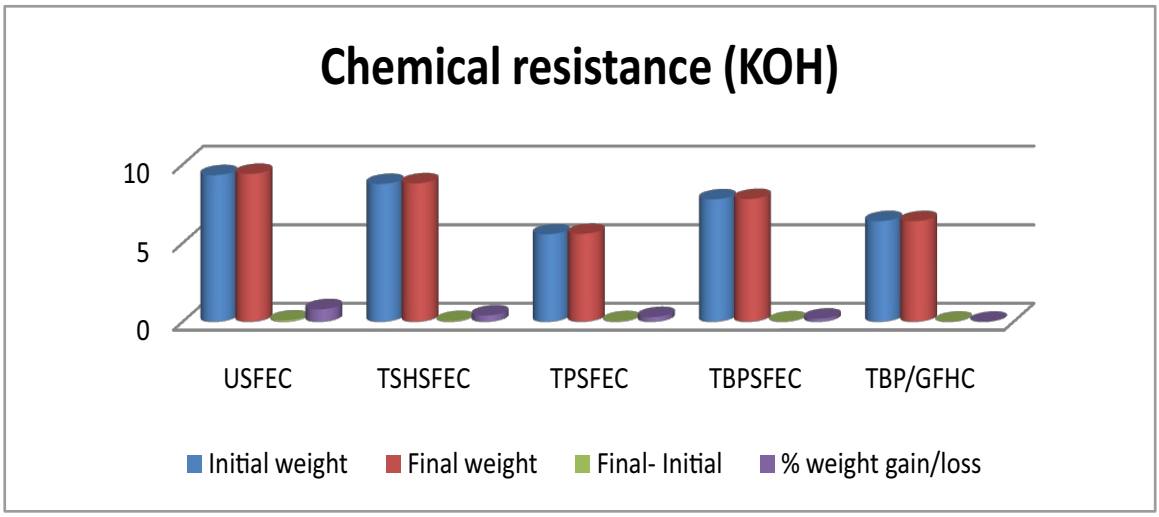

Figure 5. Chemical resistance Alkali (KOH) Test.

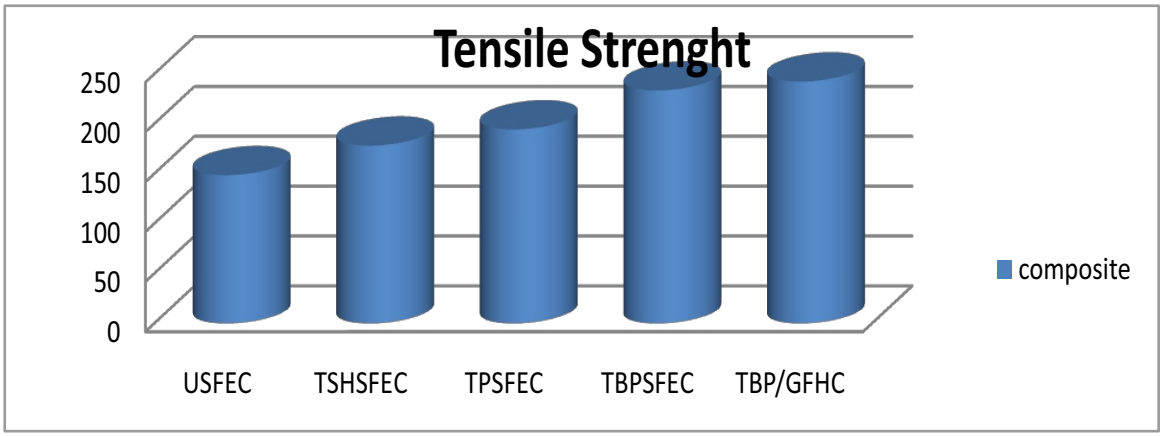

Figure 6. Tensile StrengthTest.

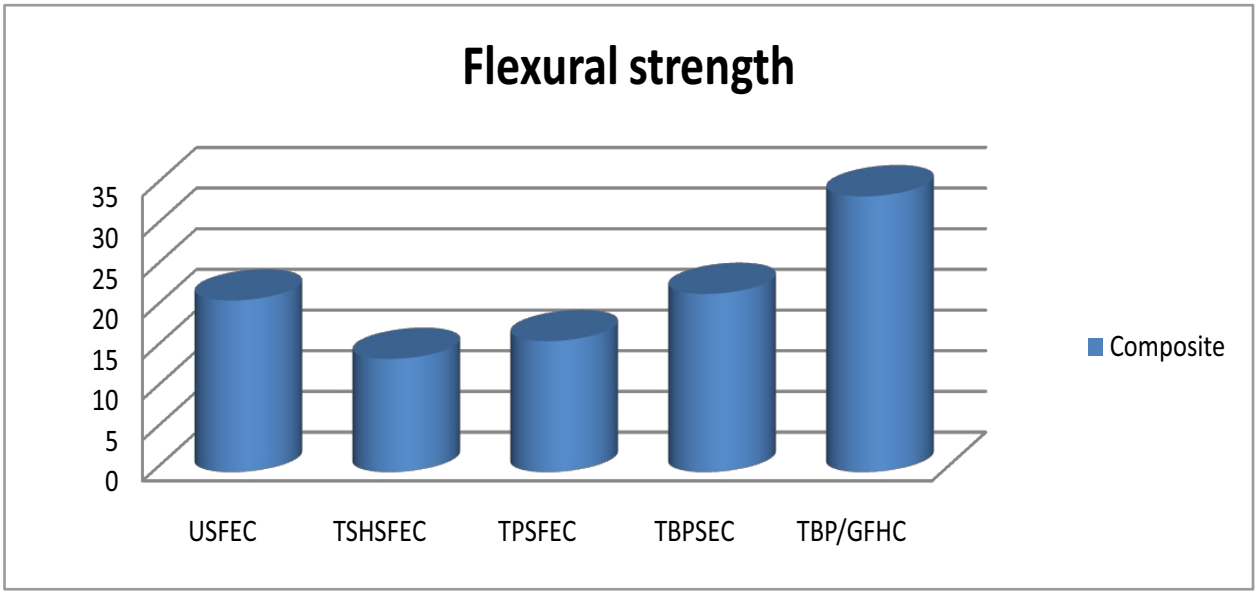

Figure 7: Flexural strength Test

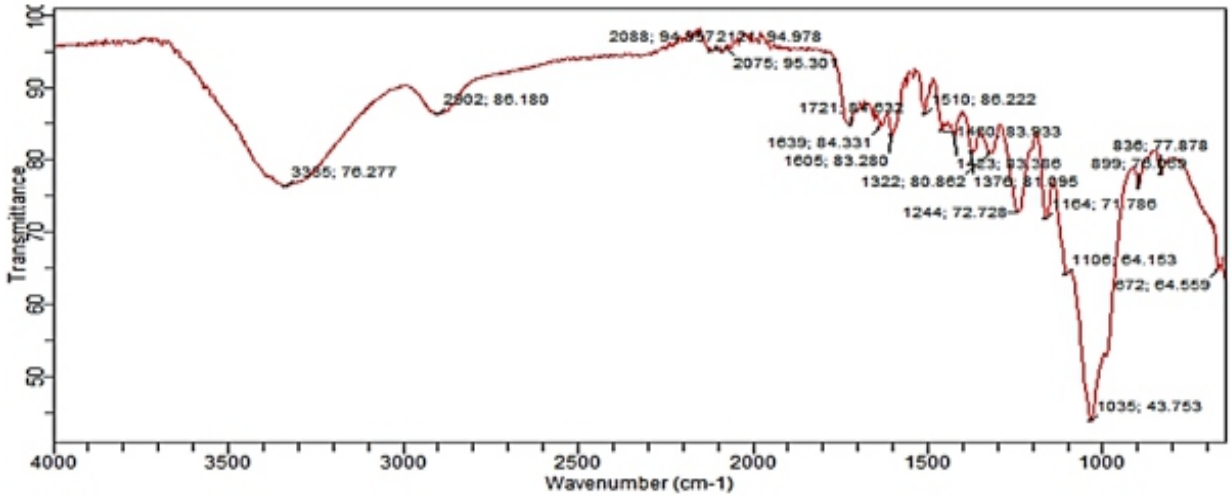

Figure 8: FTIR Spectrum of Untreated Sugarcane Fiber.

Sample	Bond	Range	Peak Absorption intensity (cm^{-1})
Untreated	O-H	3500-3000	O-H band stretching at peak 3335cm^{-1} strong and very broad
	C-OH	1160-1020	C-OH band stretching lignin at peak 1035 and 1032cm^{-1}

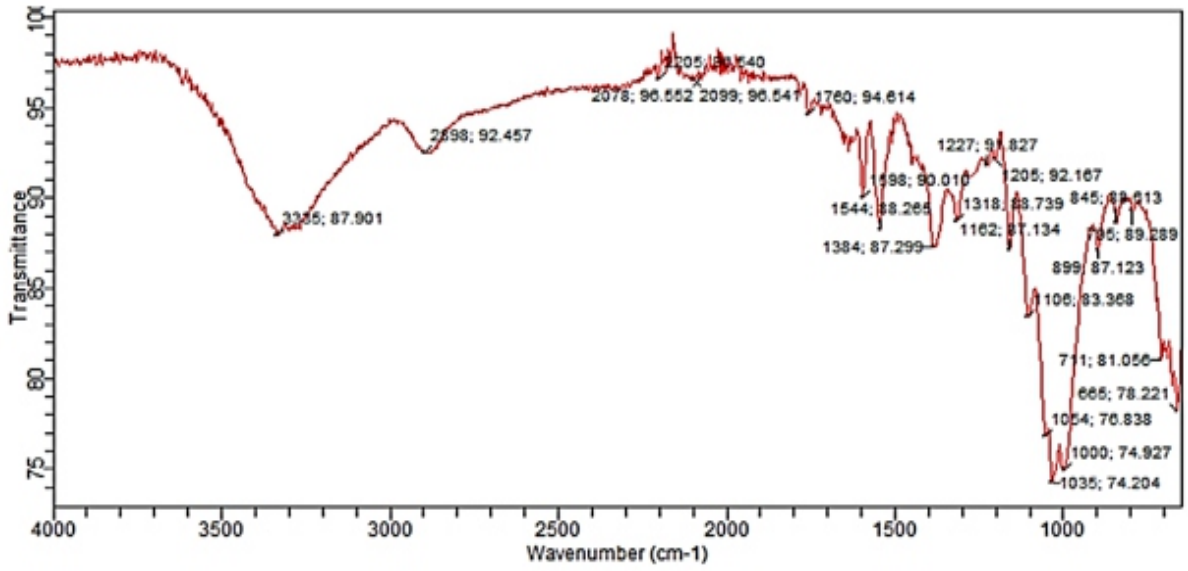

Figure 9: FTIR Spectrum of Treated Benzoyl Peroxide Sugarcane Fiber.

Table 2: FTIR Results.

	C-H	3000-2800	C-H stretching of medium aldehyde at peak 2802cm^{-1}
	CH_2	1420-1300	Stretching a symmetry bending at peak 1423cm^{-1}
Treated			
	C=O	1900-1600	C=O stretching carbonyl at peak 1760&1641cm^{-1}
	C-O	1300-1000	C-O stretching phenol at peak 1205 & 1203cm^{-1}
	C=C	1600-1475	Stretching of aromatic at peak 1544cm^{-1}
	C-C	1600-1400	Stretching alkenes at peak 1598cm^{-1}

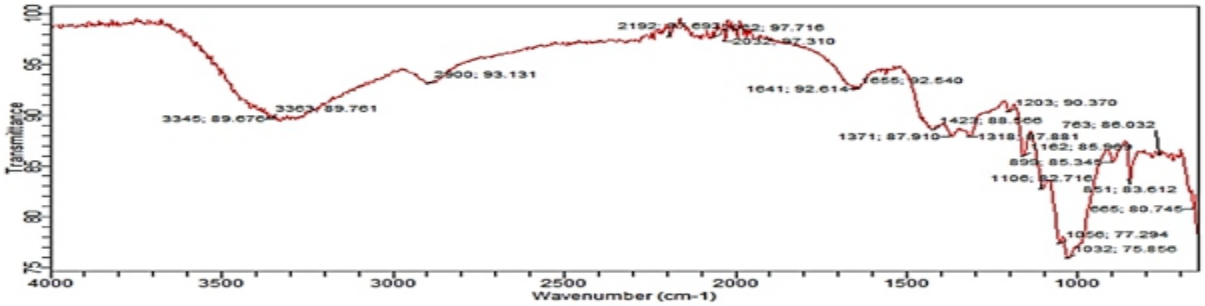

Figure 10: FTIR Spectrum of Treated Sodium Hydroxide Sugarcane Fiber.

4.0 CONCLUSION

This research work presents the fabrication of composite using sugarcane and glass fiber reinforced epoxy composite by hand lay-up method. Before fabrication the fiber undergoes treatment (Alkali, permanganate and benzolation),mechanical test (tensile and flexural) and FT-IR test. From the test, the following conclusions are drawn:the hybrid composite of BPTSC/glass fiberpossess high tensile strength,due to the hybridization with some amount of glass fiber, the composite of PPTSC and BPTSC fiber composite shows better result compared to ATSC and UTSC, natural fiber epoxy composites are generally lower in strength performance compared to hybrid composites.The incorporation of sugarcane/glass fiber enhances the mechanical properties and it lead to increases in the utilization of natural fiber in various applications.The merits of glass fibers (technical fibers) are good mechanical properties; which vary only small differences, while their demerit is difficulty in recycling.Several natural fiber composites achieve the mechanical properties of glass fiber composites and they are already applied, e.g., in automobile and furniture industries.

References

Abubakar, A (2004). Composite Blends and Biodegradable Products of Guna Protein/Cellulose Based Biocomposites *Journal of Pure & Applied Chemistry*.6: (4) 182-189.

Amine M, Nabil G, Nadia B,. (2001) Structural and thermal characterization of Moroccan sugar cane bagasse cellulose fibers and their applications as a reinforcing agent in low density polyethylene, *Composites:* Part B 52: (2) 233 – 238.

Arrakhiz F.Z., Malha M., Bouhfid R., Benmoussa K., and Qaiss A., (2013). Tensile, flexural and tensional properties of chemically treated alfa, coir and bagasse reinforced polypropylene,

Composites: Part B 47 (4), 35 – 41.

Bel - Berger, A.J., Mohammed, R.D., Taylor, A.C., Eger, C., Springer, S. and Egan, D, (1999). The Effect of Silica Nano-Particles and Rubber Particles on the toughness of Multiphase thermosetting epoxy polymers. *Journal of Material Science*, 40(18): 5083-5086.

Cao, Y., Chan, F., Chui, Y., and Xiao, H. (2012). Characterization of flax fibers modified byAlkaline, Enzyme and steam-heat treatments, *BioResources*7(3), 4109-4121.

Dadrasi A.,Fooladpanjeh S, Alavi and Gharahbagh A. (2019). Interactions between HA/GO/epoxy resin nanocomposites: optimization, modeling and mechanical performance using central composite design and genetic algorithm, *Journal of the Brazilian Society of Mechanical Sciences and Engineering* 41:(2) 63-80 ,doi: 10.1002/pc.20461.

Daniella R., Herman J.C., Maria O.H., Maria L, and Sandra M. L., (2009). Preparation and properties of HDPE/sugarcane bagasse cellulose composite obtained for thermo kinetic mixer*, Carbohydrate Polymers* 75:(4), 317 –321.

Gang Wang, Lichun Ma, Xiaobing Yang, Xiaoru Li, Ping Han, Chao Yang, Longliang Cong, WenzheSong,andGuojun Song (2018). Improving the interfacial and flexural properties of carbon fiber–epoxy composites via the grafting of a hyperbranched aromatic polyamide onto a carbon fiber surface on the basis of solution polymerization, *Journal of Applied Polymer Science*. 45;(2), 47232-47242, doi: 10.1002/ APP.47232.

Gumel, S. M., and Tijiani, A. A. (2017). Effect of Chemical Modifications on the Mechanical Properties of PiliostigmaThonningiiFibre Reinforced Epoxy Composites. *Chemistry +Environmental Sciences*. 1:(1) 1-15. https://doi.org/10.26762/ces.20170 1001.

Jawaid,M., Abdul Khalil, H. P. S and Abu Bakar .(2011). "Woven hybrid composites: Tensile andflexural properties of oil palm-woven jute fibres based epoxy composites". *Materials Scienceand Engineering* 528(15):5190–5195.

Jonoobi, M., Harun, J., Tahir, P., Zaini, L., Saiful, A.S., and Makinejad, M. (2010). "Characteristics ofnanofibers extracted from kenaf core" . *BioResources,5*, 2556–2566.

Josephine T. O., Benjamin D., (2016)Physical and Mechanical bagasse fiber for use as filler in unsaturated polyester composite. *International Journal of composite materials*, 6(2):48-54 doi:10.5923/J.CMaterials 20160602.02.

Lingtong L., Chun Y., Haibing X., Dong L., Pengcheng S., Yingdan Z. , Gang C., Xiaofei W., and Wenqing L., (2018). Improving the interfacial properties of carbon fiber–epoxy resin composites with a graphene-modified sizing agent. *Journal of Applied Polymer Science*, 136 (9) 47112-47132, doi: 10.1002/APP.47122.

Maneesh T, Singh V. K., Gope P. C., Arun K. C. (2012). Evaluation of Mechanical Properties of Bagasse-Glass Fiber Reinforced Composite*,*

Journal of Material Environmental Science, 3 :(1) 171-184.

Mathur, V.K., (2006). Composite materials from local resources *Construction and Building materials*, 20, 470–477.

Mohd R., Prabhat K. S., and Earnest V. P., (2015) Study testing & analysis of composite material based on munja fiber. *The International Journal of Engineering and Science* 4 :(4) 60-65.

Nazari G., Jafari A, Mohtasebi S., Tabatabaeefar A, Sharifi A, (2008). Effects of moisture content and level in the crop on the engineeringproperties of alfalfa stems. *Biosystems Engineering*101(2): 199–208.

Niharika, M., and Acharya, S.K. (2013). "Tensile flexural and Intermolecular sheer properties of luffacylindrical fiber reinforced epoxy composite*".International Journal of Macromolecularscience,* 3(2) 6-10.

Punyapriya M.S. and Acharya K., (2010). Anisotropy abrasive wear behavior of bagasse fiber reinforced polymer composite*, International Journal of Engineering, Science and Technology*2 : (2) 104-112.

Şahin Y and Mehmet M. İ., (2018). Stress and Rigidity Comparison and Improved Vibration Control of Flexible Carbon-Fiber and Epoxy-Glass Composite Manipulators Under End-Point Load, *Materials Research Express*, 1 (4) , 1705-1712doi: https://doi.org/10.1088/2053-1591/aaf700.

Satyanarayana, K., Arizaga, G., and Wyphych. F. (2008).Biodegradable composite based lignocellulosic fiber – An overview. *Journal of polymer science*, 34:(3) 982-1021.

Sherif M, Mahmoud F, Rashad R. M., and Hamdy E., (2012) Fabrication and Characterization of Starch Based Bagasse Fiber Composite*, Materials and Manufacturing, Parts A*, 21;(2) 9–15.

Singal P and Tiwari S.K., (2014). The effect of various treatment on the damping properties of jute fiber reinforced composite. *International Journal of Advanced Mechanical Engineering*. 4:(4) 413-424.

Sumit Das Lala, Ashish. B. Deoghareand Sushovan Chatterjee (2018). Effect of Dual Pre-treatment on Mechanical, Morphological, Electrical and Thermal Properties of Rubber Seed Shell-Reinforced Epoxy Composites. *Arabian Journal for Science and Engineering*, 44;(2)845-856. doi: https://doi.org/10.1007/s13369-018-3302-3.

Velmurugan, G., Vadivel, D., Vengalesan, S. P., and Mathiazhagan, A. (2012) Tensile analysis of natural fiber reinforces composite, *International Journal of Mechanical and Industrial Engineering*, 2(4), 2231-6477.

Venkateshwaran, N., ElayaPerumal A.,AlavudeenA.,andThiruchitrambalam M. (2011)Mechanical and water absorption behaviour of banana/sisal reinforced hybrid composites. *Materials and Design* 32: 4017–4021.

Wang, B., Panigrahi, S., Tabil, L., and Crerar, W. (2007). Pretreatment of flax fibres for use in rotationally molded biocomposites. Sage publication, *Journal of Reinforced Plastics andComposites, 26*(5), 447-463.

Xie, Y. J., Hill, C. A. S., Xiao, Z. F., Militz, H., and Mai, C. (2010). Silane coupling agents used fornatural fiber/polymer composites: A review.Composites Part A: *Applied Science andManufacturing*, 41(7), 806-819. doi:10.1016/j.compositesa.2010.03.05

Xue, L., Lope, G.T., and Satyanarayan, P. (2007). "Chemical treatment of natural fibre for use innatural fibre-reinforced composites: *A review"*. *Polymer Environment, 15*(1), 25-33.

Nigerian Journal of Polymer Science and Technology, 2019, Vol. 14, pp53-59

Received: 10/12/2018 *Accepted: 16 September, 2019*

Production of Green Free Binder From Fly Ash and Slag Industrial Waste

Sulaiman M. S* and Babayo H.
Department of Pure and Industrial chemistry, Bayero University Kano, P.M.B 3011, Kano Nigeria

***Corresponding author email:**sdanguguwa@gmail.com

Abstract
Methods of recycle and utilization of industrial waste are currently being practiced in many countries in an effort to minimize industrial waste and protect the environment. In this study, the synthesis, process, composition, water absorption, Fourier transform infrared spectroscopy (FTIR) and the mechanical properties of geopolymers generated from two different kinds of industrial waste (i.e. coal fly ash and furnace slag) were explored. For the two geopolymers with identical raw materials, variable parameters involved in the synthesis were examined to investigate the extent and degree of geopolymerization. Compression test was used to examine the compressive strength and durability. The compressive strength for geopolymers synthesized by each of fly ash and furnace slag were found to be 0.00714N/mm^2 and 0.008692 N/ mm^2 respectively. Also the result for water absorption test obtained was used to calculate the absorption percentage for both fly ash geopolymer and furnace slag geopolymer to be 0.12% and 0.01% respectively. In FTIR spectra it has seen that geopolymerisation has been achieved successfully since the major fingerprint for the geopolymer has been obtained at ~1000cm^{-1}, 3593cm^{-1}, 1644cm^{-1}, 1460cm^{-1}, 775-650cm^{-1}, 558cm^{-1}, and ~460cm^{-1}.Owing to the consistent properties of both fly ash-based geopolymer and slag-based geopolymer, they were selected to be examined as construction materials used in the production of bricks, concrete for pavement, concrete for structures (e. g bridges), highway base materials. The results showed that varying the polymer composition (e.g $SiO_2.AL_2O_3$ ratio), NaOH concentration, curing temperature can alter the tensile strength for tailored sensing applications for concrete structures.

Keywords: *Geopolymer, Green Binders, Fly ash, Slag , Waste material*

1.0 Introduction

Geopolymer binders are an emerging class of cementitious material that can be manufactured from industrial by-products, such as fly ash and slag, which can be used as 100% replacement for portland cement in construction applications (Allouche, 2013). The term "Geopolymer" was used by Davidovits to describe the inorganic aluminous-silicate polymeric gel, resulting from reaction of amorphous aluminosilicates with alkali hydroxide and silicate solutions (Aldred and Day, 2012).

Each year, the concrete industry produces approximately 12 billion tonnes of concrete. This makes the demand for Portland cement to be 1.6 billion tonnes per annum worldwide, thereby making the cement industry consuming considerable amounts of virgin materials (limestone and sand) and energy. Each tonne of Portland cement requires about 1.5 tonnes of raw material as well as 1700-1800 MJ/tonne clinker of energy. As a result, with the manufacture of one tonne of cement, approximately 0.8 tonnes of CO_2 are launched into the atmosphere making the cement industry accounts for worldwide emission of CO_2 to about 5-7% (Jeyalakshmi et. al., 2015).

Due to exponential growth in urbanization and industrialization, by-products from the steel industries such as furnace slag and coal combustion by-products (CCBs) from power plants are becoming an increasing concern for recycling and waste management. At some time, studies have revealed usage of Geopolymer in concrete as a partial replacement for Ordinary Portlanr Cement (OPC) .Geopolymer is one of the recently introduced solution to the above mentioned environmental issues, i.e disposal of industrial waste in ponds and high CO2 emissions of OPC production (Akbari et al., 2015). During past years, different raw materials which are rich in Al-Si such as fly ash, bottom ash, and slag have been used to generate geopolymer binders in order to replace OPC in concrete application in construction industry (Akbari et al., 2015). This lead to reduction in OPC consumption and consequently, decline in the CO2 emissions, since concrete is the second most used processed material in the world by weight after water (Allouche, 2013). Starting material plays an important role in the formation of geopolymer. Materials rich in silicone (like fly ash, slag and rice husk) and materials rich in Aluminum (clays like kaolin) are the primary requirement to undergo geopolymerization. The majority of studies conducted to date have used alkali silicate solutions for dissolution of raw materials to form the reactive precursors required for geopolymerisation. It has been shown that silicate activation increases the dissolution of the starting materials and give rise to favourable mechanical properties (Albakri, 2011).

The alkali-activated binders give the possibility to utilize rejected inorganic wastes; the properties of such binders are often better than those of standard Portland cement (ŠKVÁRA, et al 2005). Montes and Allouche (2013) reported that geopolymer concrete (GPC) offers high resistance to acid and sulphate attack, high compressive strength, and rapid strength gain rate and undergoes little shrinkage. Geopolymer offer high mechanical strength, along with high corrosion resistance and resistance to elevated temperatures (up to 2800˚ F). Potentially a cost effective, low cost, locally available refractory material for low-pH high temperature biomass incinerators (Allouche, 2013). Aldred and Day (2012) reported that geopolymer concretes in general including this particular geopolymer tend to have higher tensile and flexural strength relative to the compressive strength than Portland cement based concrete. This appears due to the strong bond of the geopolymer gel to the aggregate particles and would be expected to improve crack resistance of geopolymer concrete. High resistance against sulfate and chlorine corrosion, very good mechanical properties also high concentration of alkali activator limits the industrial acceptation of fly ashes as basic material.

Other advantages of geopolymer include reduction in waste material such as fly ash and bottom ash, less water consumption in comparison to OPC, less mining activities and natural minerals utilization, and higher resistance to fire and corrosion (Akbari et al., 2015) and also very resistant to many durability issues that can be plague to conventional concretes (Davidovits, 2013). Geopolymer blended concrete have been used successfully in concrete for many years in many countries throughout the world where structures have to be designed for durability requirements in very aggressive environment (Ramachandra et al., 2014). This project is aimed at producing geopolymer using fly ash and furnace slag.

2.0 Materials and Methods

2.1 Sample Collection and Characterization

The fly ash and slag samples used in this study were obtained directly from Shehu Musa Yar'adu steel rolling company Katsina State

in Nigeria as a waste from coal briquette used as source of energy in local stove, and as waste slag from their furnace respectively. Table 1 below shows their chemical composition as obtained from Shehu Musa Yar'adu steel rolling company laboratory. Also the raw fly ash and slag samples were analysed for molecular structure using Fourier transform infrared spectroscopy (FTIR). (Perkin Elmer Spectrum 100). The tensile strength, density and water absorbance was also determined using standard methods.

2.1 Materials for making Geopolymers

The alkaline activator was a combination of sodium hydroxide and sodium silicate solutions. The sodium hydroxide solids were laboratory grade in pellets form, with a specific gravity of 2.15, 97% purity. Distilled water was used for the preparation of the activator solutions.

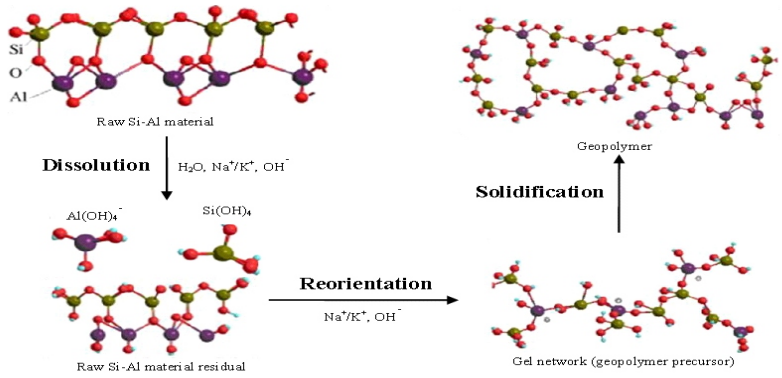

Fig 2: Sketch of a typical reaction mechanism of geopolymerization

.

2.2 Geopolymer Synthesis

375.0g of fly ash and slag were measured and put into two separate plastic containers, 14 molarity solution of Lye (41g NaOH pellets was dissolve in 60.7g of water to produce NaOH solution), which was prepared carefully due to excessive heat released during the reaction and allowed to cool down at room temperature. 36.5g sodium-silicate was also dissolve in 62.5g of water which was immediately added to the cooled Iye-solution and stirred together to make a water glass solution know as alkaline activated solution of 226.5g. The water glass was prepared twice and each was poured in to the above measured fly ash and slag samples separately and mix for 10 minutes with a mechanical mixing paddle, the mix was allowed to sit for 5 minutes, and each was poured into a mould which has already being sprayed with mold release(Pam cooking spray). The geopolymer paste was divided into two parts, one was cured in a pre-heated oven at 200°F for 4 hours, after which it was removed from the oven while the other part was cured at 30°C.The resulting four geopolymer blocks G1 for fly ash and slag cured at 30°C and G2 for fly ash and slag cured in the oven at 200°F were produced for comparison purposes.

2.3 Fourier Transform Infrared Spectroscopy

Fourier Transform Infrared spectroscopy technique is being used extensively to perform reaction product analysis on cementitious materials. Spectroscopic techniques provide molecular fingerprints of materials as every compound exhibit different types of vibrations. Sateesh(2014).The peaks arising at different wavenumbers with different intensities explain the type of bond formations and vibrations in the material matrix. This helps to identify the different compositions in a material. For alkali activated aluminosilicates the peaks determining the

silicate region are concentrated as the structure is defined by these chains. The analysis can be done to perform various studies like the changes occurring with time, temperature, mix proportions, curing conditions etc. The position of the Si-O-T peak (where T is Al or Si) is observed from the FTIR spectra of these samples. The range of Si-O-T peak for geopolymers is from 900-1200 cm−1. The position of peak varies due to factors like time, mix proportion etc. According to geopolymers theory an aluminum gel is formed at the beginning which later on forms a gel with more silicates in the structure polymerizing to form a solid product. When analyzing with time, the peak values of the Si-O-T peak can change due to physiochemical reactions. The decrease in wavenumber indicates lower force constant which means lower bond energy or strength. This provides us with information about the lengthening or changes in bond angles. Hence the changes happening in the aluminosilicate structures after the addition of alkali activators can be analyzed from the FTIR spectra of the reactionproducts. The obtained FTIR spectrum of a material is an integrated curve mapping all the peaks determining various vibrations. The peaks with higher intensities and ranges can overlap smaller adjacent bonds and form the integrated peak. These smaller peaks can be of valuable significance for analyzing the material (Sateesh2014).

Table 1: Chemical composition of fly ash and slag sample

Component	SiO2	Al2O3	Fe2O3	CaO	MgO	SO3	K2O	Na2O	TiO2	P2O5
Fly ash(wt. %)	53.79	32.97	5.51	1.84	0.92	0.46	1.76	0.37	2.1	0.15
Slag(wt. %)	22.38	8.09	2.31	37.44	3.51	7.46	1.27	<0.11	0.51	_

3.0 Results and Discussion

3.1 FourierTransformInfraredSpectroscopy

A summarized FTIR spectra peaks for fresh sample (Fly ash), room temperature geopolymer and Oven cured geopolymer (80oC*) are presented in Table 2*. The strong peak at ~1000 cm-1is associated with Al-O and Si-O asymmetric stretching vibrations and is the fingerprint of the geopolymerisation. The bands seen at 3593 cm-1 is attributed to stretching vibration of -OH and 1644 cm-1 is bending vibrations of H-O-H. Atmospheric carbonation is evident at 1460 cm-1. In the region of 775-650 cm-1, the bands are due to symmetrical vibrations of tetrahedral groups (TO4). The band at 558 cm-1 is corresponding to double-ring linkage. The peak at ~460 cm-1 is assigned to in-plane bending of Al-O and Si-O linkages.

Table 2: Summarized FTIR spectra peaks

Fly Ash			
Specimen	Fresh Sample (Fly ash)	*Room temperature* Geopolymer	*Oven cured* Geopolymer (80°C)
Peaks (cm^{-1})	3490-866	3309-866	2918-968
Slag			
Specimen	Fresh Sample (slag)	*Room temperature* Geopolymer	Oven cured Geopolymer (80°C)
Peaks (cm^{-1})	2922-877	3324-866	3324-866

3.2 Water Absorption Test

Low water absorption level is a good indicator of limited open porosity that can inhibit the high flow of water into the concrete. The durability of concrete has been evaluated in this study through parameters related to permeability. The absorption study was done to know the permeability characteristics of geopolymer concrete and was performed in accordance to ASTM C 642-82. The specimens used for this water absorption criteria test are G1 cured at room temp and G2 cured in the oven at 80 ^{o}C.

Table 3: Assessment criteria for H_2O Absorption (CSB, 1989)

Absorption %	Absorption Rating	Concrete quality
< 3.0	Low	Good
3.0 to 5.0	Average	Average
> 5.0	High	Poor

$$\text{Absorption percentage} = \frac{W2 - W1}{W1} * 100 \qquad 3.1$$

Where

W1 = weight of specimen after complete drying 80 oC (kg)

W2 = Final weight of surface dry sample after immersion in water (kg)

3.3 Durability analysis

The reliability of materials can be determined by measuring its resistance to fracture, either ductile or brittle and fracture toughness. However, durability analysis reveals both toughness and fracture types. The durability analysis is known to give a good indication of how reliable the materials are likely to be under conditions of shock. It can be obtain using the equation *(3.2)*.

$$DA = \frac{\text{Average breaking force}}{\text{Cross sectional area}} \qquad 3.2$$

$$\text{Cross sectional area} = L\,(25mm) * b\,(10mm) = 250mm2$$

$$DA\ (\text{Fly ash}) = 3.600/250 = 0.0144$$

The result shows that the material prepared are resistant to corrosion. No signs of sample deterioration were observed. In contrast to Portland cement, no visible damage of sample occurred even if they were kept in corrosive environment for days. From the result it shows that geopolymer produce from slag will be more durable compared to that of fly ash.

3.4 Compressive test

The compressive test was cal*culated using equation 3.4*

$$Fc = \frac{p}{a} \qquad 3.4$$

Where;

Fc = Rectangle compressive strength in N/mm2

P = Retangle compressive load causing failure in N

A = Cross sectional area of cube in mm^2

$$Fc\ (\text{Fly ash}) = 1.785N/250mm2 = 0.00714$$

$$\text{Fc (Slag)} = 2.173\text{N}/250\ \text{mm2} = 0.008692$$

The values of compressive strength of geopolymer materials exposed no signs of any expansion and also indicated that the curing conditions influenced the physical properties of geopolymer samples. The strength of geopolymer cured in the oven is much stronger compared to the one cured in at room temperature. Also the slag based geopolymer is stronger than the fly ash geopolymer.

4.0 Conclusion

Utilization of fly ash reduces the cost of the product where fly ash is cheaper than cement. Fly ash as Supplementary cementing materials (SCM) prevents pollution, conserves natural resources and protects the environment. The alkali-activated binders give the possibility to utilize rejected inorganic wastes. The properties of such binders are often better than those of standard Portland cement. Geopolymer binders cover a wide range of possible source materials and activators. The products resulting from the alkaline activation of fly ash exhibit an amorphous character with minority crystalline phases. The properties of alkali-activated fly ashes are dependent on the method applied to their preparation and, in particular, on the concentration of the alkaline activating agent as well as on the humidity conditions. Optimum results were obtained when the bodies were prepared under 'dry' conditions. The materials on the basis of alkali-activated fly ashes possess an excellent durability in the corrosive environment of salt solutions, they exhibit very good frost resistance and can resist the effect of temperatures of up to about 600°C. The low shrinkage and heat of hydration as well as the high tensile strength means that the material may have technical advantages over traditional concrete, particularly in structural elements subject to external restraint.

References

Abdullah M.M.A. (2011). Mechanism and Chemical Reaction of Fly Ash Geopolymer Cement. A Reviewed. International Journal of Pure and Applied scientific and Technology, 6(1), pp.35-44

Akbari, H., Mensah-Biney, R. and Simms, J. (2015) Production of Geopolymer Binder From Coal Fly Ash to make Cement- Less Concrete. Proceedings of the World of Coal Ash (WOCA). Nasvhille.

Allouche E. (2013) High Durability ‘‘Green” Inorganic Polymer Binders for Sustainable Construction..Louisiana. Technical University College of Engineering and Science.

Albakri A.M.M. (2011). Mechanism and Chemical Reaction of Fly Ash Geopolymer Cement. Journal of Asian scientific Research. 1 (5): 247-253

Aldred, J., and Day, J. (2012). Is Geopolymer Concrete a Suitable Alternative to Traditional Concrete?Proceedings of 37th conference on our world in concrete and structures. Singapore.

He, J. (2012). Synthesis and Characterization of Geopolymers for Infrastructural Applications. PhD. thesis Louisiana State University, Unpublished.

Jeyalakshmi R., Dhinesh. M., Baskar S. R., Raja, N.P. (2015). Geopolymer; Portland cement Free Binder System From Industrial Wastes. International Journals of Chem Tech Research 7(7): 2846-2854.

Davidovits, J. (2013). Geopolymer Cement: A review. Geopolymer Science and Technics, 21: 1-11

Davidovits, J. (2011). Geopolymer Chemistry and Applications 3rd Edition, Saint-Quentin, France. Institute Geopolymere.

Palomo, A., Grutzeck, M.W., Blanco, M.T.

(1999). Alkali-Activated fly ashes: A cement for the Future" Cement and Concrete Research 29:1323-1329.

Ramachangra, M..L., Anvekar S.R. and Yogananda, M.V. (2014). Recent Developments in the Indian Concrete Industry in the use of GGBS in Concrete at RMC Batching Plants as Partial Replacement to OPC Cement and its effects on Concrete Durability and Sustainability in the Indian context. International Congress on Durability of Concrete. India.

Skvara F., Jilek T. and Opecky L. (2005). GeopolymerMaterials Based on Fly Ash Ceramic-Silicate. Department of glass and ceramics institute of chemical technology praque& Department of structural mechanic, Czech Technical University, 49, 195-204.

Sunku, J. (2006). Advantage of using Fly Ash as Supplementary Cement Material (SCM) in Fiber Cement Sheet Inorganic Bounded Fiber Composite. Proceedings of 10th International Inorganic Bonded Composite Conference.

Sateesh B.M (2014). FTIR Analysis of Alkali Activated slag and fly Ash using Deconvolution Techniques. M.Sc. thesis, Arizona State University, Unpublished

Xu, H. and Van D. (2000), The Geopolymerisation of Alumino-Silicate Minerals, International Journal of Mineral Processing 59, pp. 247-266

Nigerian Journal of Polymer Science and Technology, 2019, Vol. 14, pp60-66

Received: 30/12/2018 Accepted: 02/10/ 2019

Preparation, FTIR Analysis and Morphological Studies of PVAc/Starch-g-Oleic acid Polymer blends.

[*1]Ahmad, Y. M. and [2]Musa, H.

[1]*Department of Chemistry, Sa'adatuRimi College of Education,Kumbotso,Kano. P.M.B. 3218, Nigeria.*
[2]*Department of Pure and Industrial Chemistry, Bayero University, Kano. P.M.B. 3011, Kano, Nigeria.*

[*]Corresponding Author: yusufmusa900@yahoo.com

Abstract

Oleic acid grafted cassava starch was blended with poly (vinyl acetate) PVAc, in a PVAc/starch-g-oleic acid w/w ratio of 20:80, 40:60, 50:50 and 80:20 at room temperature. The blend films were characterized by FTIR-analysis, a strong absorption band at 1150-1350cm^{-1} is due to C-O-C in the grafted starch, another peak at 1000-1260cm^{-1} in these spectra is due to C-O absorption band from the starch component, carbonyl due to PVAc appear at 1730-1737cm^{-1} and C-H stretching band at 2924cm^{-1} in all the spectra and its intensity increases upon grafting. The scanning electron micrographs (SEM) of these blends show an improved compatibility when compared with PVAc/Native starch images. However, it was observed that 50:50 PVAc/starch-g-oleic acid w/w ratio, showed better compatibility and minimum phase separation followed by 20:80 and 40:60 then 80:20. This may be due to the high oleic acid content which enhance the hydrophobicity of the blend.

Keywords:FTIR-analysis, morphological studies, polymer blends and starch-g-oleic acid.

1.0 Introduction

Blending of polymer is an interesting route for producing new materials basically due to economic aspects (Pereira et al, 2010). The miscibility between the polymers is a very important factor in producing desired blends (Utracki, 1989). Generally, most of polymer blends are incomparable, resulting in materials with weak interfacial adhesion and thus poor mechanical performances, therefore, the great challenge in the field of multiphase polymer blend research in the manipulating of the phase structure via a judicious control of the interfacial interaction between the components. Polymer modification by chain grafting is a well known strategy to modulate polymer properties or to provide them with new ones such as hydrophilicity / hydrophobicity balance, compatibility in blends and composites and self assemblingbehaviour. Etc (Bertoldo et al, 2012). One of the classical methods to ensure adhesion between the phases (reducing interfacial tension) is the used of third component a compatibilizer, which results in a finer and more stable morphology better adhesion between the phases and consequently better mechanical properties of the final product. (Elias et al 2009).

2.0 Experimental

2.1 Materials and Methods

Poly (vinyl acetate)PVAcprepared in the lab by suspension polymerization, with

molecular weight of 1133gmol^{-1} , native cassava starch, Oleic acid, DMSO, potassium persulphate, acetone, ethanol, Scanning Electron Microscope (SEM) , model No: PW100-002 magnification: 80x-100,000x, Accelerating voltage: 5-15kv, FTIR- machine (cary 630, Agilent Technology at frequency range 4000-600 cm^{-1}), vaccum oven, magnetic stirrer with hot plate, round bottom flask and glass plates.

2.2 Preparation Of Starch – Oleic Acid Graft Co-Polymers

About 3g of cassava starch was dissolved in 30ml DMSO, 15.6g Oleic acid was added to this and 0.5g $K_2 S_2O_8$ was used as catalyst. This reaction mixture was heated 100±5 ^{0}C for 6hrs in a round bottom flask with magnetic stirring. Graft polymer formed was separated by precipitation from ethanol, filtered, washed thrice with ethanol the sample was air dried at room temperature.

2.2.1 Determination of Percentage Graft Yield

Percentage of graft polymer was calculated gravimetrically. The calculation of grafting yield percentage was done using the following equation:

$$\text{Graft yield (\%)} = \frac{Wg}{Ws+Wa} \text{ X } 100$$

Where; Wg = weight of grafted polymer
Ws= weight of starch used
Wa= weight of acid used (the percentage graft yield was 17%).

2.3 Preparation OfPVAc/ Starch-g-Oleic Acid Blends

PVAc/ Starch-g-Oleic acid w/w ratio of 20:80, 40:60, 50:50 and 80:20 were prepared. these was achieved by dissolving weight percent of PVAc in acetone and weight percent of starch in DMSO, then these solution were mixed and stirred vigorously at room temperature. The resulting solution was casted onto a glass plate and allowed to dried in vaccum at 30^{0}C. same procedure was used for PVAc/ native starch blend. However, PVAc starch 20:80 ratio was to be highly brittle (no film forming) hence couldn't be characterized (Byun et al, 2012).

3.0 Results and Discussions

The native cassava starch, PVAc, Oleic acid and polymer blends were characterized by Fourier Transformed Infrared Spectroscopy (FTIR) and the spectra are presented below:

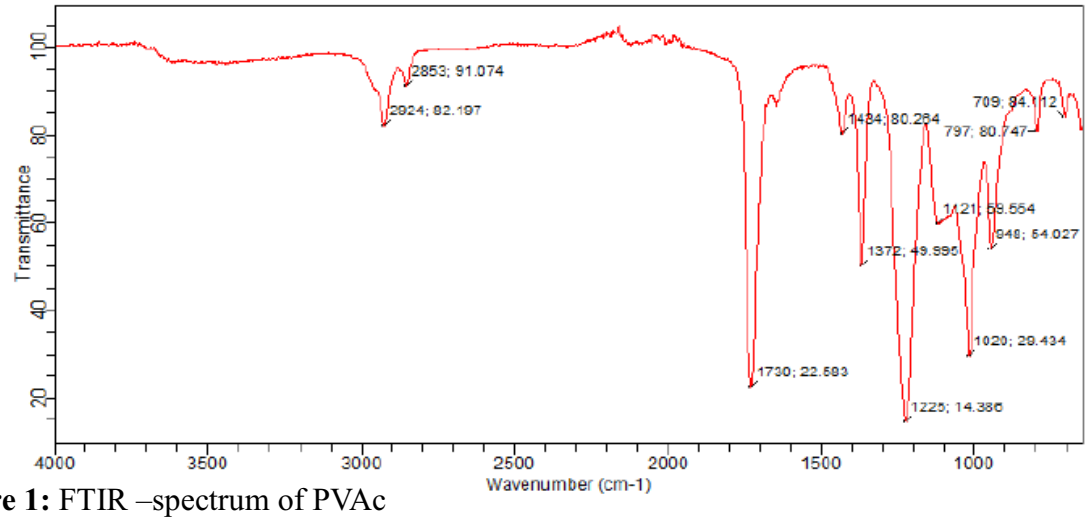

Figure 1: FTIR –spectrum of PVAc

.

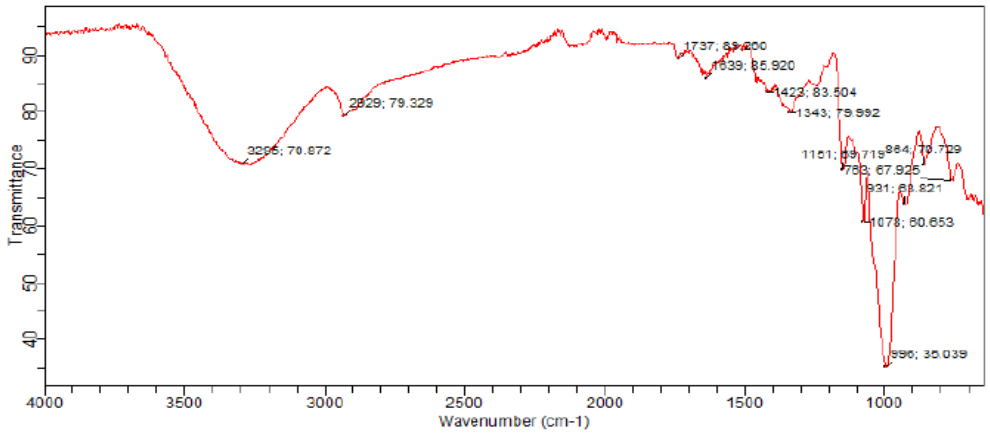

Figure 2: FTIR-spectrum of native cassava starch

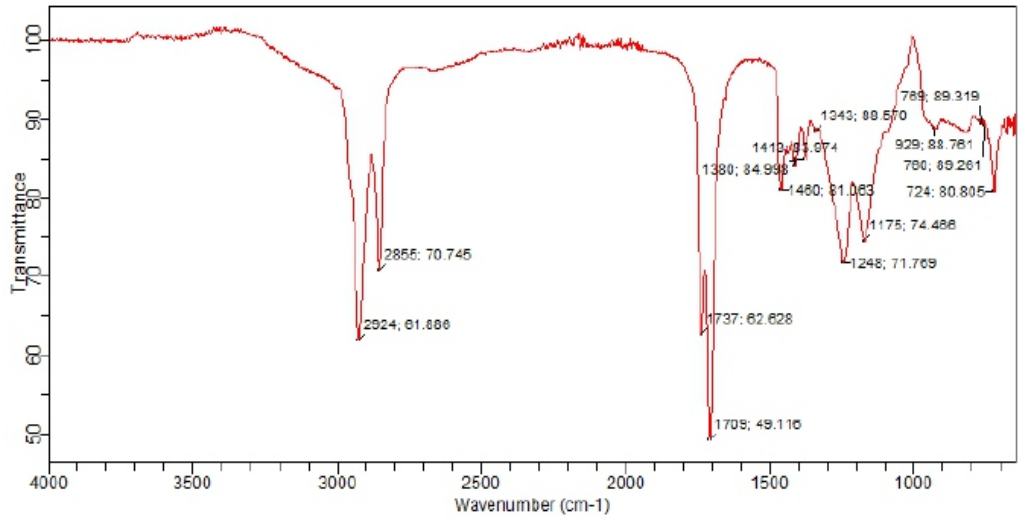

Figure 3: FTIR spectrum of Oleic acid

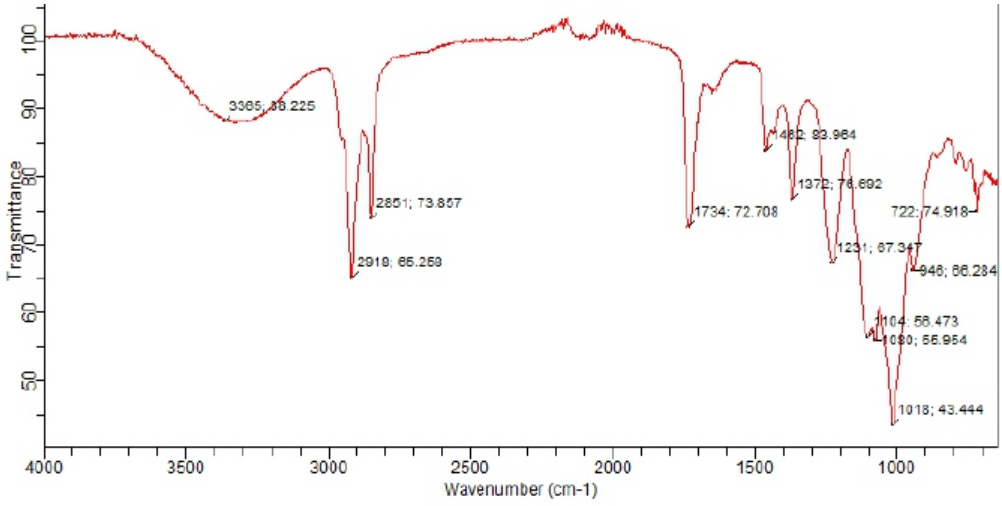

Figure 4: FTIR-spectrum of PVAc/starch -g-

Figure 4: FTIR spectrum of PVAc /starch-g-Oleic acid

The spectra of the native starch, PVAc, Oleic acid and the PVAc /starch-g-Oleic acid are shown in the figure 1-4. The introduction of the oleic acid in to the starch lead to the formation of characteristic absorption band at1231cm^{-1} in figure 4 within the range of1150cm^{-1}-1350cm^{-1}indicating C-O-C bond which is the point of interaction, peak at 1151cm^{-1} , 1078cm and 996cm all are in the range of 1000-1260cm^{-1} are due to the C-O (alkoxy) stretching band in the starch component. Strong absorption band at 1730cm^{-1} in Figure 1, 1734cm^{-1} in Figure 4, and 1737cm^{-1}in Figure 2 and 3 respectively are due to C=O from PVAc, Starch and Oleic acid.C-H stretching band appeared at 2924cm^{-1} in all the spectra and its intensity increases upon grafting. (Chai and Isah, 2013). A broad band due to hydroxyl group in the native starch appeared 3296cm^{-1} its intensity decreases upon grafting since the starch-acid reaction is through one of the primary hydroxyl group present in the starch.

3.1 Morphology of PVAc/native cassava starch blends

The micrographs of the PVAc/native cassava starch were obtained by Scanning Electron Microscopic analysis (SEM). It was observed that there was a clear spherulite in the native starch which were found in homogenity with that of PVAc in each of the blend ratios, but the lower the amount of starch the more the miscibility and the better the roughness and the compatibility as found in 80/20 (PVAc/starch ratio) though there was good interaction in (50:50 ratio) than in 40/60 which shows little craft and some defects in the morphology and phase separation (perier et al, 2010).

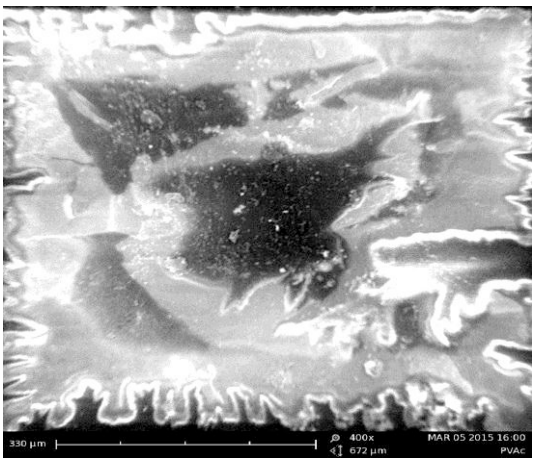

Figure 5 : PVAc 400x

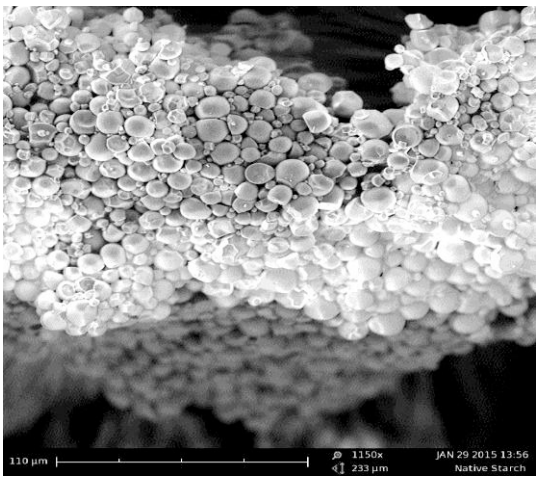

Figure 6 : Native cassava starch 1150x

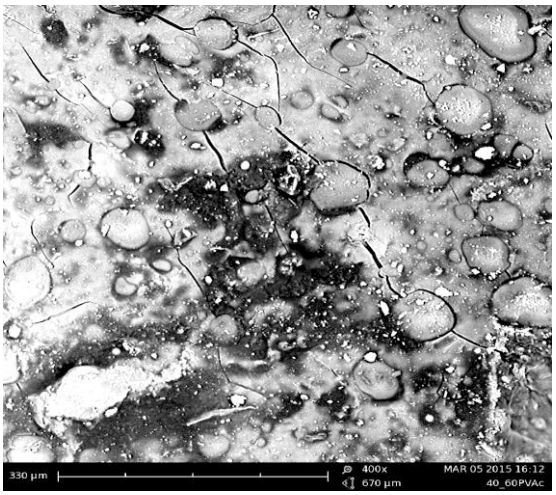

Figure 7: PVAc/ starch 40/60 400x

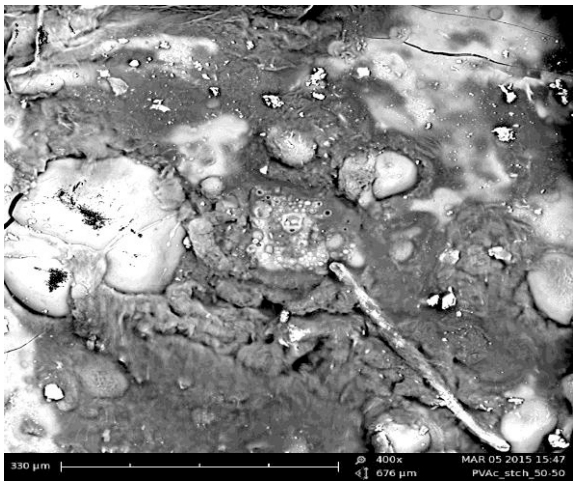

Figure 8: PVAc / starch 50/50 400x

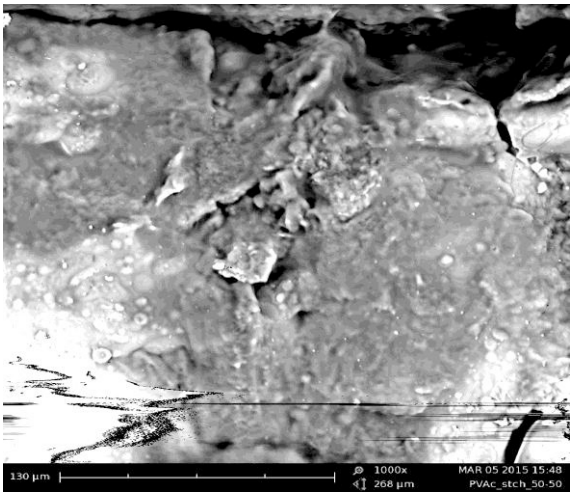

Figure 9: PVAc / starch 50/50 1000x

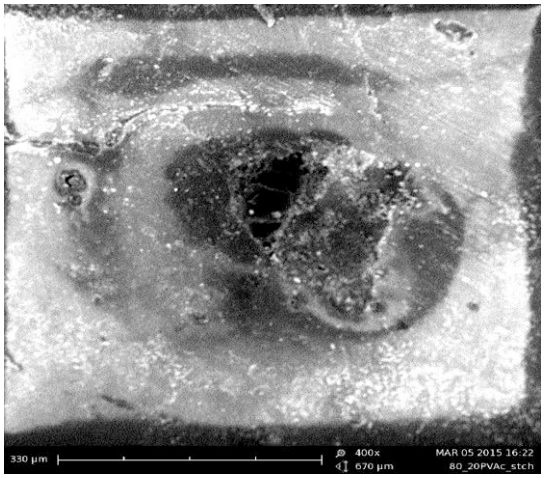

Figure 10: PVAc / starch 80/20 400x

3.2 Morphology Of PVAc/Starch-g-Oleic Acid Copolymers

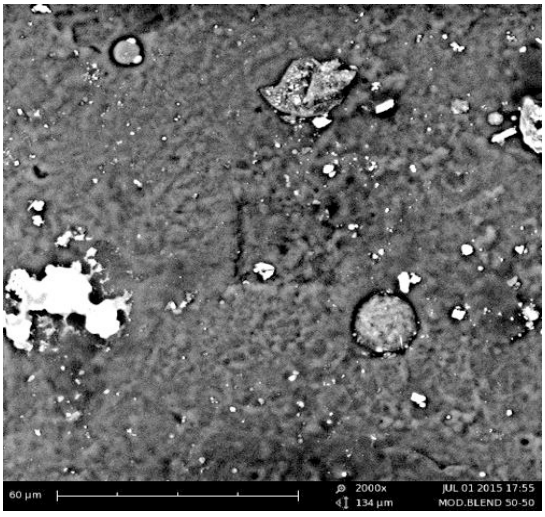

Figure 11: PVAc/starch-g-Oleic Acid 50/50, 410x

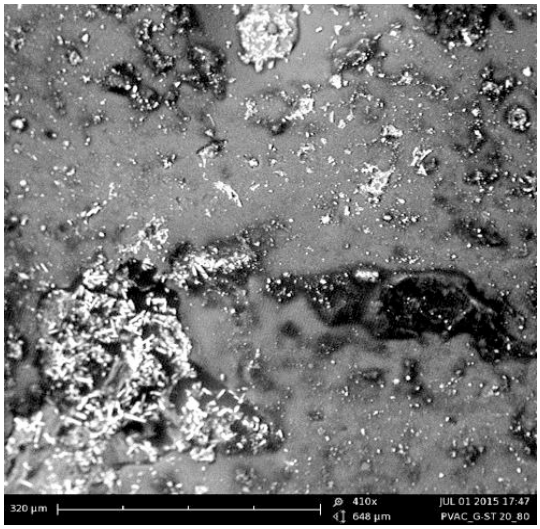

Figure 12: PVAc/starch-g-Oleic Acid 20/80,

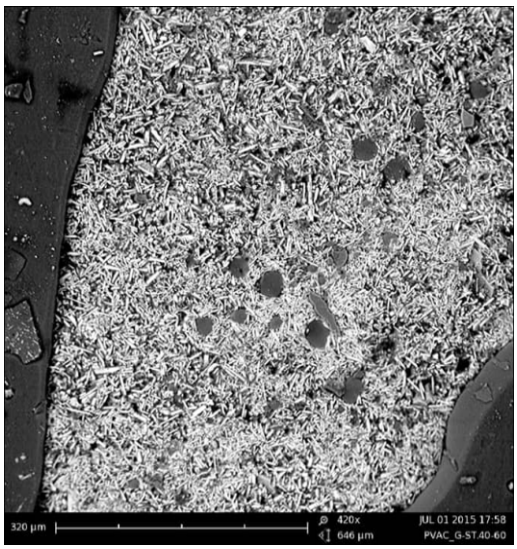

Figure 13: PVAc/starch-g-Oleic Acid 40/60, 1000x

Figure 14: PVAc/starch-g-Oleic Acid 80/20,

It was clearly observed that the micrographs of these blends of copolymers showed evidence of an improved compatibility when compared with PVAc native starch images due to introduction of long hydrocarbon chain from the acid. After grafting the spheroid in the native starch was completely destroyed due to gelatinization (Simi and Emilia, 2007). It was also observed that 50/50 PVAc/starch –g-oleic acid blend ratio shows better compatibility and minimum phase separation followed by 20/80 and 40/60 then 80/20. This may be due to high oleic acid content in the grafted starch, hence exhibited a hydrophobic nature of PVAc.

4.0 Conclusion

Poly (vinyl acetate) is a hydrophobic since its non water solving, where as cassava starch is hydrophilic due to the presence of hydroxyl groups, therefore mixing these polymers in an ordinary condition may results in blends with poor morphology and mechanical properties especially if blend with high starch content are prepared as it was found in 40/60 and the 20/80 blends ratios. The graft copolymer was characterized by FTIR, key functional groups were observed viz: C=O, C-O-C, C-H, C-O and OH as the characteristics bands.

However, morphological studies by SEM shows the effect of grafting oleic acid onto starch in yielding hydrophobic hydrophilic polymer blends with minimum phase separation and better compatibility when compared with PVAc/native starch blends.

Based on the results obtained in this research work blending synthetic polymer with modified starch by graft technique using oleic acid can serve as a possible means for producing materials which has potential application with the manufacturing biodegradable polymers for packaging, drug delivery or even as thickeners and binders in paints.

References

Bertoldo M., Federica C. and Simona B. (2012) preparation of gelatin/polyoxypropylene grafted copolymers by Isocyanate promoted "grafting onto" Reaction. Polymer journal 53. Pp. 4595

Byun Y. Whiteside S., Thomas R., Dharman M., Hughes J. and Kim Y.T. (2012). The effect of Solvent mixture on properties of Solvent Cast polylactic acid (PLA) film. *Journal of Applied polymer science* 124: *Pp*. 3577-3582.

Chai M. and Isah M.I.N (2013) the oleic acid composition effect on carboxymethylcellulose Based Biopolymers Electrolytes. Journal of crystallization process Technology 3 (1): Pp2-3.

Elias L., Fenonillot F., majeste J.C, and cassagnou Ph.(2009) Morphology and rheologyof immiscible polymer blend filled with Silica nanoparticles. 19th congress francaisMecanique Pp-1

Pereira A.G.B, Paulino A.T, Rubira A.F, and Muniz E.C (2010). Polymer-polymer miscibility in PEO/cationic starch and PEO/hydrophobic starch bleds. Express polymer letter Vol:4, No 8 page 488.

Simi C.K, and Emilia T. (2007) Hydrophobic grafted and cross-linked starch Nanoparticles for Drug Delivery, J. of Bioprocess Biosystem Eng. 30: Pp174-177

Utracki L.A and Manias E. (1989) polymer alloys and blend: thermodynamics and theology. Henser Munich

Nigerian Journal of Polymer Science and Technology, 2019, Vol. 14, pp67-74

Received: 28/08/2019 Accepted: 07/10/2019

MECHANO-FLEXURE STRAIN EVALUATION OF GRADED COCONUT FILLER ON NATURAL RUBBER REINFORCEMENT

[*1]Momoh F.P., [2]Mamza P.A.P., [3]Ajekwene K.K., [1]Eboreime A.E. and [1]Augustine A.O.

[1]Department of Polymer Engineering Technology, Auchi Polytechnic, Auchi
[2]Department of Chemistry, Ahmadu Bello University, Zaria
[3]Department of Polymer and Textile Technology, Yaba College of Technology, Yaba, Lagos.

*Corresponding author: fridymoh@yahoo.com

Abstract

Reinforced composites are considered as high performance materials if properly harnessed and formulated. In this study, the mechano-flexural strain properties of natural rubber filled with different preparation of coconut filler powder were comparatively evaluated. Coconut meat, shell, fibre and the modified shell and fibre via carbonisation were incorporated into natural rubber matrix and evaluated for mechanical, flexure-strain relationship and dynamic strength as proven indices for reinforcement. The morphological outlay, impact energy criteria and thermal ageing effect of modification on composites were also evaluated. Particle size range of 75µm was achieved using a 75µm mesh size sieve and treatment through carbonisation was effected at 600^{0}C for 3 hours. The modified variants especially the carbonised fibre showed a greater performance in dynamic energy resistance, mechanical properties, flexure-strain relationship and therefore reinforcement.

Keywords: carbonisation, composites, dynamic impact, flexure-strain and reinforcement.

1.0 Introduction

In recent times, property modification and enhancement in rubbers and composites especially for engineering designs and purposes have become paramount. The flexural modulus has to do with bending and is an intensive property that must be accurately computed and formulated for to maintain appropriate ratios and ratings of stress to strain in flexural deformation.

The flexure- strain relationship of a rubber composite to be used for designs with dynamic requirements is a sensitive matter and it should be handled as such. The flexural modulus is inversely related to deflection and a lower deflection would result in a higher modulus. A higher flexural modulus material is stiffer than a lower flexural modulus material.

The need for modification and reinforcement of composites arises due to high needs for the exhibition of good mechanical behaviour. Cost and recyclability are among the primary factors in exploiting the engineering materials for their new applications through appropriate modifications. The use of waste such as coconut shell, meat and fibre in engineering materials would serve to save our environment from untidiness and then leading to eventual wealth generation.

Khan et al, 2017, studied flexural deflections in glass/pp- based sandwich panel experimentally and numerically with the aims of its

potential applications in the automotive structures.

The tensile and flexural properties of composites made from coconut shell filler particles and epoxy resin have been studied previously by Sapuan et al, 2003. They performed several characterisation studies on composites prepared from coconut shell filler particles at three different filler contents. Their experimental results showed that tensile and flexural properties of the composites increased with the increase in the filler particle content. The composite materials demonstrate somewhat linear behaviour and sharp fracture for tensile and slight non-linear behaviour and sharp fracture for flexural testing.

Inés et al, 2018, carried out the dynamic flexural behaviour of sandwich beams, with composite face sheets and a foam core, by developing a 3-D finite element model. The comparison between numerical and experimental results in terms of contact force histories, peak force values, absorbed energy, and maximum displacement of both face sheets was satisfactory. It was revealed that the collapse of the foam core under the impact region favoured the failure of the upper face sheet.

Mansur and Aziz, 1983, studied bamboo-mesh reinforced cement composites and found that the reinforcing material could enhance the ductility and toughness of the cement matrix, and increase significantly its tensile, flexural, and impact strength.

The morphological studies of composites would be necessary to seek the interaction between the failure of a core and the failure of the composite material. This interaction is important in order to evaluate weakness point, causing a possible unexpected failure of the structure.

The present work seeks to comparatively evaluate the reinforcement properties of coconut shell, fibre, meat as well as the modified shell and fibre for use in dynamic flexure-strain applications in composites for the ultimate purpose of fitting engineering designs and manufacture.

2. Materials and Methods

2.1 Materials

The composites were made up of coconut fillers (meat, shell, fibre; carbonised shell and fibre). The thickness of each composite sheet was in the form of a bar 76.2mm x 25.4mm x 6mm. Coconut fruit (for the meat), shell and fibre were sourced in Auchi, Edo State, Nigeria. All needed additives used for the compounding process such as Zinc oxide, Stearic acid, Sulphur, MBTS, TMTD, TMQ and mineral processing oil were of pure and analytical grade. The Natural rubber used was NSR 10.

2.2 Filler Preparation

The carefully collected shells and fibres were washed in distilled water to remove debris, sands and keep other unwarranted reactions away before being oven dried at 95^0C for 2hours to remove all moisture. The coconut meat was blended and the contained oil mechanically extracted. The meat was also oven dried for 3hours at 95^0C to dry off all inclusive and remaining oil contents. Carbonisation of the shell and fibre were effected at 600^0C for 3hours in each case. The raw and carbonised materials were crushed and ground using a grinding machine. All powders; both raw and carbonised were taken through a series of sieve with mesh sizes ranging from 400µm down to 75µm in order to fully achieve an eventual particle size of 75µm used for the compounding process.

2.3 Mixing and Compounding

Distributive and dispersive mixing was effected using a two-roll mill machine at maintained roll temperature of 65^0C. A fitting formulation was designed and weighed out additives were incorporated into the rubber matrix. After 24hours of maturation and rheological determination using the ODR 2000 Rheometer, curing was carried out at 140^0C, for a period of 12 minutes at a pressure of 25psi.

2.4 Characterisation/Mechanical Properties Determination

From evaluative characterisation and physical/mechanical studies of the composite sheets certain scientific inferences and confirmations were made. The mechanical properties of the composites using standard methods (Khan et al, 2017) were as indicated in Table 1. Properties characterised were: Density, Young's modulus, Poisson ratio, Shear modulus, tensile strength, Compressive strength, Ultimate strain, Hardness and Elongation at break.

2.5 Flexure-Strain Measurement

Flexure-strain tests were performed using three point bending method in accordance to ASTM D790-03 procedure. The composite samples were tested at a crosshead speed of 2mm/min, at a temperature of 22^0C and humidity 0f 50%. The test sample was in the form of a bar 76.2mm x 25.4mm x 6mm. It was neatly cut from the composite samples so as to have smoothed edges free from cracks. The cut edges smoothen by finishing with zero number emery cloth.

2.6 Matrix Morphological studies

Scanning electron microscopy study was conducted on the compounded composites to evaluate the cell morphologies and matrix network distributions with the filled raw and carbonised fillers. Microscopic magnification was done at 1000x with a resolution of 75µm.

2.7 Dynamic Impact Test

Dynamic three point bending tests were performed. A drop weight tower instrumented to record the force exerted by the impacter, was used for testing the specimens dimensioned as 50mm width, 36mm thickness and 480mm length using a span of 450mm and impact energy of 65J. The impacter was a Charpy nose of 20mm with 7.95Kg of mass.

2.8 Thermal Ageing Effects

Using ASTM E1641, the samples were heated from room temperature to above 850^0C at a rate of 5^0C/min nitrogen to validate ageing effect on flexure-strain properties. Balance sensitivity of 0.1mg was achievable.

3 Results and Discussion

3.1 Characterisation and Mechanical Properties Evaluation

The evaluation of the mechanical properties of composites showed density increase from CMF – CCFF. The increase in density indicated that particles got packed into the matrix of the rubber thereby eliciting more of better filler-matrix interactions. The interpenetrating network between filler and rubber gets stronger with filler modification through carbonisation treatment (Chotirat et al, 2007).

The tensile strength and modulus of the composites increased with modification through carbonisation. This observation is expected and it is attributed to better filler dispersion and filler-matrix interactions; and hence a stronger reinforcement property. Carbon covalent also increased with carbonisation and fillers with higher carbon content provide greater

reinforcement (Hortola, 2015 and Momoh, 2017).

Table 1: Characterisation and Mechanical Properties of Composites with Graded Coconut Filler

Parameters	**CMF**	**CSF**	**CFF**	**CCSF**	**CCFF**
Density (Kg/M^3)	980	1200	1300	1500	1600
Young's Modulus (Gpa)	4.8	5.1	5.3	6.8	7.4
Poisson Ratio (υ)	0.16	0.14	0.12	0.10	0.09
Shear Modulus (Gpa)	0.6	0.9	1.0	1.2	1.3
Tensile Strength (MPa)	134.5	135.8	141.2	256.5	284.6
Compressive Strength (MPa)	134.2	135.1	140.0	245.4	280.6
Ultimate Strain (%)	1.12	1.23	1.45	2.68	3.14
Shore A Hardness (Å)	58.0	62.0	64.0	75.0	80.0
Elongation @ Break (%)	490.50	488.20	450.00	421.85	415.20

Legend Key
***CMF**-Coconut Meat Filler* ***CSF**-Coconut Shell Filler* ***CFF**-Coconut Fibre Filler*
***CCSF**-Carbonised Coconut Shell Filler* ***CCFF**-Carbonised Coconut Fibre Filler*

The increase in shear modulus is an indication of increase in stiffness of the composites with modification via carbonisation which leads to the creation of stiffer carbon content bonds (Momoh et al, 2017). The modification via carbonisation depressed compression and increase compressive strength of composites. Composite ductility increased and hence a corresponding improvement in reinforcement interaction levels between filler and rubber matrix (Ishak, 1995 and Momoh et al, 2016). Hardness of the composites increased with modification as a result of decrease in particle sizes. Reduction in particle size provides a greater surface area and reinforcement. The carbonised filler has a very high surface activity, which provided greater reinforcement in comparison with the raw fillers (Inés et al, 2018).Suppression of Poisson ratio of the filler to rubber matrix can dramatically impact elastomer mechanical response, with large enhancement of modulus, toughness and strength (Scott and David, 2018).

3.2 Flexure – Strain Evaluation

The flexure stress-strain relationship as depicted in figures 1 (a) and (b) gave a lucid indication of the levels of bending and deflection energy the composites filled with coconut meat, shell, fibre; as well as carbonised shell and fibre could withstand.

There was also a clear indication of the levels of bending and deflections the carbonised shell and fibre alone are capable of withstanding as showed in Figure 1 (b) above. The longitudinal elements of the beam near the bottom are stretched and those near the top are compressed, thus indicating the simultaneous existence of both tensile and compressive stresses on transverse planes. The stress distribution of beams was necessary for determining the levels of performance of the composites (Mohanty et al, 2000). Modification by carbonisation treatment on the composites gave better bending beams and an indication of positive contribution to filler-matrix interactions and therefore resulting in eventual product reinforcement.

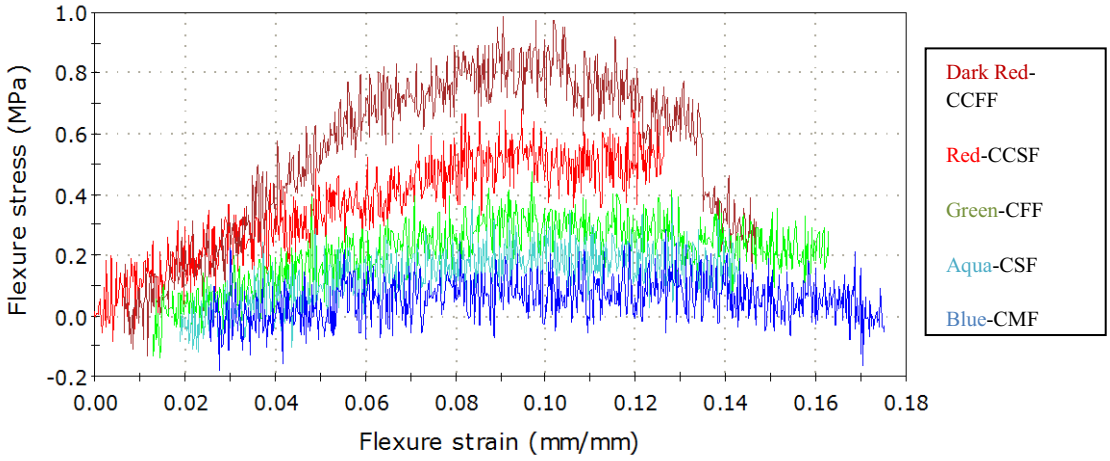

Figure 1 (a): Flexure-Strain Curve of Composites with Graded Coconut Filler

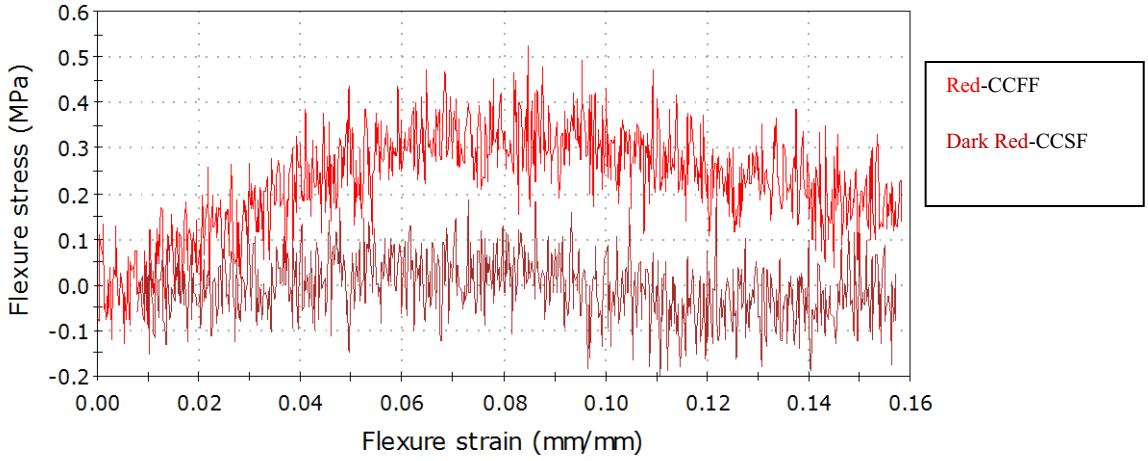

Figure 1 (b): Flexure-Strain Curve of Carbonised Coconut Fibre and Shell

The ultimate engineering stress that may be sustained without fracture is known as maximum tensile stress. The change in length of specimen divided by its original length is known as maximum tensile strain. Carbonisation results in increase in tensile stress strain and fracture or bending properties (Momoh et al, 2016).

3.3 SEM Evaluation

Optical clarity with the presence of tiny-like shinning particles could be observed with modification via carbonisation. The tiny-like particles suggested regular arrangement, properly aligned morphologies and structures which could have resulted from modification. The more glassy and structured the particles are the better the interfacial interactions between filler and the rubber composite (Eiras and Pessan, 2009). The agglomerated area created stress concentration zones which might act as a hardness initiator and therefore leading to reinforcement in mechanical properties and improved flexure-strain relationship. Large agglomerates of particles will contribute to weaker matrix and poor flexure-strain property; while tiny/fine agglomerates will contribute to stronger matrix and good flexure-strain properties as clearly depicted in the monographs plates in Figures 2 (a), (b), (c), (d) and (e) below (Momoh, 2019).

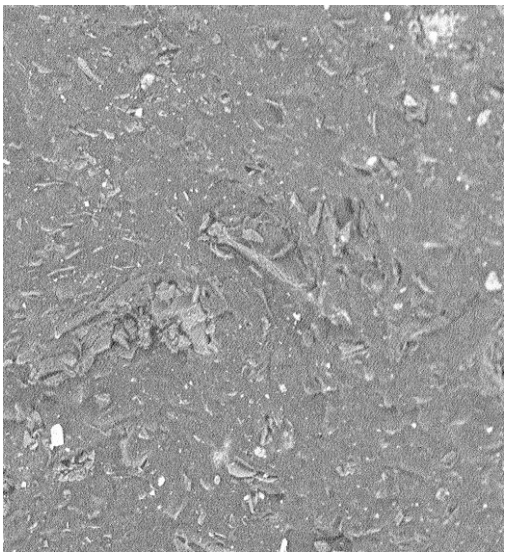

Figure 2 (a): Morphology of CCSF

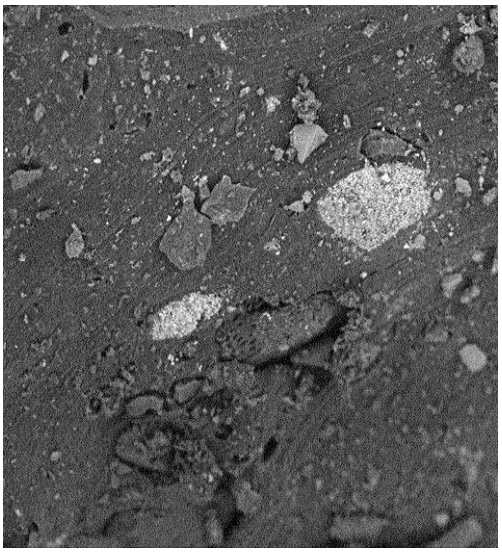

Figure 2 (b): Morphology of CCFF

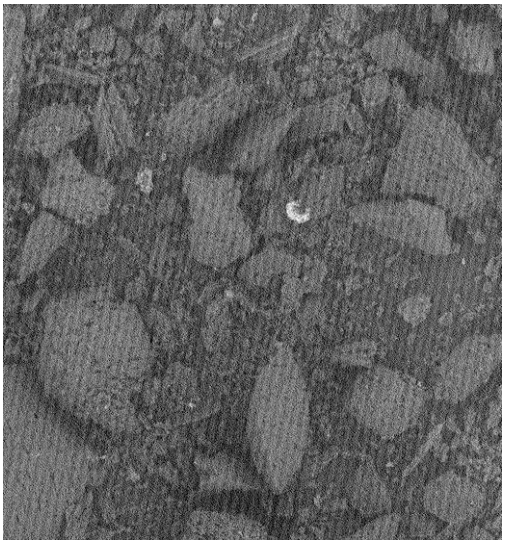

Figure 2 (c): Morphology of CMF

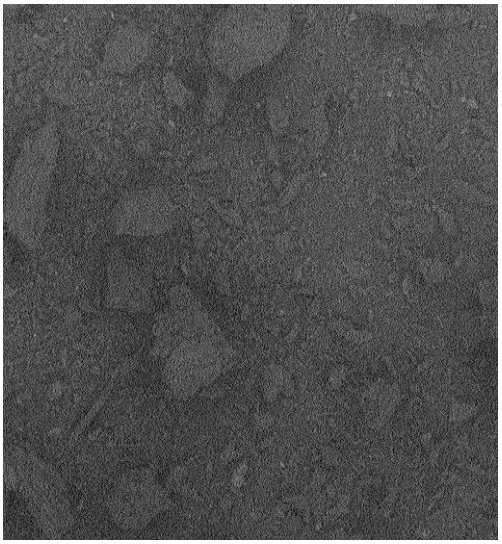

Figure 2 (d): Morphology of CSF

Figure 2 (e): Morphology of CFF

3.4 Impact Strength

The development of good mechanical properties and good flexure-strain interactional relationships also contribute to appreciable impact strength especially with the carbonised shell and fibre fillers as showed in Table 2 below:

Table 2: Impact Strength of Composites

Sample	Test 1 Joules/mm^2	Test 2 Joules/mm^2	Test 3 Joules/mm^2	Average value Joules/mm^2
CMF	60.00	61.00	60.50	60.50
CSF	63.00	64.00	62.00	63.00
CFF	66.00	65.00	66.00	65.67
CCSF	70.00	72.00	71.00	71.00
CCFF	78.00	79.00	80.00	79.00

The histogram distribution curve in Figure 3below showed a built up of impact strength produced which gave a positive report in the overall resistance of the composites to fracture and hence good reinforcement of the matrix (Momoh, 2019).

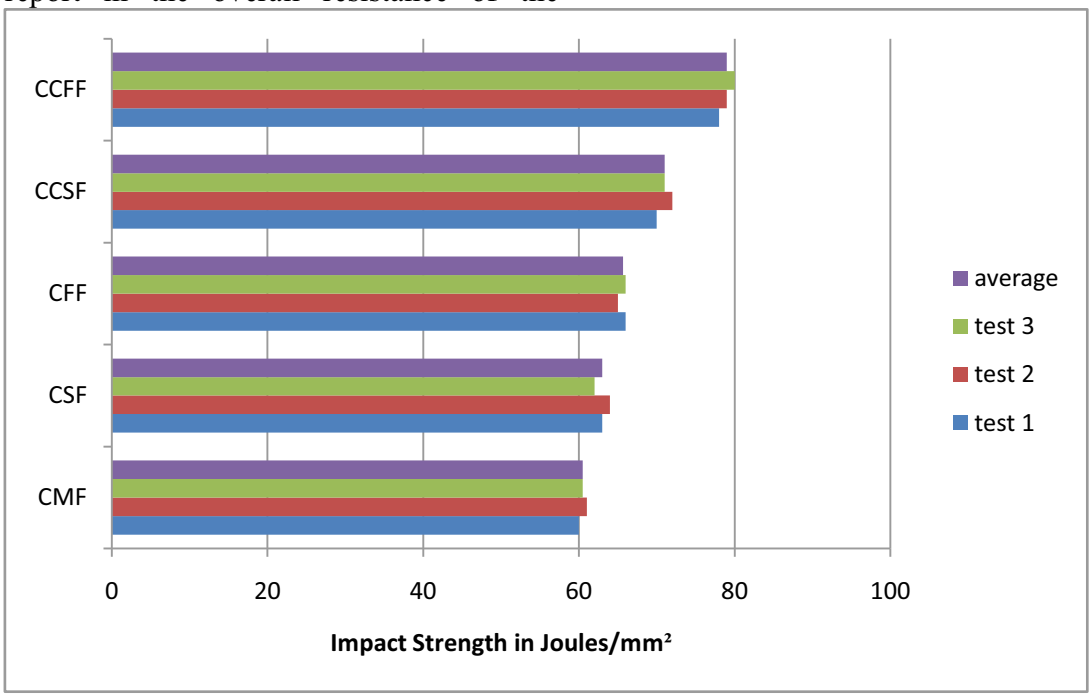

Figure 3: Impact Strength of Composites with Graded Coconut Filler

3.5 Thermal Ageing Effect on Dynamic Flexure-Strain Relationship

Dynamic flex fatigue was carried out on the samples prior to ageing and after ageing to validate potential mode of failure in service. In its simplest form flex fatigue is the cracking of rubber component due to cyclical stresses and strain. Results in Table 3 below showed positive effect of ageing on dynamic flexure stress-strain capacities of composites.

Table 3: Thermal Ageing Effect on Dynamic Stress-Strain of Composites

Samples	Initial Crack Time Prior to Ageing (Minutes)	Final Crack Time After Ageing (Minutes)
CMF	48	39
CSF	72	60
CFF	142	131
CCSF	245	238
CCFF	282	279

The intensity of effect of ageing on dynamic properties was much on CMF, CSF and CFF; but quite least on CCSF and CCFF. This showed that modification via carbonisation presented more resistant composites because the molecular matrix was dense and more thickly networked for the modified composites. The failure starts off as micro-cracking virtually at the molecular levels, and with successive cycling; it propagates into macro-cracking that ultimately resulted in composite failure.

Conclusion

Physical modification actually took place through carbonisation and molecular matrix was reinforced and strengthened. Physical/mechanical behaviour, morphological outlays and thermal resistant properties of composites got remarkably improved. Modification by carbonisation gave a clear indication of the performance of coconut filler in flexure-strain relationship. Potential surface and material hindrances were drastically eliminated during carbonisation treatment, thereby creating a high interactive surface between filler and rubber matrix of the composites as well as increase in the carbon content of the fillers.

References

Carcia-Castillo, S.K., Sanchez-Saez, S., Lopez-Puente, J., Barbero, E., Navarro, C. (2009) Impact Behaviour of Preloaded Glass/Polyester Woven Plates. Compos Sci.Technol,

Chotirat, L., Chaochanchaikul, K.,Sombatsompop, N (2007) On Adhesion Mechanism and Interfacial Strength in Acrylonitrile Butadiene Styrene/wood Sawdust Composites. International Journal of Adhesion and Adhesives, 27: 660-678.

Eiras, D., Pessan, L.A. (2009) Crystallization Behaviour of Elastomer/Filler Composites: Effect of Elastomer Polarity. Polymer, 41: 9283-9290; 355-356.

Hortola, P. (2015) Evaluating the Use of Synthetic Replicas for SEM Identification of Blood Stains (with Emphasis on Archaeological and Ethnographic Artifacts). Microscopy and Micro-Analysis, 6:1504.

Icardi, U., Ferrero, L (2009) Impact Analysis of Sandwich Composites Based on a Refined Plate Element with Strain Energy Updating. Compos Struct.

Inés Wañez, Carlos Santiuste, Sonia Sanchez-Saez (2018) FEM Analysis of Dynamic Flexural Behaviour of Composite Sandwich Beams with Foam Core.

Ishak, Z.A.M., Bakar, A. A. (1995) Investigation on the Potential of Rice Husk Ash as Fillers for

Epoxidised Natural Rubber (ENR) European Polymer Journal, 31 (3): 259-269.

Jacob OlaitanAkindapo, Ayogu Harrison, Olawale Monsur Sanusi (2014) Evaluation of Mechanical Properties of Coconut Shell Fibres as Reinforcement Material in Epoxy Matrix. International Journal of Engineering Research and Technology (IJERT), ISSN: 2278-0181

Khan, M.A., Syed, A.K., Ijaz, H., Shh, R.M.B.R. (2017) Experimental and Numerical Analysis of Flexural and Impact Behaviour of Glass/pp Sandwich Panel for Automotive Structural Applications.

Mansur, M.A., Aziz, M.A. (1983) Study of Bamboo-Mesh Reinforced Cement Composites, United Kingdom. Pp. 165-175.

Mohanty, A.K., Khan, M.A.,Hinrichsen, G. (2000) Surface Modification of Jute and its Influence on Performance of Biodegradable Jute-Fabricbiopol Composites. Composition Science and Technology, 60 (7): 1115-1124.

Momoh, F.P., Mamza, P.A.P., Gimba, C.E., Nkeonye, P. (2016) Effects of Carbonisation on Coconut Shell as Filler in Natural Rubber Compounding, Nigerian Journal of Polymer Science and Technology 11: 115-123.

Momoh, F.P., Mamza, P.A.P., Gimba, C.E., Nkeonye, P. (2017) Morphology and Crystallinity of Modified Coconut Shell Powder in Natural Rubber Development. International Journal of Innovative Research and Advanced Studies (IJIRAS) 4: 257- 262.

Momoh, F.P. (2019) Engineering Design with Polymers. Scholar Press International Book Market Service Ltd, Member of OmnicsriptumPublishing Group, Mauritius.

Sadighi, M., Pouriayevahi, H. (2008) Quasi-Static and Low-Velocity Impact Response of Fully Backed or Simply Supported Sandwich Beams. J. Sandwich Struct Mater.

Sapuan, M., Harimi, M. (2003) Mechanical Properties of Epoxy/Coconut Shell Filler Particle Composites. The Arabian Journal for Science and Engineering.

Scott, M. Smith; David, S. Simmons (2018) Poisson Ratio Mismatch Drives Low-Strain Reinforcement in Elastomeric Nanocomposites. Research Gate.

ANA INDUSTRIES LTD.

GGI INT'L (NIG) LTD

....nigerian coy, global spirit...

GGI Place: Plot 8 GGI Crescent [Opp. Mikab Filling Station] East/West Road, P. O. Box 11591, Rumuodara Port Harcourt 500001 Rivers State, Nigeria.
Tel: (+234) 84 301125, 8074036014, 8169529400, 0700GGIGROUP.
Email: ggi_group@yahoo.com, enquiries@ggigroupltd.com, Website: www.ggigroupltd.com

Lagos Office: OKIO ARIKPO (NUC) HOUSE, 5 Idowu Taylor Street, Victoria Island, Lagos.
Tel: +234(0)8172064304

Eket Office: #7 Inyang Udofa Street, Eket, Akwa Ibom State, Nigeria
Tel: +234 (0) 81720634305, +234(0)8029933955

What WE DO

- Oilfield TREATMENT CHEMICALS
- COMMODITY CHEMICALS
- Lab SERVICES
- DELIVERY TANKS & OILFIELD FACILITY UPGRADES
- Blending/Production OF OILFIELD & PROCESS CHEMICALS

AN ISO 9001:2015, OHSAS, 18001:2007 & ISO 14001:2015 REGISTERED COMPANY

PETAN MEMBER OF Chamber

IFAZ NETWORK
Network Graphics